Ultra-High Throughput HPLC-MS Analysis Using Active Flow Technology

Danijela Kocic
BSc (Honours) (Chemistry)

A thesis submitted in accord with the requisites of the degree of

Doctor of Philosophy

School of Science and Health
University of Western Sydney
Parramatta, New South Wales, Australia

August 2015

Statement of Authentication

I, Danijela Kocic, declare that the work presented in this thesis is, to the best of my knowledge and belief, original except as referenced in the text of this thesis. I hereby declare that I have not submitted this material, either in full or in part, for a degree at this or any other institution.

Signed: _____

Date: _____

Acknowledgements

I would like to thank my supervisors Prof. Andrew Shalliker and Associate Prof Gary Dennis for their help, support, guidance and patience throughout my candidature; in particular my sincere gratitude is reserved for Prof. Andrew Shalliker as my primary supervisor for the expert guidance, assistance, advice and friendship who always believed in me and encouraged me to do my best. I would like to acknowledge the Australian Post Graduate Award and The University of Western Sydney Research Award for providing me the opportunity and necessary financial assistance.

Special thanks go to Kathleen Mackenzie for introducing mass spectrometry into my life and her continuous support of my undergraduate and postgraduate studies during my work at Novartis AH R&D. I am also grateful to my colleges and friends, Sercan, Chester and Michelle for their friendship and support during my candidature.
Last but not least, I want to thank to my family and friends for their love, understanding and friendship.

Last few years were not an easy ride, both academically and personally. It was a life changing experience that I value very much. It shaped me into a better person and better scientist and I would not have it any other way.

I dedicate this thesis to
my family, my husband Miroslav and my beloved children Kristian and Marko
for their constant support and unconditional love.
I love you all dearly.

Publications published arising from this thesis

Book Chapters

1. R. A. Shalliker and D. Kocic, Recent Advances in Column Technology, in Analytical Separation Science Vol 1, Editor, Anderson Wiley-VCH (2015) (In Press).

2. R.A. Shalliker, M.J. Gray, D Kocic and S. Pravadali-Cekic, HPLC-Hyphenation, in Analytical Instrumentation Handbook, 4th Edition Ed. J. Cazes and E. Ewing. Marcel Dekker Inc New York (In review).

Journal Publications

3. D. Kocic, L. Pereira, D. Foley, T. Edge, J.A. Mosely, H. Ritchie, X.A Conlan and R.A. Shalliker, *High Through-put and Highly Sensitive LC-MS/MS Separations of Essential Amino Acids using Active Flow Technology Chromatography Columns*, *J. Chromatogr. A,* **1305** (2013) 102-108

4. D. Kocic, S. Hua, G.R. Dennis, R.A. Shalliker, *Using active flow technology columns to achieve near 'direct' injection through-put in HPLC–MS, Microchem., J.,* **118** (2014) 193-197.

5. D. Kocic, L. Pereira, T. Edge, H. Ritchie, X.A Conlan and R.A. Shalliker, *Improving quantification using chromatography columns in the analysis of labile compounds: A study on amino acids, J. Chromatogr. A,* **1375** (2015) 76-81.

6. A. Jones, S. Pravadali-Cekic, S. Hua, D. Kocic, G. Dennis, R. A. Shalliker, *Post Column Derivatisation Using Reaction Flow High Performance Liquid Chromatography Columns, JoVE* (In press)

7. S. Pravadali-Cekic, D. Kocic, A. Jones, S. Hua, G. Dennis, R. A. Shalliker, *Curtain Flow Column – Optimization of efficiency and sensitivity, J. Vis. Exp.* (In press)

8. S. Pravadali-Cekic, D. Kocic, A. Jones, S. Hua, G. Dennis, R. A. Shalliker, *Tuning a Parallel Segmented Flow Column and Enabling Multiplexed Detection, J. Vis. Exp.* (106), e53448, doi:10.3791/53448 (2015).

9. Sercan Pravadali-Cekic, Danijela Kocic, Xavier Conlan and R. Andrew Shalliker *"Multiplexed detection: Fast comprehensive sample analysis of tobacco leaf extracts using AFT HPLC columns. J.of Liq.Chromatography and Relat.Techniq.* 38 (2015) 1753.

10. D. Kocic, S. Pravadali-Cekic, A. Jones, S. Hua, G. Dennis, R. A. Shalliker , *Curtain Flow HPLC-MS for high-throughput, high sensitivity analyses, J. Vis. Exp.* (Submitted for Publication).

11. D. Kocic and R. A. Shalliker, *Using Active Flow Technology Columns For High Through-put and Efficient Analyses Incorporating Mass Spectral Detection, J. Chromatogr. A* **1421** (2015) 60.

12. D. Kocic and R. A. Shalliker, *A New Approach to Live Reaction Monitoring using Active Flow Technology in Ultra High Speed HPLC with Mass Spectral Detection, J. Mass Spectrometry,* **50** (2015) 1396.

13. S. Pravadali-Cekic, D. Kocic, P. Stevenson and R. A. Shalliker, *Outlining a Multidimensional Approach for the Analysis of Coffee using HPLC, J. Chromatogr. and Sep. Techniques*, 6:284. doi:10.4172/2157-7064.1000284.

14. D. Kocic, G.R. Dennis, W. Farrell and R. A. Shalliker, *Ultra High Speed HPLC-MS Using Active Flow Technology for High Through-put Applications, Rapid Communications in Mass Spectrometry* (Submitted for Publication).

Conferences and Presentations

1. HDR 2012 Sydney – Oral presentation -***High Through-put and High Sensitivity LC-MS using Segmented Flow Chromatography Columns***

2. R&D Topics 2012 Melbourne – Oral presentation - ***High Through-put and High Sensitivity LC-MS Analysis of Amino Acids using Segmented Flow Chromatography Columns***

3. HPLC 2012 Anaheim – Poster presentation - ***High Through-put and High Sensitivity LC-MS using Segmented Flow Chromatography Columns***

4. HDR 2013 Sydney – Oral presentation – 12th of July 2013 - ***High Through-put and Highly Sensitive LC-MS/MS Separations of Essential Amino Acids using Active Flow Technology Chromatography Columns***

5. HPLC 2013 Amsterdam - Poster presentation - ***High Through-put and High Sensitivity Analyses Using Active Flow Technology Chromatography with Mass Spectral Detection***

6. HPLC 2013 Hobart - Poster presentation - ***High Through-put and High Sensitivity LC-MS Analysis of Amino Acids using Active Flow Technology Chromatography Columns***

7. HDR 2014 Sydney – Oral presentation - ***High Through-put and High Sensitivity LC-MS using Segmented Flow Chromatography Columns***

8. HPLC 2014 New Orleans - Oral presentation - ***High Through-put Assays using Curtain Flow Chromatography Columns: A Study using Labile Compounds***

9. Virtual Symposium on Applied Separation Science (VSASS) 2015 Virtual conference - Oral presentation - ***High Through-put Assays using Curtain Flow Chromatography Columns: A Study using Labile Compounds***

10. Virtual Symposium on Applied Separation Science (VSASS) 2015 Virtual conference – three poster presentations

    I. ***High Through-put Assays using Curtain Flow Chromatography Columns***
    II. ***High Through-put Assays using Curtain Flow Chromatography Columns: A Study using Labile Compounds***
    III. ***High Through-put Assays using Curtain Flow Chromatography Columns: Near Direct Injection***

List of Abbreviations and Symbols

µL	Microlitres
σ	Standard deviation of the population
µm	Micrometre
AFT	Active Flow Technology
Ar	Argon
C	Celsius
CF	Curtain Flow
CI	Chemical Ionisation
cm	Centimetre
Da	Dalton
d_p	Particle diameter
EI	Electron Ionisation
EIC	Extracted Ion Chromatogram
ESI	Electrospray Ionisation
ESI-MS	Electrospray Ionisation Mass Spectrometry
eV	Electron Volt
g	Grams
H	Height equivalent to theoretical plate
h	Hours
h	Reduced plate height
He	Helium
HESI	Heated Electrospray Ionisation
HETP	Height Equivalent to Theoretical Plate
HPLC	High Performance Liquid Chromatography
i.d.	Internal Diameter
k	Retention factor
kV	Kilovolt
L	Column length
LC	Liquid Chromatography
LRM	Live Reaction Monitoring
M	Molarity
m/z	Mass to charge
MALDI	Matrix Assisted Laser Absorption Ionisation
mg	Milligrams
min	Minute
mL	Millilitre
mm	Millimetre
MRM	Multiple Reaction Monitoring
MS	Mass Spectrometry
MS/MS	Tandem Mass Spectrometry
MS/MS/MS	Triple Stage Mass Spectrometry
MW	Molecular Weight
MΩ	Megaohm
n	Number of peaks
N	Theoretical Plate Count
N_2	Nitrogen
ND	Not Detected
ng	Nano-gram

nL	Nano-litre
nm	Nano-meters
p.s.i.	Pounds per Square Inch
P_d	Particle size
PD	Plasma Desorption
PDI	Pulsed Direct Injection
ppm	Parts Per Million
PSF	Parallel Segmented Flow
R^2	Correlation coefficient
Q	Quadrupole
R	Resolution
RSD	Relative Standard Deviation
S/N	Signal to Noise
SE	Secondary electron
Sec	Second
SRM	Single Reaction Monitoring
SST	System Suitability Test
TIC	Total Ion Count
TOF	Time of Flight
t_R	Retention Time
TSQ	Triple Stage Quadrupole
UHPLC	Ultra High Performance Liquid Chromatography
USA	United States of America
UV	Ultra Violet
v	Velocity
V	Volt
σ	Standard Deviation of the Population

Abstract

High through-put analysis is increasingly in demand in many aspects of the analytical world. In concert with the need for high throughput, there is the need for higher sensitivity and better resolution. Further, for complex mixtures there is the need often there is a requirement for comprehensive sample characterization. These requirements are the driving forces for continuous developments in instrumentation. High performance liquid chromatography with mass spectrometry detection quickly evolved from predominantly university researcher environments to a tool that is now utilised on an everyday basis for qualitative and quantitative analyses in a wide variety of disciplines. Despite the general superiority of LC-MS as the go-to analytical tool, there are still many challenging issues and limitations, especially in relation to the interface between the LC and the MS detector.

The work undertaken in this thesis develops strategies and technology as a solution to the interface problem between LC and MS. In particular this thesis investigates how to undertake LC-MS analyses in modes that are described here as 'ultra-high' throughput, consistent with the paradigm change in the enabled workflow. Indeed, the speed of the LC-MS analyses presented in this thesis rival direct injection protocols, but with the advantage that separation takes place prior to detection. A preliminary investigation was undertaken to assess the applicability of the ultra-high speed LC-MS developed herein as a tool for monitoring live reactions that require frequent sampling for reaction rate determinations. This was achieved employing a new column technology, called Active Flow Technology (AFT), which overcomes the limitations of the interface between HPLC and MS. The two important designs of AFT that are related to this thesis are the Curtain Flow column and the Parallel Segmented Flow column.

Preface

High Performance Liquid Chromatography-Mass Spectrometry (HPLC-MS) is an integral and essential tool for almost every aspect of modern day chemical analysis. The demand for shorter analysis times and high-throughput, together with higher sensitivity and higher resolution, coupled with stringent regulatory requirements has led to the tremendous transformation and evolution of LC-MS, especially over the last 20 years. Even though HPLC-MS has had rapid development there are still many limitations and unresolved issues when it comes to coupling high performance liquid chromatography to mass spectrometry detectors. This thesis outlines these issues and focuses on demonstrating how Active Flow Technology (AFT) columns can offer a solution to the problem.

Chapter 1 is an introduction, setting the scene of the current state of chromatography and mass spectrometry. It also outlines the limitations of the modern HPLC-MS technique, which then leads to the objectives of this thesis, specifically detailing a novel approach to overcome current issues associated with improving the flow limitations at the interface between HPLC and MS. Chapter 1 introduces the use of AFT chromatography columns to applications involving MS detection and outlines the thesis objectives.

Chapter 2 outlines general experimental details. This chapter lists all the materials and methods as well as the instrumentation. It also outlines the working principles of curtain flow and parallel segmented flow columns. Any experimental information that relates solely to work reported in the experimental sections in specific chapters, however, has not been included in Chapter 2.

Chapter 3 details the performance of chromatography columns, offering a comparison between HPLC and UHPLC formats, and then compares these formats to AFT columns in HPLC mode. The practical limitations of conventional HPLC and UHPLC columns are discussed. The chapter concludes that for the purpose of high throughput work flow, AFT columns have significantly higher efficiency at high flow rates, and function at lower back pressures.

Chapter 4 introduces the use of AFT columns to HPLC-MS applications. Specifically in Chapter 4, the curtain flow version of AFT columns have been utilised. Experiments conducted in Chapter 4 demonstrate the advantages of curtain flow chromatography columns in comparison to conventional and narrow bore columns. The results in Chapter 4 show that AFT columns can be utilized for substantial gains in sensitivity when compared to traditional columns.

Chapter 5 details the importance of speed when analysing labile compounds. Mixtures of underivatized amino acids were used as test compounds to demonstrate this point. The outcome from this chapter was that curtain flow columns could be operated with higher throughput in an HPLC-MS analysis, with greater sensitivity, and as a result, the data obtained from the analysis was more accurate and with greater precision.

Chapter 6 explores the use of narrow bore AFT columns in applications of HPLC-MS. This resulted in even greater through-put than demonstrated in Chapters 4 and 5. Specifically, the research here showed that separations could be complete in time frames of less than 6 seconds, indeed approaching the speed of direct injection protocols.

Chapter 7 expands further on the application of high-through put HPLC-MS using narrow bore AFT columns. The work demonstrates the approach to automation of the AFT-MS at high throughput, highlighting the benefits of operating at very high volumetric flow rates. This technique was termed Pulsed Direct Injection (PDI). This chapter details principles of this novel technique and demonstrates its effectiveness for HPLC-MS analyses.

Chapter 8 is a short chapter that provides information on the method robustness, reproducibility, limits of detection, calibration range and linearity of PDI AFT-MS. Furthermore, mass spectral data was also assessed for quality, determining whether current mass spectrometer data acquisition rate is sufficient to adequately define a chromatographic peak at high speeds, especially when a large number of transitions were being monitored simultaneously. The chapter concludes the AFT-MS operating at very high flow rates can be a feasible technique, although the user should be aware

of the limitations in data acquisition and hence must consider how best to undertake selective ion monitoring.

Chapter 9 is a chapter on future directions, specifically detailing preliminary work on the uses PDI AFT-MS as a means to monitor chemical reactions in real time. This was a brief chapter that used the degradation of amino acids in acidic solution as a test demonstrating how the rate of degradation could be determined as the reaction proceeded.

Chapter 10 is the general conclusion of this project, tying together the outcomes and objectives of this study.

Table of Contents

Acknowledgements **.....i**

Publications published arising from this thesis iii

Conferences and Presentations v

List of Abbreviations and Symbols.....vi

Abstract viii

Preface ix

1 Introduction 1

1.1 Mass spectrometry 2

1.1.1 History 2

1.1.2 Components of ESI-MS 3

1.1.2.1 Ion Source 3

1.1.2.2 Mass Analyser.....5

1.1.2.3 Detector.....6

1.1.3 Ionisation techniques.....6

1.1.3.1 Electrospray Ionisation 7

1.1.3.2 The ESI Mass Spectrum.....10

1.2 Separations involving Chromatography and Mass Spectrometry 10

1.2.1 The evolution of HPLC and column technology 11

1.2.2 Current Applications of LC-MS.....13

1.2.3 Leading trends and future of separations and mass spectrometry.....13

1.3 Active Flow technology..... 14

1.3.1 Curtain Flow Chromatography.....14

1.3.2 Parallel Segmented Flow Chromatography.....16

1.4 Research problems, project aim and objectives..... 18

2 General Experimental..... 19

2.1 Introduction 20

2.1.1 Chemical and reagents 20

2.1.2 Chromatographic Conditions 20

2.1.3 Mass Spectrometry parameters 20

2.1.4 Instrumentation UPLC-MS/MS 22

2.1.4.1 Isocratic Method – Mass Spectrometry. 22

2.1.5 Curtain flow Chromatography Columns – Operation.....22

3 Assessing the Suitability of Active Flow Technology Columns for High Through-put Separations 23

3.1 Introduction 24

3.2 Experimental 25

3.2.1 Chromatography Columns 25

3.2.2 Chemicals and Reagents 25

3.2.3 Chromatographic Separation 26

3.3 Results and Discussion. 26

3.3.1 Conventional HPLC and UHPLC columns 26

3.3.2 Conventional HPLC and AFT columns – 5 μm particle formats 28

3.3.3 The Performance of AFT columns in 2.1 and 4.6 mm i.d. formats– 5 μm particle formats. 31

3.4 Conclusion 35

4 High Through-put and Highly Sensitive LC-MS/MS Separations of Essential Amino Acids using Active Flow Technology Chromatography Columns 36

4.1 Introduction 37

4.1.1 Curtain Flow Chromatography. 37

4.2 Experimental 38

4.2.1 Chromatography Columns. 38

4.2.2 Chemicals and Reagents 38

4.2.3 Instrumentation UPLC-MS/MS 38

4.2.3.1 Gradient Method. 38

4.2.4 Mass Spectrometry Parameters 39

4.3 Results and Discussion 39

4.4 Conclusion 48

5 Improving Quantification Using Curtain Flow Chromatography Columns in the Analysis of Labile Compounds: A Study on Amino Acids 49

5.1 Introduction 50

5.2 Experimental 50

5.2.1 Chromatography Columns. 50

5.2.2 Instrumentation UPLC-MS/MS 50

5.2.3 Mass Spectrometry Parameters 50

5.2.4 Quantification Protocol 50

5.2.5 Column Testing. 51
5.3 Results and Discussion 51
5.4 Conclusion 59
6 Using Active Flow Technology Columns to Achieve Near 'Direct' Injection Through-put in HPLC-MS 60
6.1 Introduction 61
6.2 Experimental 62
6.2.1 Chromatography Columns 62
6.2.2 Chemicals and Reagents 62
6.2.3 Instrumentation 62
6.2.4 Mass Spectrometry Parameters 62
6.2.5 Chromatographic Separation 62
6.3 Results and Discussion 63
6.4 Conclusion 69
7 Pulsed Direct Injection for Ultra-Fast HPLC MS Analyses 70
7.1 Introduction 71
7.2 Experimental 72
7.2.1 Chemicals and Reagents 72
7.2.2 Chromatography Columns. 72
7.2.3 Instrumentation HPLC-MS/MS 72
7.2.4 HPLC-MS/MS analysis 72
7.3 Results and Discussion. 73
7.4 Conclusion. 79
8 Validation of the Pulsed Direct Injection Process 80
8.1 Introduction 81
8.2 Experimental. 82
8.2.1 Chemicals and reagents 82
8.2.2 Instrumentation 82
8.2.3 Instrument set up 83
8.3 Results and Discussion. 83
9 Future Directions: Application of Pulsed Direct Injection and Active Flow Technology in Reaction Monitoring 90

9.1 Introduction 91
9.2 Experimental. 92
9.2.1 Chemicals and reagents 92
9.2.2 Standard preparation 92
9.2.3 Instrumentation 92
9.2.3.1 Instrumental method for amino acid analysis 92
9.2.4 Instrument set up 92
9.3 Results and Discussion. 92
9.4 Conclusion. 95
10 Conclusion 96
10.1 Concluding Remarks 97
References 100

List of Figures

Figure 1.1 Flow diagram of the processes involved in the MS detection. 3
Figure 1.2 Ion source with capillary needle spraying towards the orifice of the sample cone [17] 4
Figure 1.3 Ion path of a triple stage mass spectrometer, Q1 and Q3 are mass-resolving quadrupoles, and Q2 is functioning as a collision cell. 5
Figure 1.4 Schematic representation of the electrospray ionisation process. 8
Figure 1.5 Formation of Taylor cone at the end of capillary needle. 9
Figure 1.6 A typical ESI-mass spectrum acquired in positive ion mode. 10
Figure 1.7 Curtain flow column with AFT fittings at the column inlet and outlet demonstrating the multi-port radial flow splitting process. 15
Figure 1.8 Concept of virtual "wall less" column. The inner cylinder represents the wall less MP flow. 15
Figure 1.9 Active Flow Technology end fitting with multiple ports. As detailed in reference [90,91]. 16
Figure 1.10 Illustration of flow stream splitting (left – AFT radial flow split; centre – 50% post column split on a conventional column; right – 30% post column split on a conventional column, “typical” chromatographic responses. 17
Figure 1.11 Parallel Segmented Flow Column with multi-port AFT fitting on the column outlet. 17
Figure 3.1 HETP curves obtained on a conventional 1.9 µm particle packed column in a 2.1 mm i.d. format (red) and a conventional 5 µm particle column in a 4.6 mm i.d. format. 28
Figure 3.2 HETP curves obtained on a conventional 5 µm particle packed column in a 4.6 mm i.d. format (black) and a PSF 5 µm particle column in a 4.6 mm i.d. format with an outlet segmentation ratio of 43% through the centre (blue). 29
Figure 3.3 HETP curves obtained on a conventional 5 µm particle packed column in a 4.6 mm i.d. format (black) and a PSF 5 µm particle column in a 4.6 mm i.d. format with an outlet segmentation ratio of 21% through the centre (blue). 30
Figure 3.4 Comparison between the separations obtained on conventional 2.1 mm i.d. columns packed with 1.9 µm (red) and 5 µm (black) particles. 32
Figure 3.5 HETP curves obtained on a 4.6 mm i.d. PSF column packed with 5 µm particles operating with a 21% outlet segmentation ratio (black) and a 2.1 mm i.d. PSF

column in a 2.1 mm i.d. format packed with 5 μm particles with an outlet segmentation ratio of 21% through the centre (blue).....32

Figure 3.6 HETP curves for the 1.9 and 5 μm particle packed columns in conventional UHPLC and AFT (21% segmentation ratio), all in 2.1 mm i.d. formats: Toluene (□), propylbenzene (○), butylbezene (Δ). Black trace 2.1 × 50 mm, 1.9 μm, Green trace 2.1 × 30 mm, 1.9 μm, and Blue trace 2.1 × 50 mm, 5 μm. 33

Figure 3.7 Chromatograms illustrating the separations obtained on the conventional UHPLC column (red trace) in a 2.1 × 30 mm, 1.9 μm format and the PSF column with a 21% outlet segmentation ratio (black trace) in a 2.1 × 50 mm, 5 μm format. Both separations were obtained at equal numbers of theoretical plates. 35

Figure 4.1 Extracted ion chromatograms of phenylalanine derived from each of the three columns. Trace (a) is the chromatogram obtained on the 4.6 mm i.d. conventional column, trace (b) for the 2.1 mm i.d. conventional column and trace (c) is the CF column. Note the rising baseline is due to the gradient change and this is not apparent on the AFT column.....40

Figure 4.2 Calibration curves for tryptophan obtained on each of the columns: curtain flow column (O), 4.6 mm i.d. conventional column (▲) and 2.1 mm i.d. conventional column (■).....42

Figure 4.3 Plot illustrating S/N responses for each of the amino acids. Cross hatched = 2.1 mm i.d. conventional column, shaded = 4.6 mm i.d. conventional column, and hollow = curtain flow column. Amino acids from left to right are: valine, threonine, lysine, methionine, histidine, phenylalanine, arginine, tyrosine, and tryptophan.....43

Figure 4.4 Comparison of the signal intensity responses for each of the amino acids. Cross hatched = 2.1 mm i.d. conventional column, shaded = 4.6 mm i.d. conventional column, and hollow = curtain flow column. Amino acids from left to right are: valine, threonine, lysine, methionine, histidine, phenylalanine, arginine, tyrosine, and tryptophan.....44

Figure 4.5 The plots showing the noise contributions for each of the three columns for extracted ion chromatograms of phenylalanine. Note the time axis is expressed as a fraction of the total run time, i.e. normalised time between 0 to 1. Each plot represents the first 20% of the total time. (a) curtain flow column, (b) 2.1 mm i.d. conventional column and (c) 4.6 mm i.d. conventional column. The response corresponding to the void time is represented by the dip in the baseline. 45

Figure 4.6 The plots showing the noise contributions for each of the three columns for extracted ion chromatograms of methionine. Note the time axis is expressed as a fraction of the total run time, i.e. normalised time between 0 to 1. Each plot represents the first 20% of the total time. (a) curtain flow column, (b) 2.1 mm i.d. conventional column (bold) and (c) 4.6 mm i.d. conventional column. 46

Figure 4.7 Plot of the baseline noise response for the EIC for m/z 150 (methionine) on the same scale as that for phenylalanine in Figure 4.5. Data illustrated is the same as in Figure 4.6. 46

Figure 5.1 Extracted ion chromatograms of phenylalanine derived from each of the three columns. Trace (a) is the chromatogram obtained on the 2.1 mm i.d. conventional column, trace (b) for the 4.6 mm i.d. conventional column and trace (c) is the CF column. 52

Figure 5.2 Plot of column efficiency (N) versus injection volume, for alkylbenzenes tested on a conventional 2.1 mm i.d. column. 53

Figure 5.3 Illustration of the peak shape for the toluene band as a function of the injection volume. Flow rate 0.44 mL/min, mobile phase 40/60 water/methanol (column 2.1 mm format).....54

Figure 5.4 Calibration curves for phenylalanine obtained on each of the columns: Figure (a) is the calibration curve obtained on the 2.1 mm i.d. conventional column, figure (b) for the 4.6 mm i.d. conventional column and figure (c) is the CF column. 55

Figure 5.5 (a) Extracted ion chromatograms of phenylalanine derived from each of the three columns at the beginning of the sequence. Black trace is the chromatogram obtained on the 2.1 mm i.d. conventional column, red trace is for the 4.6 mm i.d. conventional column and blue trace is CF column. Pre-beginning of the sequence; Post-end of the sequence. 57

Figure 6.1 Illustration of the peak profiles for butylbenzene eluting from the 2.1 mm i.d. format columns. The flow rate on both the conventional and the PSF columns was 2.5 mL/min. 64

Figure 6.2 Extracted ion chromatograms of the amino acid separations undertaken on a 50 × 4.6 mm i.d. conventional column at flow of 1 mL/min; MP composition was 5% methanol in isocratic mode. Flow to the MS detector was 1 mL/min. 65

Figure 6.3 Extracted ion chromatograms of the amino acid separations undertaken on a 50 × 4.6 mm i.d. PSF column at flow of 5 mL/min; MP composition was 5% methanol in isocratic mode. Flow to the MS detector was 1 mL/min. 65

Figure 6.4 Calibrations obtained for tyrosine on conventional and PSF columns. Chromatography conditions are same as in Figures 6.2 and 6.3. 66
Figure 6.5 Extracted ion chromatograms of the amino acid separations undertaken on a 30 mm × 2.1 mm i.d. conventional column at flow of 1 mL/min.; MP composition was 5% methanol in isocratic mode. Flow to the MS detector was 1 mL/min. 68
Figure 6.6 Extracted ion chromatograms of the amino acid separations undertaken on a 30 mm × 2.1 mm i.d. conventional column at flow of 1 mL/min.; MP composition was 5% methanol in isocratic mode. Flow to the MS detector was 1 mL/min. 68
Figure 7.1 HETP curves acquired for the solute butylbenzene on a conventional 50 × 2.1 mm column (squares) and an AFT 50 × 2.1 mm column (hollow circles); both packed with 5 μm Hypersil GOLD particles. The AFT column was operated in parallel segmented flow mode, with 21% of the solvent from eluting from the radial central exit port. Only the radial central flow was processed by the UV detector. 74
Figure 7.2 Total ion chromatograms (10 replicate injections) of 10 amino acids (200 ng/mL). 75
Figure 7.3 Extracted Ion chromatograms (10 replicate injections) of phenylalanine (200 ng/mL). 76
Figure 7.4 Calibration curves based on peak area for each amino acid. 76
Figure 8.1 Extracted Ion Chromatogram of Piroxicam in a single component sample (10 injections). 84
Figure 8.2 Extracted ion chromatogram of piroxicam in single component sample. 85
Figure 8.3 Extracted Ion Chromatogram of 3 Pharmaceuticals: acetaminophen, caffeine and piroxicam (10 injections). 86
Figure 8.4 Extracted ion chromatogram of Piroxicam in a three component sample mix..... 86
Figure 8.5 Six Amino acids zoomed in (one injection)..... 88
Figure 8.6 Extracted Ion Chromatogram of phenylalanine in 6 compounds sample mix -95 points across the peak derived from Figure 8.5. 88
Figure 8.7 Phenylalanine in 20 compounds mix – 25 points across the peak derived from Figure 8.5. 89
Figure 9.1 Total Ion Count for 10 injections of phenylalanine, tryptophan and tyrosine, prepared in 5M Nitric acid. 93
Figure 9.2 Extracted Ion Chromatogram of phenylalanine derived from Figure 9.1. 94
Figure 9.3 Extracted Ion Chromatogram of tyrosine derived from Figure 9.1. 94
Figure 9.4 Extracted Ion Chromatogram of tryptophan derived from Figure 9.1. 94

Figure 9.5 Degradation of three amino acids over 7 minutes. (Note, tyrosine was relatively stable in 5M Nitric acid) 95

List of Tables

Table 2.1 Individual collision energy and tube lens offsets for amino acids. 21
Table 2.2 Individual collision energy and tube lens offsets for pharmaceutical compounds. 21
Table 4.1 Calibration curve for each amino acid analysed on each of the three columns. 41
Table 4.2 Measurement of the reproducibility in the determination of the peak height for each amino acid based on the analysis of the 100 ng/mL standard for each amino acid. Total injections = 12 on each column.....47
Table 4.3 Calculated concentrations of each amino acid in apple juice derived from analyses undertaken on all three columns. The analysis was undertaken on a 1:10 diluted sample of apple juice.....48
Table 5.1 Slope and correlation coefficient for each set of calibration data for each amino acid on the conventional 2.1 and 4.6 mm i.d. columns and the 4.6 mm i.d. CF column.....56
Table 5.2 Injection reproducibility and degree of standard degradation for each amino acid on each of the three columns.....58
Table 6.1 Plate counts measured using the second moment method. Mobile phase 60/40 water/methanol, flow rates 5 mL/min on the 4.6 mm i.d. columns, and 2.5 mL/min on the 2.1 mm i.d. columns, UV detection.....64
Table 7.1 Injection to injection precision (RSD) of each amino acid at each level of standard concentration based on peak area measurements. Number of replicates for each concentration = 10. Calibration curve linear correlation (r^2) values are included. ..77
Table 7.2 Injection to injection precision (RSD) of each amino acid at each level of standard concentration using peak height measurements. Number of replicates for each concentration = 10. Calibration curve linear correlation (r2) values are included...78
Table 7.3 Concentration (ng/mL) and (RSD) values of each amino acid for apple and beetroot samples using area responses.....78
Table 8.1 Piroxicam data as a single component and in a 3 component mixture. 84
Table 8.2 RSD values for 6 amino acids in 6 and 20 component mixes.....87
Table 8.3 RSD of respective amino acids in different eluting bands. See Figure 8.5 for chromatogram. 87

Chapter 1.

Introduction

1.1 Mass spectrometry

Since its beginnings, about 100 years ago, mass spectrometry (MS) has become an important research tool. Mass spectrometry is used to measure the molecular weights of molecules in the gaseous ionic state. This has applications in chemistry, physics and biology. With its wide application, mass spectrometry has been developing in various avenues, forcing changes to supporting instrumentation [1].

1.1.1 History

The history of MS goes back to early 1900 with J.J. Thomson at Cambridge University's Cavendish Laboratories whose studies on electrical discharges in gases led to the discovery of the electron in 1897 [2]. In the first decade of the 20th century, Thomson constructed the first mass spectrometer, for which he was awarded the Nobel Prize in 1906 "*in recognition of the great merits of his theoretical and experimental investigations on the conduction of electricity by gases* [3]."

In order to study analytes in mass spectrometry, they must be in the gaseous state and then converted to ions. Mass spectrometry has become one of the most sensitive and widely used analytical tools.

The major obstacle in determining the molecular weight of a compound by MS has been maintaining molecules in an intact state and avoiding their fragmentation to smaller molecular weight compounds during the ionisation process. In the early days, ionisation methods like electron impact ionisation and chemical ionisation were developed, but they could not overcome the propensity of the molecule to undergo fragmentation. This problem became increasingly important in the mid-1980s when the determination of the molecular mass of proteins became necessary [4]. Properties of proteins, being thermally labile, polar and non-volatile, made them challenging to ionize with conventional techniques which led to their structural decomposition. The development of Electrospray Ionisation (ESI) in 1989 by Fenn helped overcome these problems. Fenn was able to ionize proteins without fragmentation by multiple charging, which further resulted in lower mass to charge (*m/z*) ratios and thus yielding acceptable m/z ranges suited to today's mass analysers [5]. Soon, ESI-MS became a standard method for the determination of the mass of biomolecules. Today, ESI-MS is widely used for characterisation of proteins, their three-dimensional structure, amino acid sequencing, etc [6,7]. In 2002, Fenn won a one-quarter share of the Nobel prize as an inventor of ESI-MS "*A few years ago the idea of making proteins or polymers "fly" by electrospray ionisation (ESI) seemed as improbable as a flying elephant, but today it is a standard part of modern mass spectrometers*" as stated by the Professor Fenn in his Nobel lecture [8].

Apart from biology, ESI-MS had a big impact towards detailed understanding of inorganic chemistry, organic, and metal-organic complexes. Further improvement came along when ESI-MS was coupled with high performance liquid chromatography (HPLC), creating a very powerful technique which combined separation modes and structural elucidation, covering the analysis of small molecules as well as large molecules in complex mixtures.

1.1.2 Components of ESI-MS

The standard set up of an ESI-mass spectrometer comprises three components: an ion source, a mass analyser and a detector. The ion source is the front part of the instrument kept within the ion chamber where molecular ions are produced. Molecular ions are then transferred to the mass analyser and transported to the detector the mass spectrum. Figure 1.1 is a flow diagram of the processes involved in the MS detection.

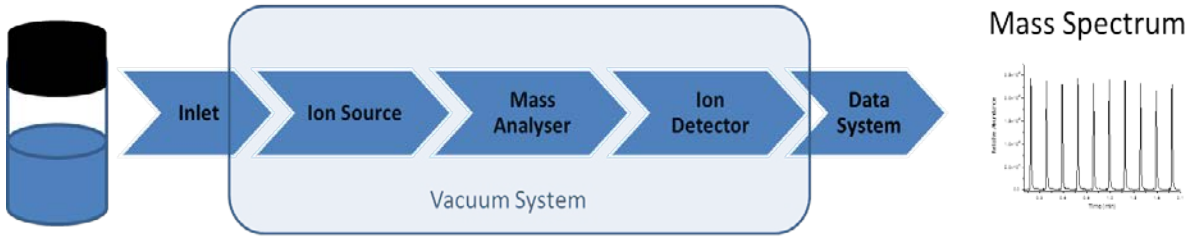

Figure 1.1 Flow diagram of the processes involved in the MS detection.

1.1.2.1 Ion Source

The first ion source suitable for LC-MS analysis was invented and designed by Fenn in the mid-1980s [9-11]. This ion source was later optimized by numerous scientists in order it improve robustness [12-16]. The primary objectives of the ion source are transformation of the analyte from the liquid phase to the gas phase and subsequent ion formation. This process is done in two stages. Firstly the liquid sample is dispersed into highly charged droplets. In the second stage, these droplets are decomposed due to desolvation producing smaller and more highly charged offspring droplets. This process continues until charged molecular ions are formed [12]. Generally, the sample is introduced as a dilute solution to the ion source *via* a heated metal capillary (0.2 mm i.d. and 60 mm in length, instrument dependent) within the electrospray probe, at typical flow rates ranging from 100 to 300 μL/min (heavily dependent of the instrument and the column used). A

voltage (1000 - 6000 V) is applied to the tip of the metal capillary relative to the sampling cone. The relative distance between the two is typically 1 to 3 cm (again very dependent on which instrument and the flow rate). The electrical field enables dispersion of the solution into a fine mist of highly charged electrospray droplets. This process is enhanced using a sheath gas that is pumped together with solvent through the capillary to ensure efficient nebulization. On the outside of the capillary, a heated auxiliary gas is used to promote complete desolvation, as well as keeping the spray concentrated towards the orifice of the sample cone, see Figure 1.2. These two gases enable evaporation of the solvent by complete desolvation and nebulization, and the charged molecules enter into the mass analyser.

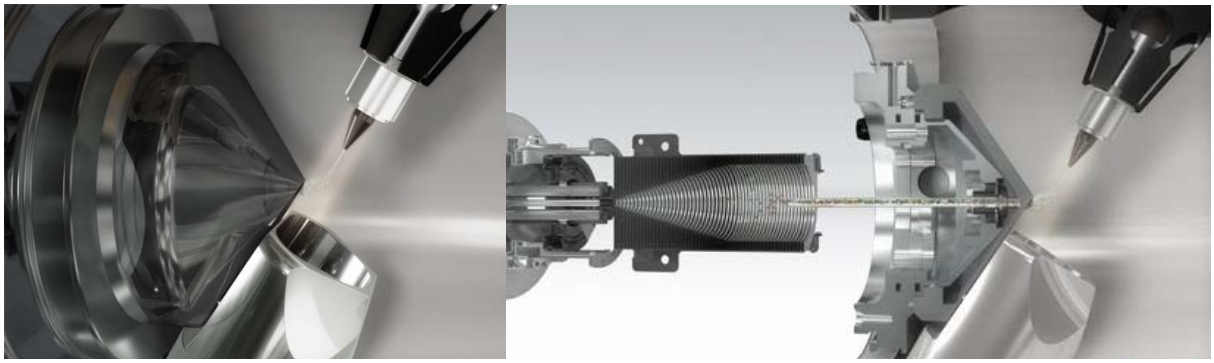

Figure 1.2 Ion source with capillary needle spraying towards the orifice of the sample cone [17] .

Capillary and gases can be heated up to 300°C. Apart from desolvation, drying gas and heat from the capillary assist with the robustness and reduction of cluster formation [16]. Charged analytes, released from the charged droplets by desolvation are passed from the ion chamber without fragmentation (depending of the instrument setting) at atmospheric pressure into the entrance of the mass analyser, which is kept at very high vacuum. This typical set up of the spray is modified to suit different needs so a number of different electrospray designs are available, e.g. ultrasonic nebulizer electrospray, electronic spray, nano-electrospray, etc.

Nano-electrospray was introduced by Will and Mann [18,19] and is a very widely used technique. The advantages of the nano-electrospray technique are very low sample concentration (nanomole/mL), small sample volume (1-2 microliters), low flowrates (20-50 nL/min), and low voltages (0.5-1.1 kV). Nano-electrospray voltage is normally applied via an electrically conducting coating enabling the formation of 200 nm charged droplets (instead of 1-2 μm as is the case for traditional ESI). This technique was found to be useful in the analysis of peptides and proteins [19-21].

1.1.2.2 Mass Analyser

The mass analyser or mass filter is positioned at the centre of the mass spectrometer. The mass analyser utilises magnetic and electric fields to manipulate the trajectories of charged ions in a mass depended manner. It sits behind the ion source and the focussing ion optics in the high vacuum area and its main objective is to separate molecules based according to their mass to charge ratio (*m/z*) before charged ions are passed to the detector. There are many different mass analysers available [22]; five of the main designs are quadrupole, time of flight, ion-trap, orbitrap and magnetic sector mass analysers. Each has their own strengths and weaknesses and selection of the suitable mass analyser is dependent on the many factors including resolution, nature of the analyte, mass range, detection limit, scan acquisition time, etc. A typical triple stage mass spectrometer is presented in Figure 1.3.

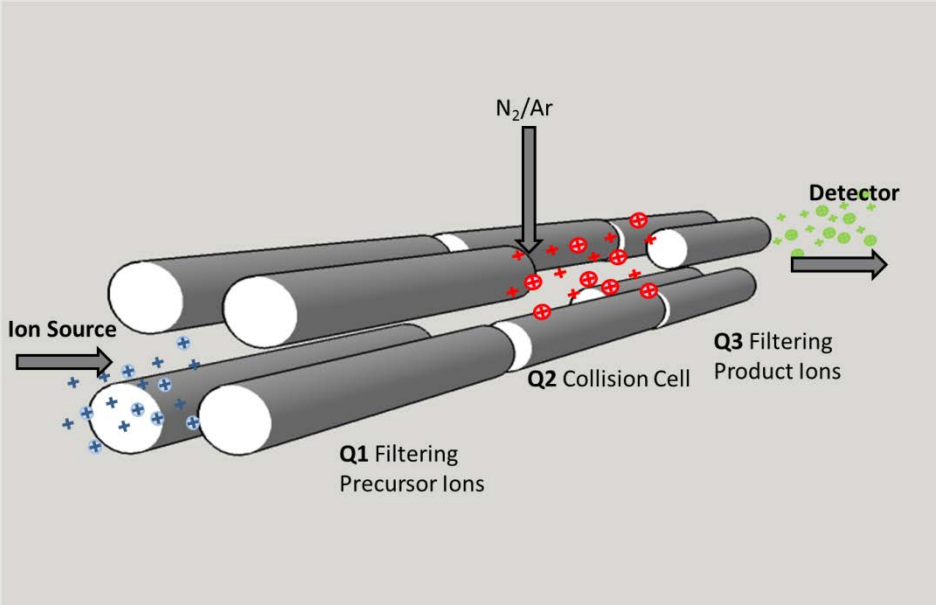

Figure 1.3 Ion path of a triple stage mass spectrometer, Q1 and Q3 are mass-resolving quadrupoles, and Q2 is functioning as a collision cell.

In order to obtain increased structural information, specificity and/or sensitivity, it is common for instruments to have two or more mass analysers in tandem, e.g. MS/MS, MS/MS-Trap, MS-Orbitrap, MS/MS/MS, etc. With multistage mass analysers, there may be two mass analysers separated by a collision cell in which ion fragmentation occurs. This collision cell is filled with an inert gas (N_2, Ar, He) and the charged precursor molecular ions are bombarded by the collision gas molecules causing them to fragment into product ions.

1.1.2.3 Detector

The easiest and simplest way to detect charged particles is to use a Faraday cup or ion-to-photon detector [23]. A key driving force for advancements in analytical techniques is to achieve lower limits of detection. Consequently the number of molecules leaving the mass analyser is increasingly smaller and some form of amplification is required in order to obtain detection. Therefore, detectors in mass spectrometry rely on the use of an electron multiplier to increase sensitivity. Typically, the electron multiplier multiplies incident charges [24-27]. The fundamental principle is ions strike a conversion diode (made out of a metal or semiconductor plate), which is held at high voltage. Consequently, secondary electrons (SE) are emitted, accelerated and focused onto the second dynode (at positive potential) which emits several electrons which strike a third dynode etc. A typical discrete-dynode electron multiplier has between 12 and 24 dynodes. This set up of a sequence of dynodes leads to an increased number of electrons emitted from each dynode, subsequently creating a shower of electrons after the last dynode. The operating gain is between 10^4 and 10^8, depending on the instrument parameters and design. This current output is converted to a voltage signal, and translated into signal intensity by means of an analog-to-digital converter.

There are several designs of multipliers: discrete dynode electron multipliers, channel electron multipliers, microchannel or multichannel plates (MCPs), etc. Suitable detectors are selected on the basis of several factors: sensitivity, speed, gain, dynamic range, etc.

1.1.3 Ionisation techniques

The basic principle of the mass spectrometer involves the use of magnetic and electric fields to manipulate charged particles (ions) in a vacuum. In order to do that, analytes have to be ionized and in gas phase. This is easily achieved when sample is in a gaseous phase or highly volatile, but when the sample is in a liquid phase it must undergo desorption prior to transformation from neutral to the charged state (actual ionisation). These two processes (desorption and ionisation) are usually separate, however, the term “ionisation” typically refers to both of these processes.

The first ionisation method was electron ionisation (EI), and due to its limitations was advanced into chemical ionisation (CI) introduced in 1966 [28] and then plasma desorption (PD) in 1974 [29]. The advantage of CI and PD is the formation of protonated (or deprotonated) ions compared to the less stable radical ion formation that occurs during EI-MS. Neither EI nor CI were, however, capable of efficiently ionizing polar and thermally labile biological compounds, and this was a factor that lead to the development of PD, which was the first type of the “soft ionisation” processes suitable for the ionisation of biomolecules with molecular weights (MW) up to 100,000. Since the ionisation of large and non-volatile molecules was a major driving force for the

development of ionisation techniques, the need for more structural information and the need for analysis in aqueous solutions were significant factors in the drive to develop better ionisation processes. These subsequently lead to the development of electrospray ionisation (ESI) [10,11,18,30] and matrix assisted laser desorption ionisation (MALDI) [31-33], both of which have revolutionized the analysis of biological substances. In the scope of this thesis, ESI will be discussed in detail.

1.1.3.1 Electrospray Ionisation

Electrospray ionisation dates from the early 1960s and appears to be credited to the works of Dole and co-workers [34]. The ESI process involves spraying a solution of the sample through a highly charged capillary needle at atmospheric pressure [35] (Figure 1.4). The spraying process is aided by the use of a nebulizing gas. Charged droplets are produced that contain positive or negative ions, which are solvated with solvent molecules. A heated gas is applied to the charged droplets to enable solvent evaporation. The desolvation process decreases the droplet size, leading to the columbic repulsion between the charges present in the droplet and further the droplet fission leading to the formation of individual gas phase analyte ions (that critical point is known as the Rayleigh limit), that are guided through ion optics into the mass analyzer. ESI can produce singly or multiply charged ions.

The number of charges retained by a particular analyte depends on several factors, such as the size, chemical composition, and higher order structure of the analyte molecule, the solvent composition, the presence of co-solutes, and the instrument parameters. For small molecules (< 2000 Da) ESI typically generates singly, doubly, or triply charged ions, while for large molecules (> 2000 Da) ESI can produce a series of multiply charged ions. The production of multiply charged analytes in ESI-MS was a contentious issue in the 1990s [34-37], but later works of Kelly and co-workers demonstrated that in positive ion mode, ESI produced protonated ions (positively charged) and in negative ion mode produced deprotonated analyte (negatively charged) [37].

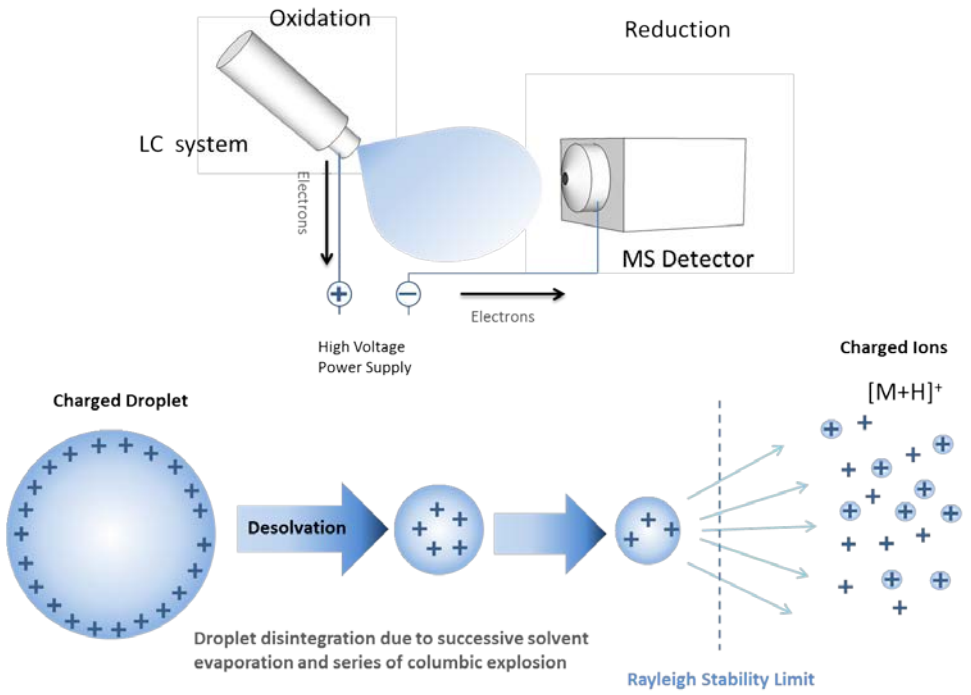

Figure 1.4 Schematic representation of the electrospray ionisation process.

During the process of electrospray ionisation, analytes are transformed from the liquid phase to the gas phase. This transformation involves three major stages: production of charged droplets, disintegration of charged droplets and ion formation from charged droplets.

a) Production of charged droplets.

Initially, analyte is presented to the ion source as a solution which is injected through a highly charged capillary, producing charged droplets. This process involves an electrochemical reaction of the solvent forcing electrons towards, or away from, the metal capillary, depending on its polarity [36]. The ion source can be considered as a form of electrolytic cell [37] where oxidation of the solvent will lead to the positive ion mode and reduction of the solvent will produce the negative ion mode [37-39]. Polar solvents (water, methanol, and acetonitrile) easily undergo electrochemical reactions and for that reason are frequently used in ESI-MS [40].

Prior to the electrospray, formation of a "Taylor cone" occurs due to repulsion of ions in the jet from the capillary. At the Rayleigh stability limit, a stream of small charged droplets is formed in a process called 'electrospray". The formation of "Taylor cone" is illustrated in Figure 1.5 [18,35,41-43].

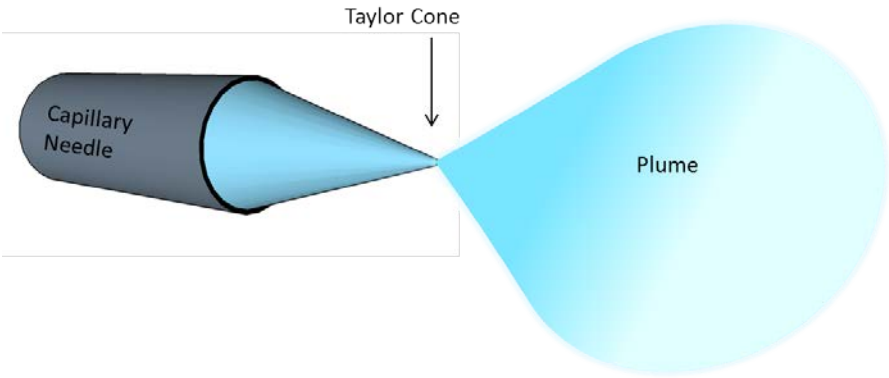

Figure 1.5 Formation of Taylor cone at the end of capillary needle.

This phenomena was first observed by Sir Geoffrey Taylor [42]. The Taylor cone forms when a voltage is applied to a liquid in spraying nozzle, which causes the liquid to form an elliptic shape. A spray is emitted from the Taylor cone leading to the formation of much smaller and highly charged droplets. While in flight, solvent evaporates from these charged droplets leaving neutral particles causing an increase in the field density at the surface of the droplet leading to a subsequent formation of the next Taylor cone. This process occurs every in microseconds, creating smaller and smaller charged particles until Coulomb fission [44-46] occurs and all the solvent is evaporated leaving only individual charged ions.

In positive ion mode a positively charged aerosol is formed, while in negative ion mode, a negatively charged aerosol is formed [40].

At this stage, an initial charged droplet produces much smaller offspring droplets with a much higher charge-to-mass ratio. [47]. The lifetime of the charged droplets is dependent on many parameters (temperature, solvents, gasses, spray voltage) and typically is a few milliseconds [48] and these are the factors that influence charging of the analyte.

b) Formation of Gas-Phase Analyte Ions from the Charged Droplets

The final step of the mechanism, ion formation, is still under debate [12,49,50]. However, several mechanisms were proposed and the two main ones are the Charged Residue Model [51,52] and the Ion Evaporation Model [53].

The charged residue model was firstly hypothesized by Dole and is based on continuous solvent evaporation and Coulomb fission, until charged droplets reach 1 nm in radius and contain only one analyte molecule then charges are transferred from the droplet onto the analyte [34]. The principle of the Ion Evaporation Model is emission of the solvated ions from the charged droplet [53,54]. Based on this theory, charged ions can be formed before reaching the size of a single

analyte droplet. This theory was proposed by Iribarne and Thomson [53,54] and it was experimentally supported [55,56]. An extended theory of ion formation was proposed by Fenn [52] where he proposed that the analyte remains neutral within a charged droplet and the charge is on the surface of the droplet. This process is extensively described in references [30,43].

1.1.3.2 The ESI Mass Spectrum

The mass spectrum is the mass distribution of all detected ions in a sample. The ions produced by ESI generally have multiple charges, and with the set of appropriate parameters neutral molecules should be protonated (in positive mode) or deprotonated (in negative ion mode) into molecular ions. The mass spectrum is typically represented where the y - axis represents relative abundance of ions and the x - axis represents the mass to charge ratio (*m/z*) of the analyte (Figure 1.6).

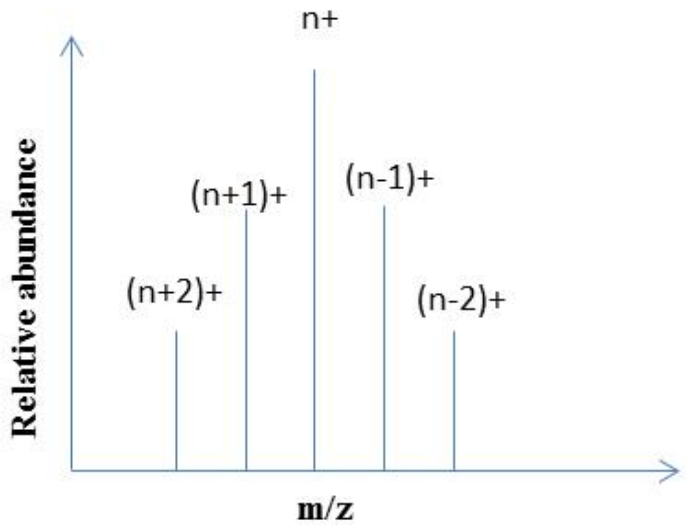

Figure 1.6 A typical ESI-mass spectrum acquired in positive ion mode.

The peak with the highest intensity (the most abundant peak) is called the "base peak" and the unit for *m/z* is Th (in honour of J.J. Thomson). The principles required for molecular mass determination of the given analyte has been extensively discussed in references [57-59].

1.2 Separations involving Chromatography and Mass Spectrometry

Chromatography is a technique for the physical separation of chemical components in mixtures. Separation is achieved according to the distribution of sample molecules between two phases, in

liquid chromatography these two phases are the mobile (liquid) phase and the stationary (solid) phase. Separation of analytes occurs due to a different intermolecular forces between the analytes, the mobile and stationary phases depending on the characteristics of the different analytes. The first use of chromatography dates from the early 1900s [60] when the Russian botanist Mikhail Semyonovich Tsvet separated plant pigments using this technique. He subsequently coined the name 'adsorption chromatography' based on the separation of coloured dye pigments. Another major step in the development of chromatography was in the 1940s with the work of Lederer, Synge and Martin [61,62] whos work pioneered the development of reversed phase chromatography – the precursor for today's modern liquid chromatography techniques.

Due to the huge variety and nature of complex mixtures, a wide range of chromatographic techniques have developed that are tailored for the separation of the species being analysed. Of importance in this thesis, however, is the technique referred to as liquid chromatography (LC) specifically High Performance Liquid Chromatography (HPLC), or in its latest guise, Ultra-High Performance Liquid Chromatography (UHPLC). Applications for each of these techniques will be discussed in more detail in later Chapters.

1.2.1 The evolution of HPLC and column technology

HPLC is a powerful analytical technique that enables the separation of different analytes from within complex mixtures that can subsequently be detected, their amounts quantified, and potentially their structures identified. An important component in this development of HPLC has been column technology, because advances in column technology have enabled ever more complex samples to be analysed, more efficiently, faster, and with lower limits in detection [63-66]. Coupling HPLC with mass spectrometry came as a natural progression in the development of more sophisticated and more powerful analytical tools [67-70].

While HPLC-MS may be considered as a powerful analytical technique, a major factor that limits its performance is sample through-put. A factor contributing to lower through-put is the drive towards the use smaller particle packings in columns used in liquid chromatography so as to improve separation, especially sensitivity, since smaller particles generate narrower sample distributions subsequently increasing the peak height. However, as the particle size decreases then the operational linear velocity must be increased to maintain optimal chromatographic performance. However, as the linear velocity increases so too does the volume of eluent entering the mass spectrometer. To decrease the volumes of eluent, the column internal diameter is typically decreased to 2.1 mm and sometimes 1 mm i.d., rather than the analytical format (4.6 mm i.d.). This decreases the solvent load to the MS by almost 5-fold for the 2.1 mm i.d. column, yet the same

linear velocity through the column can be maintained. Thus the separation can be undertaken in a timely fashion, with no adverse effect to the MS. This appeared to be a suitable solution to the problem of solvent removal prior to the mass spectrometer while at the same time being able to utilise the latest developments in particle technology. Consequently there is a reduction, or rather a compromise in the performance of the chromatographic column, primarily as a result of wall effects [71] and the management of extra-column dead volume contributions [72].

It is well known that the wall effect is an important contributor to band broadening in the chromatographic migration process, largely as a result of increased degree of packing heterogeneity in the wall region. The ratio of the wall area to that of the overall column cross sectional surface area on a 4.6 mm i.d. column is less than half that for the 2.1 mm i.d. column. Hence, the wall effect is a more serious contributor to the loss of efficiency observed on 2.1 mm i.d. columns. A recent study by Gritti and Guiochon [72] showed exactly this; the loss in optimal column performance in a 2.1 mm i.d. column format compared to the 4.6 mm i.d. column format (based on the reduced plate height, *h*) for superficially porous particles, with diameters between 1.7 to 2.7 µm, was between 13 and 42% depending on particle size, column length and manufacturer. This loss was attributed largely to the long range eddy dispersion term, a factor dependent in part on the homogeneity of the radial packing density. Although this length scale of the eddy dispersion term is generally small with respect to the radius of the column, it is between 10 to 15% of the radius on narrow diameter columns (2.1 mm), while around 2% on 4.6 mm i.d. columns [72]. Hence, a reduction in the column radius results in a relative increase in the contribution made by the wall effect [72]. Another factor that significantly affects the performance of the 2.1 mm i.d. format is related to the extra-column dead volume contributions, which rapidly decreases the efficiency as the peak volume decreases. Although this is not an insurmountable limitation, it nevertheless requires substantial care to minimize its effects, and it is often overlooked, and places practical limitations to the employment of columns with internal diameters less than 2.1 mm, unless equipment specifically designed for the task is employed – i.e. nano-flow systems.

The use of narrower diameter columns may also limit sensitivity, since one aspect of sensitivity in mass spectrometry is related to the mass load on the column. As the column internal diameter decreases so too does the volume and mass load – effectively in proportion to the square on the column radius. Hence, there are potential limitations to regulatory compliance for some standard methods of analysis, which may demand the use of injection volumes beyond the capacity of the narrower bore columns.

For the most part, operators of mass spectrometers that require some form of separation ignore the loss in the separation performance they observe when using narrow bore columns

because of the very big advantage associated with the reduced eluent load that is presented to the MS detector. This is especially so when 4.6 mm i.d. columns are employed since, in order to satisfy the volumetric solvent load to the MS, the 4.6 mm i.d. column is often operated at flow rates well below the optimum for these columns, especially as the particle size decreases, another reason why MS users often employ the 2.1 mm column format.

1.2.2 Current Applications of LC-MS

LC-MS is an analytical technique providing sensitive, specific, reliable and robust qualitative and/or quantitative analysis. This technique is becoming increasingly important in clinical laboratories and in the analysis of complex biological samples [73,74]. Some applications involve analyses relating to inherited disorders in the metabolism of amino acids [75-77], neonates with suspected errors in metabolism [78], identification and quantification of haemoglobin variants [79], diabetic monitoring [80], drug monitoring [81], and food and agricultural analysis [82,83]. Recent modification to the mass spectrometer and innovation of nano-spray further broadened the potential applications towards proteomic and metabolomics analyses.

1.2.3 Leading trends and future of separations and mass spectrometry

There is substantial evidence that suggests HPLC-MS is the quintessential analytical technique for quantification and sample identification employed in bioanalysis. Despite MS/MS detection being highly specific and sensitive, the need for a separation step is crucial in order to obtain higher quality data - ion-suppression (or ion enhancement) induced by the presence of interfering co-eluting compounds within complex mixtures [84-87] can be problematic. In order to overcome these difficulties, great emphasis should be placed on sample separation in order to overcome matrix effects as well as maximize mass spectrometry separation power and monitor compounds simultaneously. Furthermore, chromatographic separation is imperative when dealing with compounds with the same molecular mass and/or very similar fragmentation patterns, since these are effectively impossible to accurately differentiate without chromatographic separation [88,89]. There will be continued growth in this area of analytical sciences because of the substantial information obtained, and as such, the mass spectrometer is more often becoming method of choice [66].

However, there is still need for new strategies that improve the interface between HPLC and MS, and in particular strategies that address the issue of maintaining column efficiency as the column internal diameter decreases, and at the same time, offer a means of reducing the solvent load to the MS.

1.3 Active Flow Technology

Recently, a new suite of column technologies has been developed, which is referred to as Active Flow Technology (AFT). Two prior PhD theses [90,91] from this research group have discussed this technology in considerable detail and the technology is described only briefly herein. These columns provide the best features available through large and smaller internal diameter columns. Two of the important column designs in the AFT range are the Curtain Flow (CF) and the Parallel Segmented Flow (PSF) columns. The design of these columns is such that the wall effect is effectively eliminated, with the result being more efficient solute migration through the bed of the chromatography column, free from the deleterious effects of inhomogeneous packing near the wall. Furthermore, the amount of solvent that is delivered to the MS using AFT columns is reduced, and in fact, tunable by the analyst to obtain optimal performance [92]. An AFT column in a 4.6 mm i.d. format for example can be tuned to deliver the same volume of solvent to the MS as a standard 2.1 mm i.d. format column when operated at the same linear velocities. Likewise the AFT column could also be tuned to deliver the same volume load to the MS as a 3.0 mm i.d. column. Perhaps most importantly for an MS user, a 2.1 mm i.d. column can be tuned as a virtual 1 mm i.d. column, but with far greater separation efficiency than a physical 1 mm i.d. column [93].

1.3.1 Curtain Flow Chromatography

In Curtain Flow Chromatography (CF) the sample is introduced into the radial central region of the column inlet surrounded by a curtain flow of mobile phase. This curtain flow inhibits the migration of solute to the wall during passage along the column. In essence a ‘wall-less’ column is established that obeys in principle the infinite diameter column concept [94]. The sample introduction process in the curtain flow column is distinct from the manner in which sample is introduced into a standard column, where the sample is distributed by a frit across the entire radial cross section of the column inlet, and homogeneity of the sample distribution is assumed, albeit, it is likely not to be the case [95].

The design of the CF column was detailed by Camenzuli, et al. [96], and an illustration of the column design is presented in Figure 1.7. The details of the operation of CF columns will be discussed here, especially with respect to how it serves MS applications. The introduction of the sample into the central section of the bed at the column inlet is achieved using a specially designed inlet fitting [92,96], which has multiple entry ports. The flow of mobile phase from the injector feeds into a port aligned with the radial center of the column inlet. Mobile phase that by-passes the

injector feeds into port(s) that are aligned with the outer rim of the column. No sample is in this outer portion of the mobile phase. The volumetric flow rate ratio between these two streams is around 40% feed into the radial central port and 60% feed into the peripheral port for the columns utilized in the current study, although the operator can vary this ratio by +/- 5% without unduly affecting efficiency. These ratios may vary depending on the stationary phase material, i.e., particles compared to monoliths. A frit is located inside the inlet fitting, which is made in three parts: a central portion of the frit is porous, and this is aligned with the central inlet port, an outer portion of the frit is also porous, and this is aligned with the ports on the outer rim of the column inner wall. These two porous portions of the frit are separated by an impermeable barrier. There can be no cross-flow of sample from the central section of frit into the outer wall portion of frit. Hence the sample enters the bed in the central region of the column with the outer region of the column having mobile phase only passed through it. The schematics of the end fitting with annular rings are presented in Figure 1.9. The sample consequently moves down the column which is operated in an infinite diameter mode or as a wall-less column. Sample exits the column through end fittings that are the same as the inlet fitting, but with different tuning functions applied, specific to the application [92,96,97].

Figure 1.7 Curtain flow column with AFT fittings at the column inlet and outlet demonstrating the multi-port radial flow splitting process.

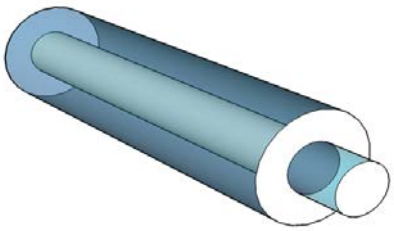

Figure 1.8 Concept of virtual "wall less" column. The inner cylinder represents the wall less MP flow.

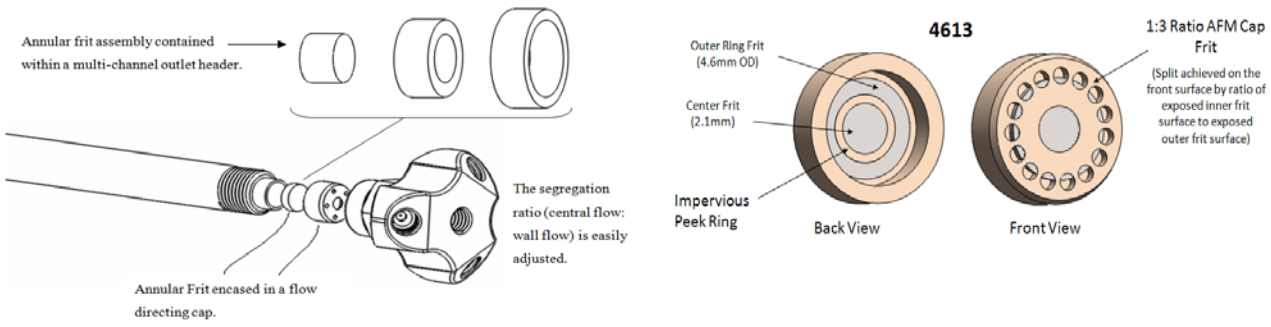

Figure 1.9 Active Flow Technology end fitting with multiple ports. As detailed in reference [90,91].

For example, the volume ratio of flow that exits the column through the radial central exit port can be tuned to suit the detection requirements [92]. If 21% of the flow exits the column from the central exit port of a 4.6 mm i.d. column then the same volume load is presented to the detector as if a 2.1 mm i.d. conventional column was employed. This concept is discussed in detail in Chapter 5 where this variable is referred to as the 'virtual' column [92]. Using these specially designed fittings at the inlet and the outlet ensures that a true wall-less column is established and its design is presented in Figure 1.9 and concept of virtual column is presented in Figure 1.8. Operation of these wall-less columns in chromatographic separations has shown that the sensitivity in UV detection is increased by almost 3-fold [98]. This phenomenon is a major advantage of AFT columns where we have practically on column splitting but this process is not the same as post column flow stream splitting. The principle of AFT on-column splitting is radial and the most efficient portion of the column is used for the separation, and then this flows to the detector. Whereas in post column flow stream spitting, the entire peak is sampled, including the dilute diffuse tailing section of the peak. The diagram of simulated flow splitting between AFT column and post columns splitting is presented in Figure 1.10. The benefits of CF to MS applications were explored in this project since MS detectors with electrospray ionisation, once coupled to an LC separation are also subsequently sensitive to the concentration response.

1.3.2 Parallel Segmented Flow Chromatography

PSF columns are very similar to CF columns but in PSF mode, the special fitting is mounted only on the column outlet (Figure 1.11). The column inlet is unchanged leaving the sample injection process identical to the conventional column. As a consequence of this design, the central radial flow stream through the column bed is separated from the wall region flow inside the column and sectioned within the frit delivering only the peak apex (without the wall region) to the detector. The

relative portion of flow from these two regions can be varied to almost any desired ratio through pressure management in order to optimise various functional aspects of the column technology. The process of pressure management and subsequent adjustment of the segmentation ratio at the column outlet has been described in detail [97,99-101]. The design of a PSF column is presented in Figure 1.11.

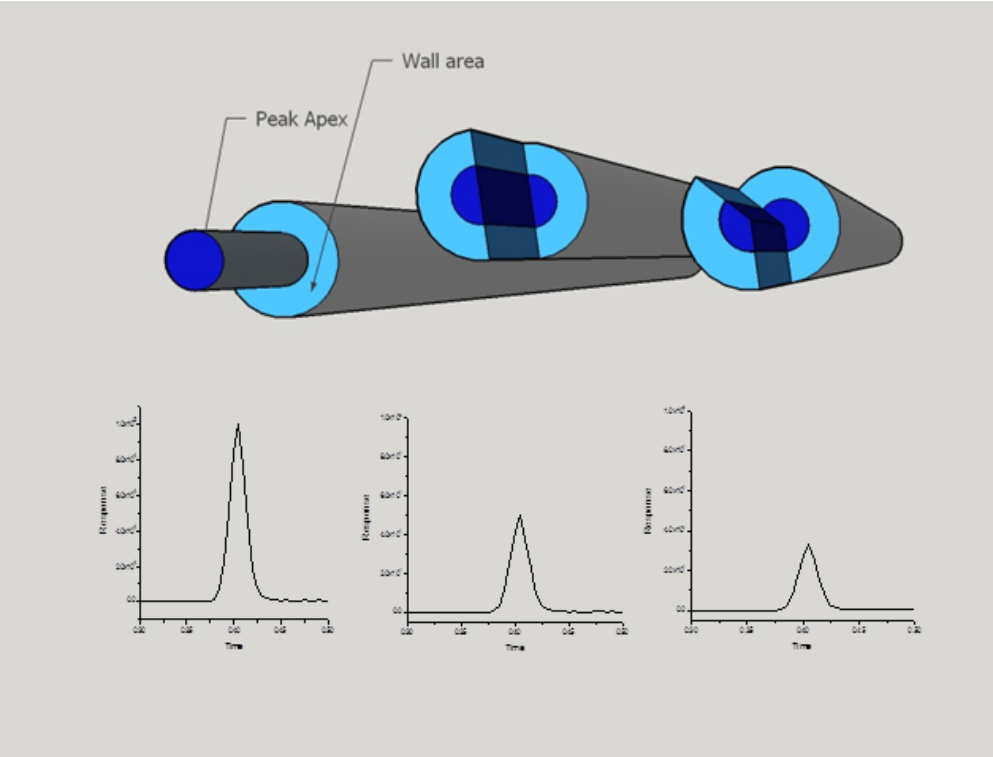

Figure 1.10 Illustration of flow stream splitting (left – AFT radial flow split; centre – 50% post column split on a conventional column; right – 30% post column split on a conventional column, "typical" chromatographic responses.

Figure 1.11 Parallel Segmented Flow Column with multi-port AFT fitting on the column outlet.

1.4 Research problems, project aim and objectives

The principle objective of this research thesis is improving the interface between High Performance Liquid Chromatography and Mass Spectrometry detection (MS). There are two main issues with this interface. One issue lies in the MS being a flow restricting detector, limiting high speed analysis to the capability of the MS to dispose of the solvent and present the sample to a high vacuum source [102]. The second limitation lies in maximizing the efficiency of the HPLC column, so that scaling down the column diameter does not necessarily equate to a sacrifice in separation performance, especially when operated at very high flow velocities. Currently, the industrial standard for processing solvent is around 1 to 1.5 mL/min of volumetric flow from the HPLC column, the lower limit being needed for highly aqueous mobile phases, and decreasing further if the sample components are unable to tolerate high temperature ESI protocols. While these volumetric flow rates are high in the context of narrow bore columns in HPLC, it is hypothesized that current HPLC (or UHPLC) columns in narrow bore format perform with efficiency levels that are well below the desired operational ideals of these columns, and as such, the separation component is sacrificed in the pursuit of assay through-put.

The objectives of this thesis are therefore to:

(1) Demonstrate that Active Flow technology (AFT) columns offer higher separation efficiency than UHPLC columns in conventional formats, and that these AFT columns operate at lower back pressure.

(2) Demonstrate that AFT columns with MS detection yield increased sensitivity compared to columns in conventional format.

(3) Demonstrate that improvements in both separation speed and assay through-put yields greatly improved assay robustness.

(4) Develop new protocols for assays that involve HPLC and MS detection which approach the speed of direct injection MS protocols.

(5) Develop new technology that enables effective reaction monitoring suitable for the optimization of organic synthesis.

Chapter 2.

General Experimental

2.1 Introduction

This chapter outlines the general experimental for the majority of experiments done in this project. The general instrumental requirements and their operations, supply of chemicals and reagents are noted in this chapter. Specific variations are noted in the subsequent Chapters.

2.1.1 Chemical and reagents

All mobile phases were prepared from HPLC-grade solvents purchased from Merck Australia Pty Ltd. Amino acids were purchased from Sigma Aldrich (Castle Hill, New South Wales, Australia). Milli-Q water (18.2 MΩ cm) was prepared in-house and filtered through a 0.2 μm filter. Formic acid was purchased from Chem-Supply Pty Ltd, Gillman, South Australia.

For assays involving amino acids (Chapters 4 to 9) the amino acids were weighed and used to prepare a mixed stock solution at the concentration of 100 μg/mL in HPLC grade methanol. The stock solution was diluted in water to prepare a working range of solutions for calibration, typically from 25 ng/mL to 750 ng/mL.

2.1.2 Chromatographic Conditions

All chromatography columns were either purchased or donated by ThermoFisher Scientific (Runcorn, Cheshire, United Kingdom). All columns were packed with Hypersil GOLD stationary phases with either 5 or 1.9 μm particles as noted in the relevant text. The columns used throughout this study were either 30 or 50 mm in length and either 2.1 or 4.6 mm in internal diameter. These varieties are noted in the specific text where applicable. Some of the columns used in this work were conventional columns, some were parallel segmented flow columns and some were curtain flow columns, and these were noted in the relevant text.

2.1.3 Mass Spectrometry parameters

Mass spectrometry detection on the TSQ Vantage was achieved using electrospray ionisation in positive ion mode using single reaction monitoring (SRM). The following MS parameters were used for optimised detection: vaporiser temperature was set at 500°C, capillary temperature was set to 350°C; sheath gas was set at the rate of 60 units, auxiliary gas flow at 40 and sweep gas flow at 5 units. Spray voltage was maintained at 3.5 kV.

Collision energy and tube lens offsets were individually optimized for each compound and presented in Tables 2.1 and 2.2 together with precursor and product ions. Data processing was performed using LC Quan software (Thermo Fisher Scientific, San Jose, USA). Volume flow to the detector remained constant for all analyses (1 mL/min), unless otherwise stated.

Analyte	**Precursor ion *m/z***	**Product Ion *m/z***	**SRM Collision Energy (eV)**	**Scan Time (s)**	**S-Lens (V)**
Valine	118.113	71.104	10	0.025	42
Threonine	120.093	102.312	17	0.025	51
Isoleucine-Leucine	132.15	85.2	10	0.025	36
Lysine	147.15	83.2	15	0.25	50
Methionine	150.07	54.953	16	0.025	47
Histidine	156.083	109.382	14	0.025	48
Phenylalanine	166.098	119.495	13	0.025	49
Arginine	175.109	69.065	21	0.025	56
Tryptophan	205.08	188	9	0.025	48

Table 2.1 Individual collision energy and tube lens offsets for amino acids.

Analyte	**Precursor ion *m/z***	**Product Ion *m/z***	**SRM Collision Energy (eV)**	**Scan Time (s)**	**S-Lens (V)**
Caffeine	195.2	137.5	19	0.005	73
Piroxycam	332.0	94.1	19	0.005	98
Acetaminophen	152.0	109.3	16	0.005	70

Table 2.2 Individual collision energy and tube lens offsets for pharmaceutical compounds.

2.1.4 Instrumentation UPLC-MS/MS

Chromatographic separations were carried out using a Thermo UHPLC system coupled with a TSQ Vantage mass spectrometer equipped with HESI II source (Thermo Scientific, San Jose, USA). The UHPLC component was an Ultimate 3000 equipped with a quaternary pump, UV detector, and auto injector with an in-line degassing unit. This system was operated as supplied from the manufacturer.

2.1.4.1 Isocratic Method – Mass Spectrometry.

In the isocratic elution of amino acids, the mobile phase composition was 95/5 v/v water/methanol (+ 0.1% formic acid). In the isocratic elution of pharmaceutical compounds, the mobile phase composition was 60/40 v/v water/methanol (+ 0.1% formic acid).

2.1.5 Curtain flow Chromatography Columns – Operation

In all cases the mobile phase delivery to any curtain flow column was set such that 40% of the total inlet flow entered the column through the radial central inlet port, and 60% of the total inlet flow entered through the peripheral ports. This flow proportioning was obtained using a split flow configuration set prior to the injector. Since the outlet of the CF column also has an AFT fitting, the outlet flow proportions - radial central exit flow: peripheral exit flow is variable. In this work, the specific flow proportions that were employed at the outlet side of the column are noted in the relevant sections of text. These flow proportions were either 43% or 21% from the radial central exit port, as noted in the relevant text. Injection volumes were scaled to the column cross-sectional surface area and were 1.04 μL for the 2.1 mm i.d., and 5 μL for the 4.6 mm and 4.6 mm CF i.d. columns.

Chapter 3.

Assessing the Suitability of Active Flow Technology Columns for High Through-put Separations

3.1 Introduction

An ever increasing priority in analytical chemistry, and the fields of science that it supports, is improving work-place productivity. One mechanism by which work-place productivity can be improved is by decreasing the time required to undertake an assay. This was, in part, the driving force behind the development of the 'new field' of separation science - ultra-high performance liquid chromatography (UHPLC), which encompasses the conjoint advances in column technology and the instruments designed to utilise their separation power.

As scientists seek to discover more about complex samples, sensitivity in an assay is always at the forefront of technological developments. With this in mind, and the need to develop faster separations, the drive towards UHPLC-type separations was inevitable. In any assay that involves a chromatographic separation, the analyte is transported through some form of separation device. In liquid chromatography this device is a chromatography column, and here the discussion will be limited to columns that are packed with particles rather than monolithic structures, pillared arrays etc. Sample is passed through the porous bed and specific retention mechanisms ultimately result in the separation of the targeted analyte species. In the process of this transportation through the column, the analyte band disperses into a broader distribution, described by well researched phenomena according to the classical Van Deemtner equation, and other relationships that have since been developed, i.e., the Knox equation, the Giddings equation. Nevertheless, if the advances made in detection devices are ignored, in other words, let us just consider the contribution or perhaps the limitation of the chromatography column to the sensitivity of an analysis, then it is apparent from Equation 3.1 that the response at any location (x) is related to the standard deviation of the normal distribution represented by the analyte peak profile [103]

$$R = \frac{1}{\sigma\sqrt{2\pi}} e^{-\frac{1}{2}\left(\frac{x-\mu}{\sigma}\right)^2} \qquad (3.1)$$

where R is the response and σ is the standard deviation of the population. Hence, any factor that leads to an increase in band broadening of an analyte peak will result in a decrease in the height of the peak (reduction in response) since the standard deviation of the band will increase. Therefore column efficiency is important since the number of theoretical plates (N) is related to the variance of the sample band distribution according to Equation 3.2 [103,104]

$$N = \frac{t_r^2}{\sigma^2} \qquad (3.2)$$

where t_r is the retention time of the analyte and σ^2 is the variance of the analyte peak (square of the standard deviation of the population distribution). If we therefore start with the assumption that all chromatography columns irrespective of particle size are packed equally well then it becomes immediately obvious from Equations 3.3 and 3.4, that columns packed with smaller particles will result in narrower sample distributions, and therefore peak height will increase [103,104].

$$H = \frac{L}{N} \tag{3.3}$$

$$h = \frac{H}{d_p} \tag{3.4}$$

where H is the height equivalent to a theoretical plate, L is the column length, d_p is the particle diameter and h is the reduced plate height. Therefore, to maintain a constant reduced plate height at a specified column length, the sample distribution must decrease as particle size decreases, and that being the case, the peak height will increase (given a constant amount of sample).

Hence on this premise, UHPLC technology was developed. However, as will be discussed in this chapter, there are limitations that underpin the assumptions that all columns irrespective of the particle size are packed, or at least perform, equally well. It is therefore the aim of this chapter to define the operational limitations of UHPLC column technology and demonstrate how AFT columns can be adapted to high through-put assays.

3.2 Experimental

3.2.1 Chromatography Columns

In this chapter conventional and AFT chromatography columns were tested. The conventional columns were 2.1 mm × 50 mm, and 2.1 mm × 30 mm, both packed with 1.9 μm particles, and 4.6 mm × 50 mm, packed with 5 μm particles. Two AFT columns in parallel Segmented Flow (PSF) mode were also employed, with geometries of 2.1 mm × 50 mm and 4.6 mm × 50 mm, both packed with 5 μm particles.

3.2.2 Chemicals and Reagents

All mobile phases were prepared from HPLC-grade solvents purchased from Thermo Fisher Scientific (North Ryde, New South Wales, Australia). Alkyl-benzene standards were purchased

from Sigma-Aldrich (Castle Hill, New South Wales, Australia). Milli-Q water (18.2 MΩ cm) was prepared in-house using a Millipore (Kilsyth, Victoria, Australia) system and filtered through a 0.2 μm filter. Stock standards was prepared in a water/methanol mobile phase (20/80) by adding 40 μL of toluene, 160 μL of propylbenzene and 400 μL of butylbenzene and made up to 25 mL.

3.2.3 Chromatographic Separation

Separations were performed on a Thermo Ultimate 3000 UHPLC system equipped with a quaternary pump, inline degassing unit, auto injector and a variable wavelength UV detector (set at 254 nm for this study using a detection frequency of 200 Hz). Separations were performed under isocratic elution conditions using a water/methanol mobile phase (40/60). Column performance was tested at various flow rates between 0.04 mL/min to 5 mL/min depending on the column format. Injection volumes were either 1 μL (2.1 mm i.d. format columns) or 5 μL (4.6 mm i.d. format columns).

Data analysis was undertaken using the integration functions of the Chromeleon software, where plate heights were measured using the second moment method.

3.3 Results and Discussion.

3.3.1 Conventional HPLC and UHPLC columns

As a starting point to evaluate the performance of AFT columns for high through-put analyses, a comparison between UHPLC columns and HPLC columns in conventional column formats must firstly be undertaken. For that purpose the efficiency and sensitivity in analyses undertaken on columns packed with 1.9 μm and 5 μm particles, both based on the Hypersil GOLD stationary phases were compared. Bearing in mind that the purpose of this study was to test the competitiveness of AFT columns against UHPLC column formats for high through-put assays, the 1.9 μm particle packed UHPLC column was in a 2.1 mm i.d. format, which was chosen because it maximised both the efficiency and through-put capabilities of this column technology. Whereas the 5 μm particle packed column was in a 4.6 mm i.d. format, so chosen to maximise the efficiency of this column, given there is the inherent understanding that conventional HPLC column technology is not competitive with UHPLC technology when productivity is a key assay criterion. It is well known that the heat generated through viscous frictional heating that stems from the high pressure environment of the 1.9 μm particle packed column is dissipated more efficiently from the 2.1 mm i.d. format column compared to the 4.6 mm i.d. format, hence the 4.6 mm i.d. format column was

not tested packed with 1.9 μm particles [105-107]. A negative aspect on this approach, however, is that extra column dead volume has a more serious effect on the smaller internal diameter column than for the larger, but as will be revealed throughout this Chapter, only the 2.1 mm i.d. column format is capable of realising outcomes that can be deemed to be high through-put assays. In tests that involve the AFT column formats, studies were undertaken in both the 2.1 and 4.6 mm i.d. format columns so as to gauge the outcome of both efficiency and speed in assays designed for high through-put work flow, especially given that the detector in later Chapters is a mass spectrometer. The justification for the comparison between the 1.9 μm particle packed column to the conventional 5 μm particle packed column is based on the premise that the AFT columns used in this thesis are primarily prepared from 5 μm particles.

The efficiency of the retention processes for each of the alkyl-benzenes for both the 1.9 and 5 μm particle packed conventional columns are shown in Figure 3.1. Considering firstly the data for the more strongly retain alkyl-benzene (butyl benzene), the minimum in the HETP curve for the 1.9 μm particle packed column was around 6.5 micron (7690 plates) compared to 12.5 micron (4028 plates) on the 5 μm particle packed column (both evaluations based on the second moment method for determining N). On the 1.9 μm particle packed column the minimum increased to 6.9 micron (7210 plates) and 8.9 micron (5590 plates) for the less retained species propylbenzene and toluene respectively. This decrease in performance, especially for the weakly retained toluene (27%) [90], was likely due to the more significant extra column dead volume contributions to band broadening, which were not corrected for in this study since primarily we are interested in experimental outcomes that can be expected to be realised in the analysis of real samples.

In comparison, there was a slight gain in the transport efficiency for the less retained species on the 4.6 mm i.d. 5 μm particle packed column, indicating that the extra column dead volume was largely insignificant on this column format. The minimum in the HETP curve for this column was 11.6 micron (4322 plates) and 11.2 micron (4452 plates) for propylbenzene and toluene respectively. This data clearly shows that, as expected the UHPLC column format performs more efficiently, at least with respect to the number of theoretical plates that are generated per separation. That being said, it is also worth realising that while the UHPLC column yields the highest number of theoretical plates, and hence it may be deemed to be more ‘efficient’, the actual reduced plate height (h) on the 5 μm particle packed column is far superior. For example, the h-values of each of the three alkyl-benzenes are 2.2, 2.3 and 2.5 for toluene, propylbenzene and butyl benzene, respectively, while on the 1.9 μm particle packed column the h-values were 3.4, 3.6 and 4.7 for the same compounds respectively. This clearly shows that it is either more difficult to pack an efficient

small particle column, or, it is difficult to use these columns to yield their best operating performance [108].

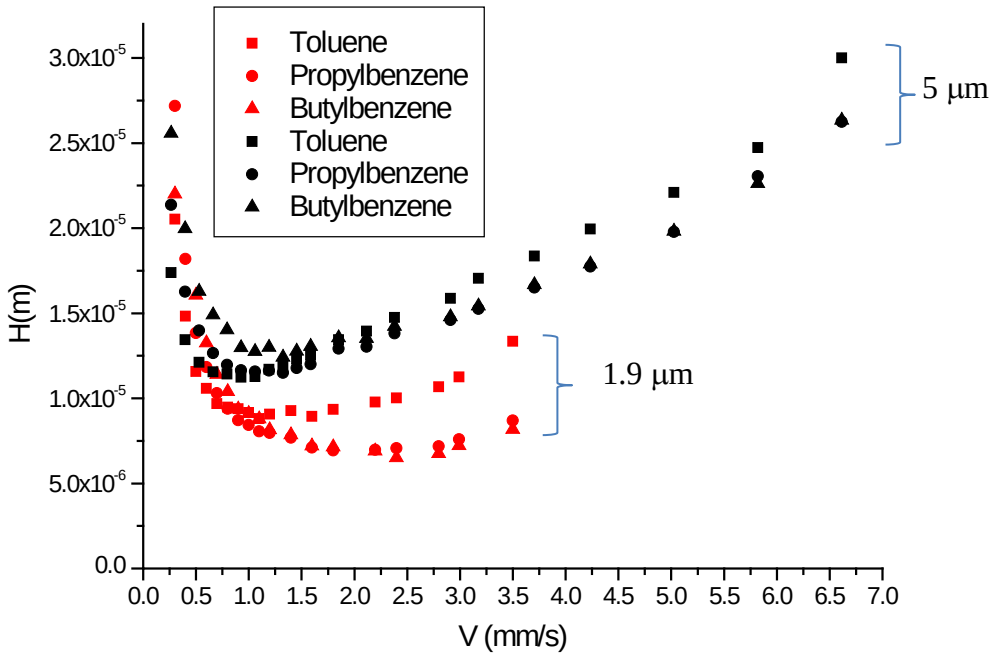

Figure 3.1 HETP curves obtained on a conventional 1.9 µm particle packed column in a 2.1 mm i.d. format (red) and a conventional 5 µm particle column in a 4.6 mm i.d. format.

3.3.2 Conventional HPLC and AFT columns – 5 µm particle formats.

The previous section verified that smaller particle size packed columns yielded greater separation power and more sensitive analyses. Therefore, as a starting point to determine the viability of AFT columns for high through-put sensitive analyses, the performance of AFT columns packed with 5 µm particles was compared to 5 µm particle conventional columns. Both column formats were identical, i.e., 50 × 4.6 mm formats.

The AFT column was operated as both a virtual 2.1 and a virtual 3.0 mm i.d. column, meaning that 21% of the flow eluted from the radial central exit port in the case of the virtual 2.1 mm i.d. column and 43% of the flow eluted from the radial central port for the virtual 3.0 mm i.d. column. HETP curves for the AFT column operating as the 'virtual' 3.0 mm i.d. column are shown in Figure 3.2.

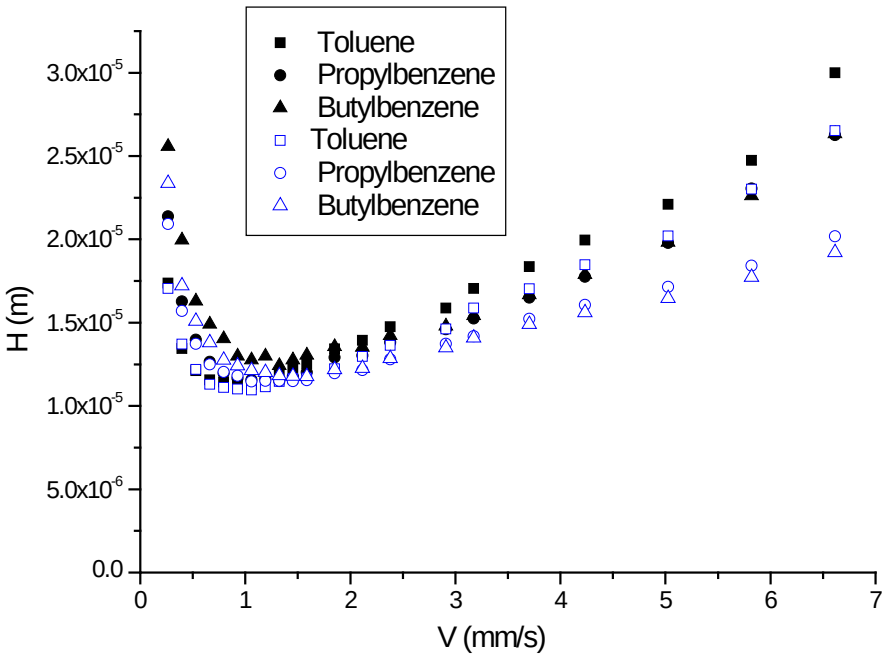

Figure 3.2 HETP curves obtained on a conventional 5 µm particle packed column in a 4.6 mm i.d. format (black) and a PSF 5 µm particle column in a 4.6 mm i.d. format with an outlet segmentation ratio of 43% through the centre (blue).

Evaluating firstly the more retained analyte, butylbenzene, it is apparent that the minimum of the HETP curve for the virtual 3.0 mm i.d. column was 11.8 micron (4250 plates), which is slightly more than a 5% gain in efficiency compared to the conventional column of the same particle size. For the less retained solutes, propylbenzene and toluene, the minimum in the HETP curve was 11.5 (4360 plates) and 10.9 micron (4560 plates) respectively, each representing gains of less 2.5%. As was the case for the conventional 5 µm particle packed column, the AFT column was also tolerant to the extra column dead volume. Although the gain in efficiency at the minimum of the HETP curve was virtually insignificant, importantly the gain in the efficiency at the higher flow rates that would correspond to high through-put were far more substantial for the AFT column. For example, at the flow rate of 5 mL/min the number of theoretical plates obtained on the virtual 3.0 mm i.d. AFT column for the butylbenzene band was 2600 plates, compared to 1900 on the conventional column, at a gain of around 37%. For propylbenzene and toluene the gain in plates AFT versus a conventional column was 30% and 14% respectively; indicating promising performance gains for high throughput activities.

The HETP curves for the AFT column operating as the ‘virtual’ 2.1 mm i.d. column are shown in Figure 3.3.

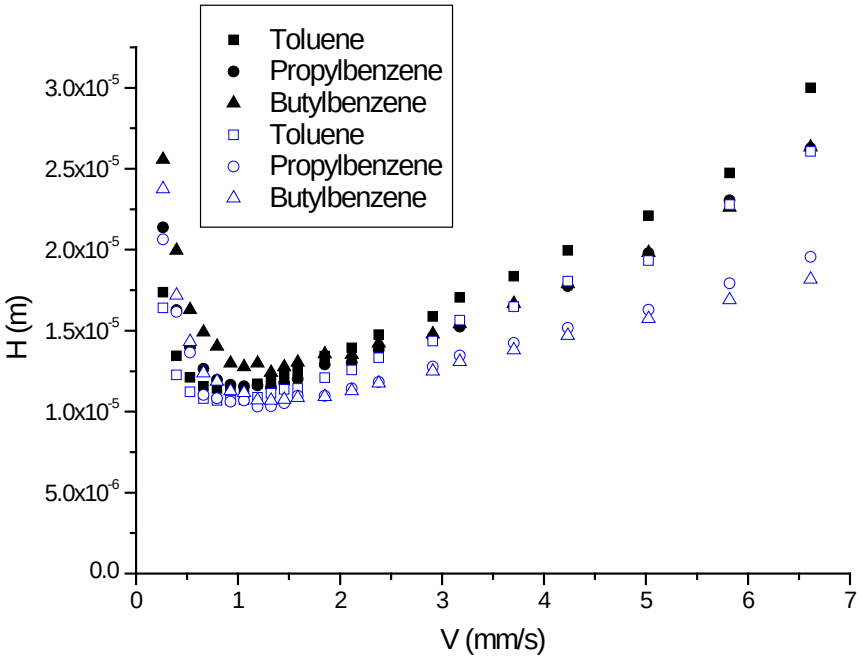

Figure 3.3 HETP curves obtained on a conventional 5 µm particle packed column in a 4.6 mm i.d. format (black) and a PSF 5 µm particle column in a 4.6 mm i.d. format with an outlet segmentation ratio of 21% through the centre (blue).

For the more retained analyte, butylbenzene, the minimum of the HETP curve for the 2.1 mm i.d. virtual column was 10.6 micron (4680 plates), which is slightly more than a 16% gain in efficiency compared to the conventional column of the same particle size. For propylbenzene and toluene the minimum in the HETP curve was 10.3 (4850 plates) and 10.6 micron (4680 plates) respectively, each representing gains of around 12%. As was the case for the virtual 3.0 mm i.d. column, the virtual 2.1 mm i.d. column is also reasonably tolerant of the extra column dead volume. As was also the case with the virtual 3.0 mm i.d. column the gain in efficiency was more substantial at the higher flow rates – at the flow rate of 5 mL/min the number of theoretical plates obtained on the AFT column for the butyl benzene band was 2750 plates, compared to 1900 on the conventional column, at gain of around 45%. For propylbenzene and toluene the gain in plates AFT versus a conventional column was 35% and 15% respectively; indicating even greater promise in performance gains for high throughput activities, especially for a flow rate limited detector such as the mass spectrometer.

3.3.3 The Performance of AFT columns in 2.1 and 4.6 mm i.d. formats– 5 μm particle formats.

Since the emphasis on the performance of AFT columns is focused on high through-put applications, it is necessary to scale down the column format since the pumping mechanism of the Ultimate 3000 cannot exceed 8 mL/min. The previous section showed that the AFT columns packed with 5 μm particles yielded gains in efficiency of around 30 to 45% compared to conventional columns when operated at 5 mL/min. Therefore in order to increase the throughput further the column internal diameter was reduced to 2.1 mm. This reduction from 4.6 to 2.1 amounts to a scaling factor of five. Hence a separation undertaken at 1 mL/min on a 2.1 mm i.d. column is equivalent to a separation undertaken at 5 mL/min on a 4.6 mm i.d. column. Since an objective of this thesis was to evaluate the usefulness of AFT with MS detection in high through-put applications, only the segmentation ratio of 21% through the radial central exit port was tested as this minimised the flow to the MS.

Prior to any discussion that relates to the performance of AFT columns in a 2.1 mm i.d. format, however, it is worth considering the relative sensitivity and efficiency between conventional columns in identical 2.1 mm i.d. formats, one packed with 1.9 μm particles, the other with 5 μm particles. Visually this is illustrated in Figure 3.4, which compares the separation of the alkyl benzene three-component mixture obtained at flow rates that yielded approximately the same retention times on both columns, i.e. 0.88 mL/min on the 5 μm particle packed column and 0.7 mL/min on the 1.9 μm particle packed column. Clearly the separation achieved on the 1.9 μm particle packed column was superior, and hence an investigation into the performance of AFT columns compared to UHPLC columns in conventional format is warranted. Therefore, the HETP curve for each of the three analytes (toluene, propylbenzene and butyl benzene) obtained on the AFT 2.1 mm i.d. column packed with 5 μm particles, and operated with a 21% segmentation ratio are shown in Figure 3.5. For ease of comparison, the HETP curves for each of the solutes is overlaid with the HETP curves obtained for the 4.6 mm i.d. AFT column operated with an outlet segmentation ratio of 21%. From this set of data it is apparent that the 2.1 mm i.d. AFT column and the 4.6 mm i.d. AFT column almost the same separation efficiency, except, however, the 2.1 mm column was able to be operated at flow rates five-times higher than the 4.6 mm format.

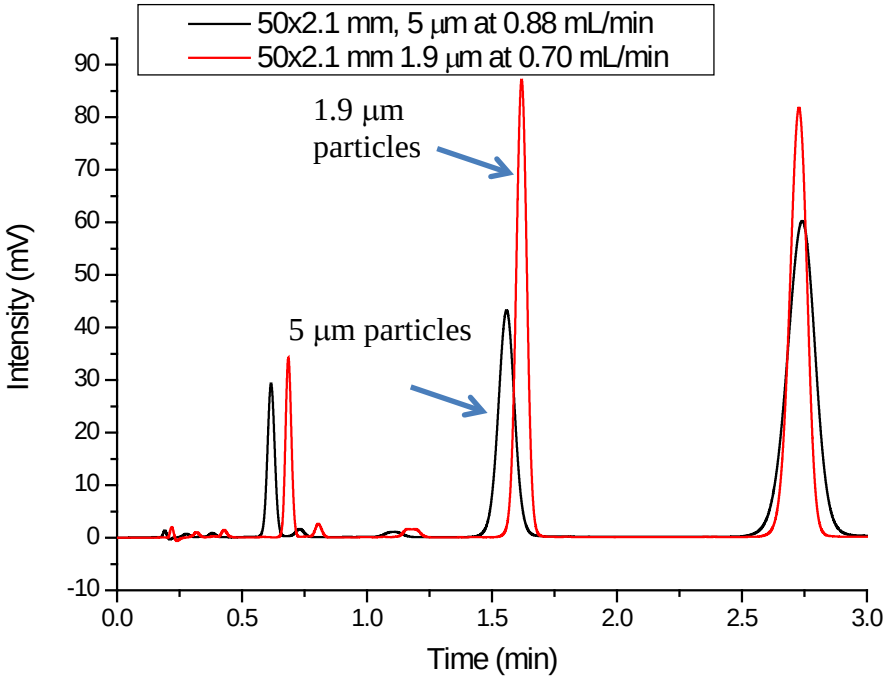

Figure 3.4 Comparison between the separations obtained on conventional 2.1 mm i.d. columns packed with 1.9 µm (red) and 5 µm (black) particles.

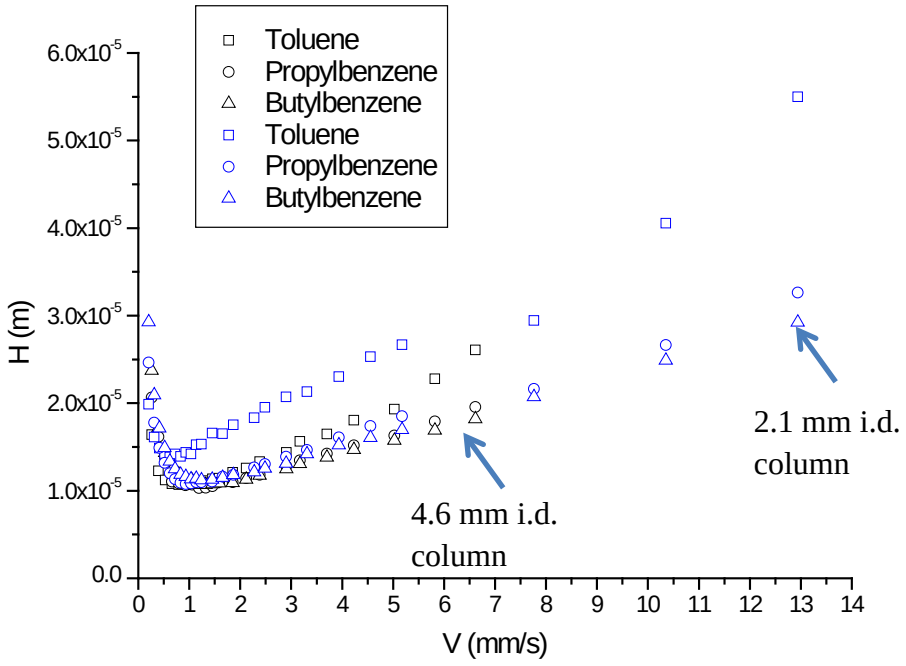

Figure 3.5 HETP curves obtained on a 4.6 mm i.d. PSF column packed with 5 µm particles operating with a 21% outlet segmentation ratio (black) and a 2.1 mm i.d. PSF column in a 2.1 mm i.d. format packed with 5 µm particles with an outlet segmentation ratio of 21% through the centre (blue).

Conventional 1.9 μm UHPLC columns and 5 μm AFT columns for high through-put assays.

HETP curves for the 1.9 and 5 μm particle packed columns in conventional UHPLC and AFT (21% segmentation ratio), both in 2.1 mm i.d. formats are shown in Figure 3.6. Both these sets of data were plotted in Figures 3.1 and 3.3 respectively. However, for simplicity they are replotted and overlaid. As was the case for the comparison between the UHPLC column and the conventional 5 μm particle packed column, the HETP is superior on the UHPLC column compared to the AFT column. However, a limiting factor associated with the use of the UHPLC column is that the maximum flow rate that could be tested was 0.7 mL/min which generated a pressure of almost 10000 p.s.i. In comparison, the HETP curve for the 2.1 mm i.d. AFT column was tested up to the flow rate of 2.8 mL/min, which is 4 times faster. As a consequence it was clear that in order for the conventional UHPLC column to function at the same or a similar through-put capabilities as the AFT column, either the internal diameter of the UHPLC column would have to be reduced or its length decreased.

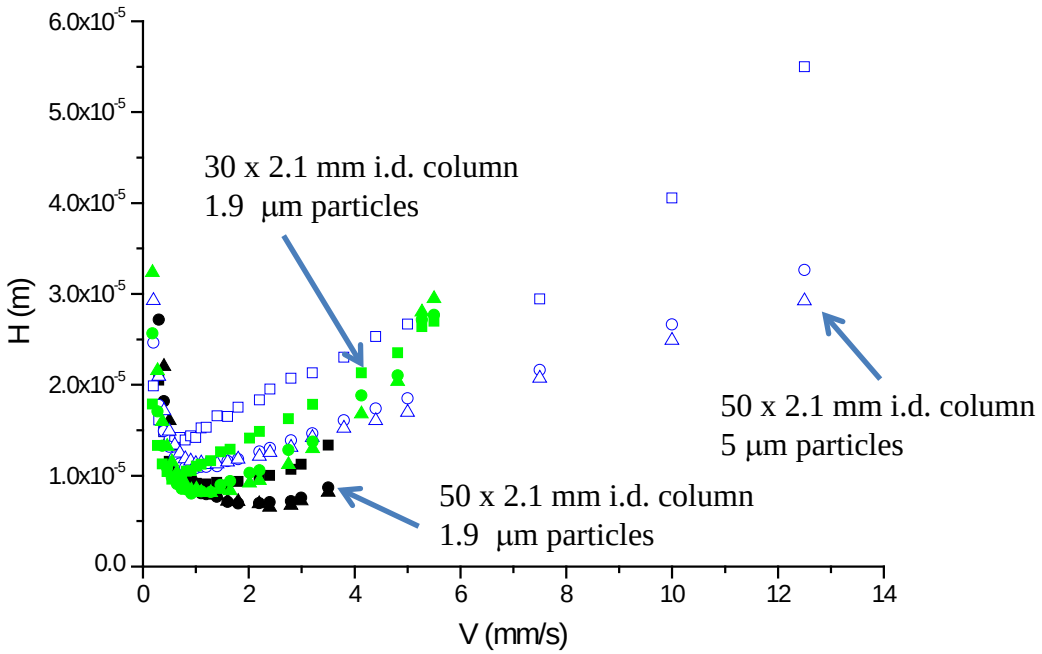

Figure 3.6 HETP curves for the 1.9 and 5 μm particle packed columns in conventional UHPLC and AFT (21% segmentation ratio), all in 2.1 mm i.d. formats: Toluene (□), propylbenzene (○), butylbezene (Δ). Black trace 2.1 × 50 mm, 1.9 μm, Green trace 2.1 × 30 mm, 1.9 μm, and Blue trace 2.1 × 50 mm, 5 μm.

While the effect of decreasing the column internal diameter would likely result in the greatest gains in separation speed, it would also likely result in the higher loss in efficiency due to the extra column dead volume contributions. AFT columns in 2.1. mm i.d. formats were, for example, compared against 1 mm i.d. columns, and in all aspects of efficiency the AFT columns were superior [93]. Hence for that reason this was not tested here. Therefore in order to increase the through-put for the UHPLC column format, the column length was decreased from 50 mm to 30 mm. This enabled the maximum flow rate to be increased to 1.2 mL/min for operating pressures near 10000 p.s.i., and the HETP curve for this 30 mm UHPLC column packed with 1.9 μm particles is shown in Figure 3.6 . From this data it is firstly apparent that the performance of the 30 mm i.d. format column is inferior to the 50 mm i.d. format. The minimum HETP achieved for butyl benzene was 8.3 micron compared to 6.5 micron on the 50 mm column, both of which are smaller than the 5 μm AFT column at the minimum in the HETP curve (11.2 micron). However, the number of theoretical plates achieved on the 30 mm UHPLC curve at the optimal flow rate was only 3690 plates, 770 less than the 50 mm AFT column packed with 5 μm particles. Hence the number of plates available for the separation on the AFT column is greater than on the UHPLC column at optimum flow for efficiency. Furthermore, the pressure at this optimum flow was 2500 p.s.i. on the UHPLC column compared to 500 p.s.i. on the AFT column. The outcome was even more favourable for the AFT column when the separation was pushed to maximum through-put, defined by the flow rate limitation of each respective column, i.e. at a pressure limit of 10000 p.s.i. for the UHPLC column and 6000 p.s.i. on the AFT column. At the maximum pressure, the number of theoretical plates on the UHPLC column was 1020 at a flow rate of 1.2 mL/min (pressure = 9300 p.s.i.), whereas on the AFT column the number of theoretical plates was 1711 at 2.5 mL/min (pressure = 5300 p.s.i.). At these operational levels the separation on the AFT column was 0.94 minutes compared to 1.2 minutes on the UHPLC column. That is a decrease in separation time of 21%, and with a gain in efficiency of 67%. The chromatograms shown in Figure 3.7 compare the separations obtained on each of these columns near the limits of operation. Clearly the AFT separation is superior, both in terms of speed and efficiency. In order for both columns to offer the same level of efficiency, measured according to the number of theoretical plates, the flow rate on the UHPLC column cannot exceed 0.9 mL/min (a depicted in Figure 3.7). At that flow rate the analysis time was 1.58 minutes, almost 70% longer than the AFT separation.

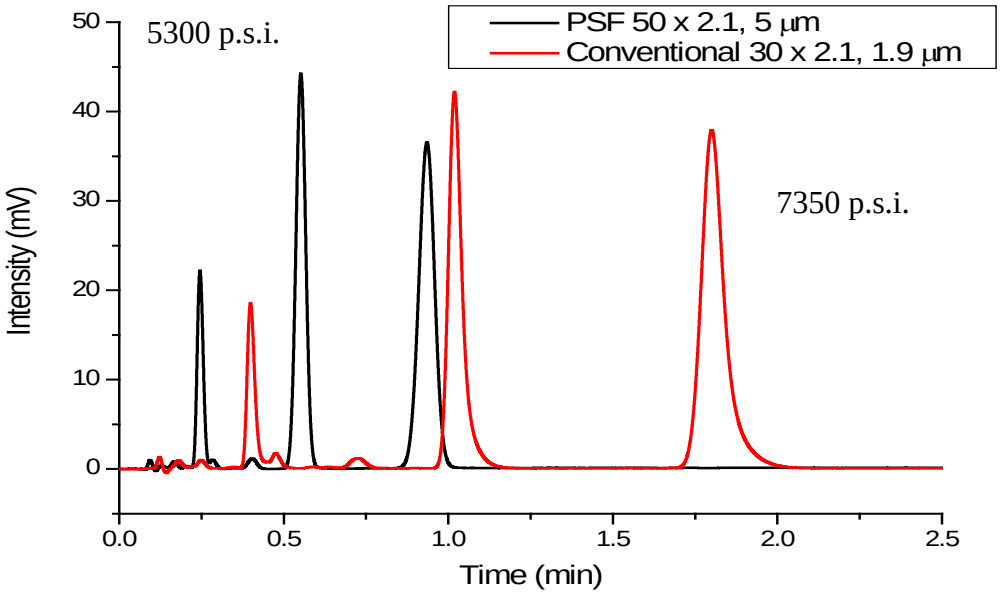

Figure 3.7 Chromatograms illustrating the separations obtained on the conventional UHPLC column (red trace) in a 2.1 × 30 mm, 1.9 µm format and the PSF column with a 21% outlet segmentation ratio (black trace) in a 2.1 × 50 mm, 5 µm format. Both separations were obtained at equal numbers of theoretical plates.

3.4 Conclusion

Data presented in this Chapter clearly showed that small particle columns had increased performance compared to larger particle columns; however, it is difficult to use these columns to yield their best operating performance. Furthermore, use of AFT columns packed with 5 µm particles had higher efficiency of around 30 to 45% compared to conventional columns when operated at high flow rates (5 mL/min). This is especially advantageous for high-throughput analysis with mass spectrometry detection. Use of AFT columns in narrow bore column formants packed with larger particles further demonstrated superiority in speed and sensitivity when compared to same inner diameter conventional columns packed with sub 2 micron particles.

.

Chapter 4.

High Through-put and Highly Sensitive LC-MS/MS Separations of Essential Amino Acids using Active Flow Technology Chromatography Columns

4.1 Introduction

HPLC-MS is a powerful analytical technique, but there are two factors that limit the performance; sample through-put and column efficiency. Both these factors are inter-related. The key aspect of the limitation in performance is the drive towards smaller particles in liquid chromatography. As the particle size decreases the linear velocity must be increased to maintain optimal chromatographic performance. However, as the linear velocity increases so too does the difficulty in reducing the solvent volume prior to sample entry into the mass spectrometer. To account for solvent removal, column internal diameters are decreased. Commonly, the 2.1 mm i.d. column is employed instead of the analytical format with a 4.6 mm internal diameter. This decreases the solvent load by almost 5-fold, yet the same linear velocity can be maintained. This appears to be a suitable solution to the problem of solvent removal prior to the mass spectrometer while at the same time being able to utilise the latest developments in particle technology. However, it is a compromise in the performance of the chromatographic separation [72], primarily as a result of wall effects [71].

MS users have become accustomed to using narrow bore columns, as this is nowadays a better approach than employing post column flow stream splitting and analytical scale columns. Nevertheless, the use of narrower diameter columns may limit sensitivity, since one aspect of sensitivity in mass spectrometry is related to the mass load on the column. As column internal diameter decreases so too does the volume and mass load – effectively in proportion to the square on the column radius. Furthermore, narrow bore columns are generally recognised as offering a lower level of separation performance, since the wall effect is more serious and managing the extra column dead volume is more difficult that for analytical scale columns. However, for the most part, operators of mass spectrometers that require some form of separation ignore the loss in the separation performance because of the very big advantage associated with the reduced solvent load that is presented to the MS detector. This is especially so when 4.6 mm i.d. columns are employed since, in order to satisfy the volumetric solvent load to the MS the 4.6 mm i.d. column is often operated at flow rates well below the optimum for these columns, especially as the particle size decreases, another reason why MS users employ the 2.1 mm format.

4.1.1 Curtain Flow Chromatography.

In this chapter CF columns have been employed. The sample introduction process and principle operation have been detailed in Section (2.1.5).

4.2 Experimental

4.2.1 Chromatography Columns.

For more details refer to Section 2.1.2. The column set used in this Chapter consisted of conventional columns having internal diameters of 2.1 or 4.6 mm, and also a 4.6 mm i.d. CF column. All columns were 50 mm in length.

4.2.2 Chemicals and Reagents

For more details refer to Section 2.1.1.Apple juice was obtained from a local supermarket, filtered through a 0.2 μm filter and diluted 10-fold for analysis.

4.2.3 Instrumentation UPLC-MS/MS

For more details refer to Section 2.1.4.The mobile phase flow rate was adjusted so the volume presented to the MS detector was always 1 mL/min (therefore the 4.6 mm i.d. and the 2.1 mm i.d. conventional columns were both operated at 1 mL/min). However, the 4.6 mm CF column was operated at 5 mL/min with an outlet segmentation ratio of 20% (i.e. 20% of the flow exited the column from the central exit port to the detector – that is 1 mL/min went to the detector). At this flow rate the linear velocities on the 2.1 mm i.d. conventional column and the 4.6 mm CF column were the same.

Since the ESI-MS detector is sensitive to concentration, injection volumes were scaled in accordance to the column cross sectional area so that sample components at elution, and hence presentation to the MS, would be at constant concentration [98]. Hence injection volumes were 1.04 μL for the 2.1 mm i.d., and 5 μL for the conventional 4.6 mm and 4.6 mm CF i.d. columns. Samples and standards were injected in at least triplicate.

4.2.3.1 Gradient Method.

When gradient elution was undertaken (noted in the relevant sections) the initial mobile phase composition was 95/5 water/methanol (+ 0.1% formic acid) and the final mobile phase composition was 35/65 water/methanol (+ 0.1% formic acid). On the 4.6 mm i.d. conventional column, the gradient duration was 6 minutes, after which the mobile phase was returned to the original conditions (1 min.). On the 2.1 mm i.d. conventional column and 4.6 mm i.d. CF column the gradient duration was 1.2 minutes (since the flow velocity was 5× greater than the 4.6 mm i.d. conventional column), after which the system would be returned to the initial conditions in 0.2 minutes. All columns were equilibrated with five column volumes of mobile phase prior to the next injection. The cycle time of the 4.6 mm i.d. conventional column was therefore 5 times that of either the 2.1 mm i.d. conventional or 4.6 mm i.d. CF columns.

4.2.4 Mass Spectrometry Parameters

The MS parameters for optimised detection are outlined in Section 2.1.3. The collision energy and tube lens offsets were individually optimized for each compound and presented in Table 2.1, together with precursor and product ions. Data processing was performed using LC Quan software. (Thermo Fisher Scientific, San Jose, USA). Volume flow to the mass spectrometer remained constant for all analyses (1 mL/min).

4.3 Results and Discussion

A requirement of this study was that the flow rate to the MS remained constant for each of the columns tested. In that way the MS detection conditions remained unchanged and thus differences in detection responses could be assigned solely to the chromatographic performance. The flow rate to the MS was set at 1 mL/min. This was chosen for two reasons: (1) the MS performance was reliable over long term operation, although close to its limits of operation given the high aqueous content of the mobile phase: and (2) the 4.6 mm i.d. standard column was operated at close to its optimal performance with respect to the chromatographic efficiency. Thus providing a reference operating under almost ideal chromatographic conditions.

Correspondingly the conventional 2.1 mm i.d. column was also operated at 1.0 mL/min, but this flow rate was well above the optimum with respect to column efficiency. The 4.6 mm i.d. CF column operating with a 20% outlet segmentation ratio was operated at 5 mL/min. At this flow rate 1 mL/min exited the column from the central exit port into the MS. The flow velocity on this column was exactly the same as for the 2.1 mm i.d. column. That is, both the 2.1 mm i.d. conventional and the curtain flow columns would offer the same kinetic performance, all things being equal. Hence the CF column functioned essentially as the ‘virtual’ 2.1 mm i.d. column, but in curtain flow mode [3,5]. It is important to reiterate that a 2.1 mm i.d. conventional column was not operated at its optimal chromatographic flow rate (~ 0.2 mL/min) since at this flow rate the through-put would be just 20% that of the curtain flow column; the objective of this study being the comparison of through-put and sensitivity. The purpose of the conventional 4.6 mm i.d. column on the other hand, was to provide a reference with respect to chromatographic efficiency, but at 1/5th the speed.

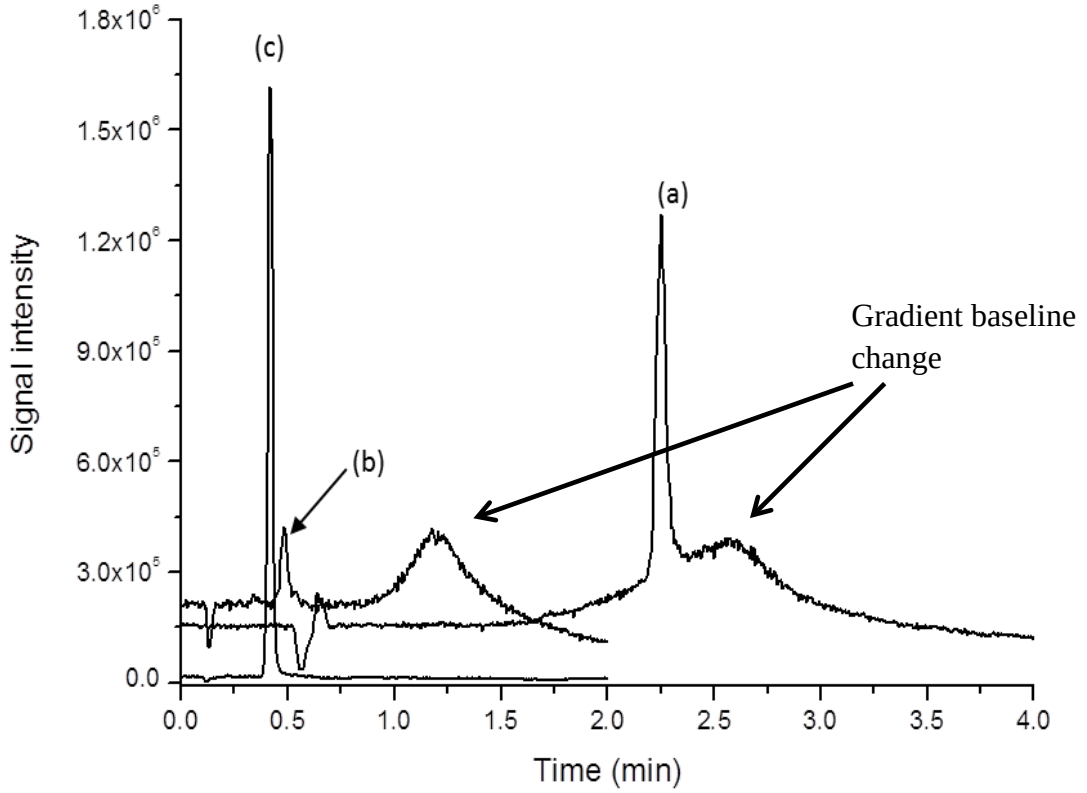

Figure 4.1 Extracted ion chromatograms of phenylalanine derived from each of the three columns. Trace (a) is the chromatogram obtained on the 4.6 mm i.d. conventional column, trace (b) for the 2.1 mm i.d. conventional column and trace (c) is the CF column. Note the rising baseline is due to the gradient change and this is not apparent on the AFT column.

The chromatographic profiles shown in Figure 4.1 are extracted ion chromatograms (EICs) of phenylalanine measured from separations on each of the three columns. Trace (a) is the chromatogram obtained on the 4.6 mm i.d. conventional column, trace (b) is for the 2.1 mm i.d. conventional column and trace (c) is the CF column. The retention time for phenylalanine was 2.25 min on the 4.6 mm i.d. conventional column and 0.48 min on the 2.1 mm i.d. standard column. In comparison, the retention time on the CF column was 0.42 min. The retention times on both the 2.1 mm standard column and the CF columns were approximately 20% that of the standard 4.6 mm i.d. column, because the linear velocity of the mobile phase in both cases was 5-times higher. Slight differences in the retention times between the 2.1 mm i.d. standard column and the CF column were apparent even though their linear velocities were equivalent because the gradient was initiated at the time of injection. Strictly, the gradient should have been started prior to injection to compensate for the system dead volume, thereby minimizing any isocratic component of elution. However, it was reasoned that most analyses are not undertaken using injection delay techniques, particularly since the pre-gradient isocratic solvent flow can be beneficial in the removal of unwanted contaminates

within the sample injection plug. Consequently retention was delayed on the 2.1 mm standard column since the dead-volume contribution from the system was a higher proportion of column volume. For all intents and purposes, the retention times on the 2.1 mm standard column and the CF column are equivalent, effectively operating 5-times faster than the 4.6 mm i.d. standard column.

Using these flow conditions it is immediately apparent that the most intense signal response was observed using the CF column, even though just 20% of the mobile phase entered the MS. The chromatograms of phenylalanine derived from CF columns were in the order of twice the sensitivity (based on peak height) of the conventional 4.6 mm i.d. format column, and approximately seven to eight times that of the conventional 2.1 mm i.d. format column. This shows how well the CF mode of injection concentrates the sample in the radial central region of the column, given that 80% of the mobile phase was directed to waste. The intensity of the signal obtained from extracted ion chromatograms provides a somewhat distorted view of the analysis. Analytical sensitivity is not solely related to the signal response, rather the ratio of the signal response to that of the noise (S/N). Therefore, in order to better determine the level of analytical sensitivity obtained from each column a series of calibration data were obtained on each column, and the S/N response measured. Calibration curves for tryptophan are shown in Figure 4.2. For each column the calibration was linear as detailed in Table 4.1.

Amino Acids	2.1 mm Conv. (Slope)	4.6 mm Conv. (Slope)	Curtain Flow (Slope)	2.1 mm Conv. (r^2)	4.6 mm Conv. (r^2)	Curtain Flow (r^2)
Histidine	1042	1563	3532	0.83	0.89	0.996
Lysine	927	2221	2093	0.95	0.97	0.96
Arginine	1545	1840	6853	0.95	0.94	0.94
Valine	1948	4943	10391	0.993	0.97	0.95
Methionine	680	2074	4600	0.998	0.994	0.98
Tyrosine	1035	2904	7401	0.994	0.994	0.993
Isoleucine/Leucine	12870	61019	50815	0.993	0.996	0.98
Phenylalanine	4278	17068	30261	0.997	0.996	0.992
Threonine	1682	5942	10046	0.998	0.995	0.998
Tryptophan	1133	5466	10045	0.994	0.998	0.998

Table 4.1 Calibration curve for each amino acid analysed on each of the three columns.

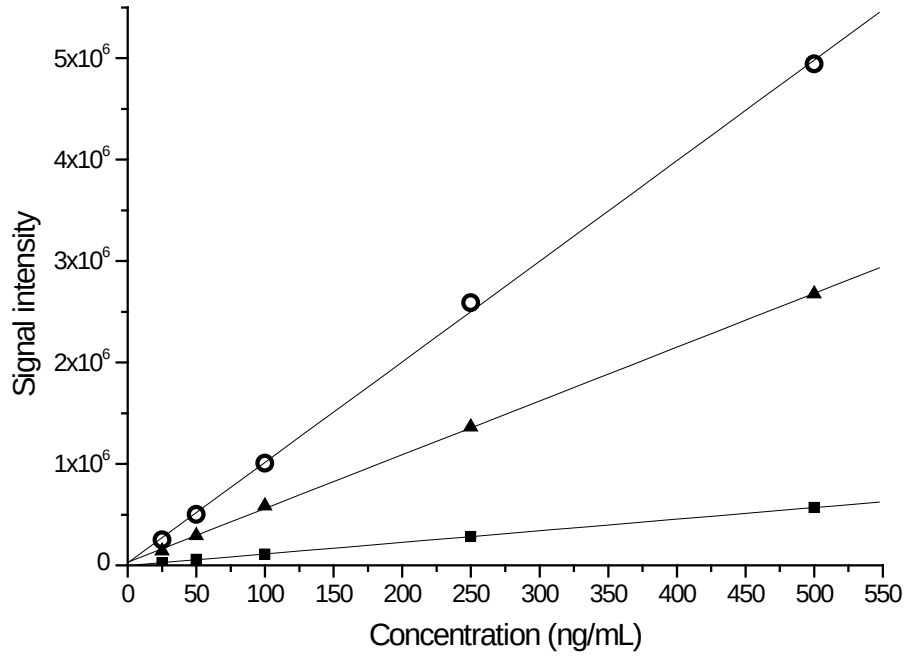

Figure 4.2 Calibration curves for tryptophan obtained on each of the columns: curtain flow column (O), 4.6 mm i.d. conventional column (▲) and 2.1 mm i.d. conventional column (■).

The S/N response was subsequently derived from this experimental data for the separations undertaken on each column. The magnitude of the noise response was determined using the *LCQuan* software, using manual measurement of RMS noise measured across 20% of the total run time using baseline immediately prior to, or immediately after the peak of interest. Irrespective, for each amino acid the noise was measured at the exact same mobile phase composition across all three columns. Figure 4.3 illustrates the S/N responses for each of the amino acids. For comparison the signal intensities are shown in Figure 4.4. Clearly, by accounting for the contribution of the noise component in the chromatographic profiles, the sensitivity of the analytical analysis using the CF mode of operation is far greater than either of the standard columns. For some amino acids the analytical sensitivity observed in the CF mode of operation was up to 20 times that of the conventional 4.6 mm i.d. column (average across the 9 amino acids = 7.8), and up to 66 times that of the standard 2.1 mm i.d. column, with a mean of 37 and a median of 44. In order to understand the gain in analytical sensitivity observed when using curtain flow columns, the plots in Figure 4.5 show the noise contributions for each of the three columns for extracted ion chromatograms of phenylalanine obtained on blank injections that were run in the sequence of standardisation. Being blank injections no amino acids were observed to elute, but the magnitude of the noise response

observed in the extracted ion chromatograms for the various amino acids could be calculated. The magnitude of the noise observed on the 2.1 mm i.d. column was in the order to 10000 units, while on the 4.6 mm i.d. column, the noise was reduced to ~ 3000 units. On the CF column, however, the noise was less than 1000 units. In addition, the background response observed on the 2.1 mm i.d. conventional column was in the order of 210,000 units and 160,000 units on the 4.6 mm i.d. conventional column. On the curtain flow column, however, the baseline was offset by the background noise by just 15,000 units, an order of magnitude less than the 2.1 mm i.d. column. Clearly the contamination of the signal response of the curtain flow column is far reduced compared to the conventional columns. Furthermore, the solvent front observed in Figure 4.5 on the curtain flow column was almost absent compared to the very large dips in the signal response seen on the conventional columns.

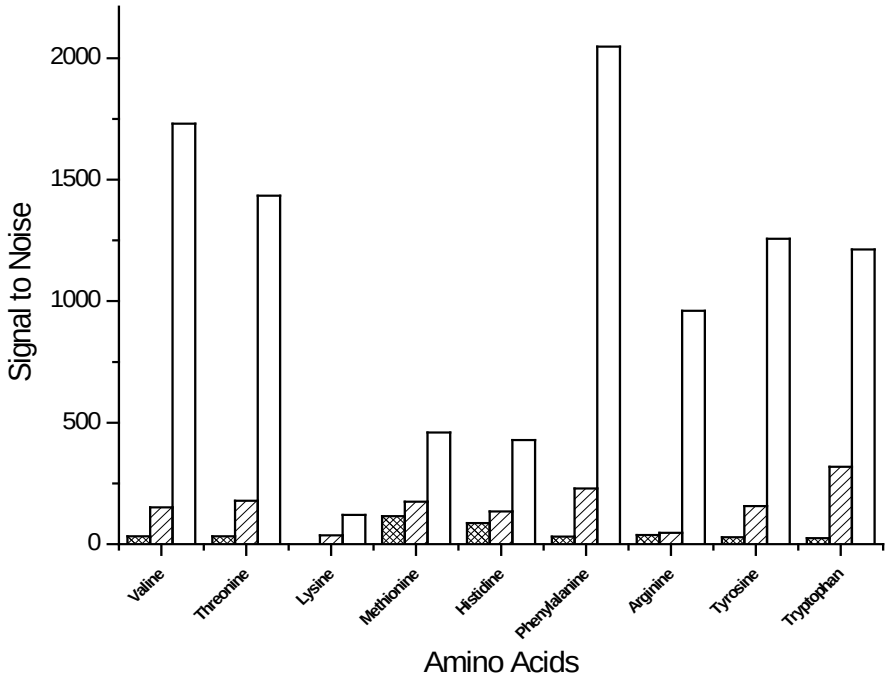

Figure 4.3 Plot illustrating S/N responses for each of the amino acids. Cross hatched = 2.1 mm i.d. conventional column, shaded = 4.6 mm i.d. conventional column, and hollow = curtain flow column. Amino acids from left to right are: valine, threonine, lysine, methionine, histidine, phenylalanine, arginine, tyrosine, and tryptophan.

An observation from Figure 4.3 (S/N response for each amino acid) shows that the gain observed in the CF mode of operation was not uniform across all amino acids. At first this would appear to be an effect resulting from the CF mode of operation, however, this is not the case.

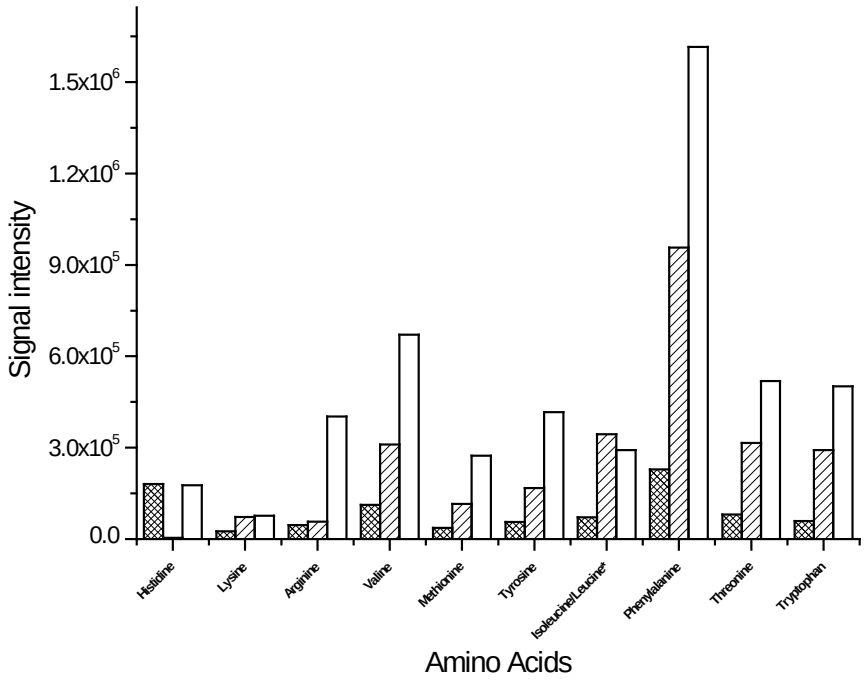

Figure 4.4 Comparison of the signal intensity responses for each of the amino acids. Cross hatched = 2.1 mm i.d. conventional column, shaded = 4.6 mm i.d. conventional column, and hollow = curtain flow column. Amino acids from left to right are: valine, threonine, lysine, methionine, histidine, phenylalanine, arginine, tyrosine, and tryptophan.

In fact, this variability stems from the conventional columns. To illustrate this point, the baseline noise for extracted ion chromatogram of methionine, derived from the same blank injection as used for the phenylalanine blank injection, is illustrated in Figures 4.6 and 4.7.

The *y*-axis in Figure 4.7 is exactly the same as in Figure 4.5 for visual comparison, while in Figure 4.6, the *y*-axis has been expanded to magnify the noise. From the chromatograms in Figures 4.6 and 4.7, in comparison to Figure 4.5, it is apparent that the range of the noise response on the conventional 2.1 mm i.d. column is very substantially reduced, while that for the curtain flow column remained essentially unchanged. As such the gain in S/N response CF: 2.1 mm i.d. conventional column was just 4 fold. Furthermore, the background response for both the conventional columns was reduced by an order of magnitude to just 15-20,000 units. The effect of the injection void is substantially greater on the conventional columns than the curtain flow column.

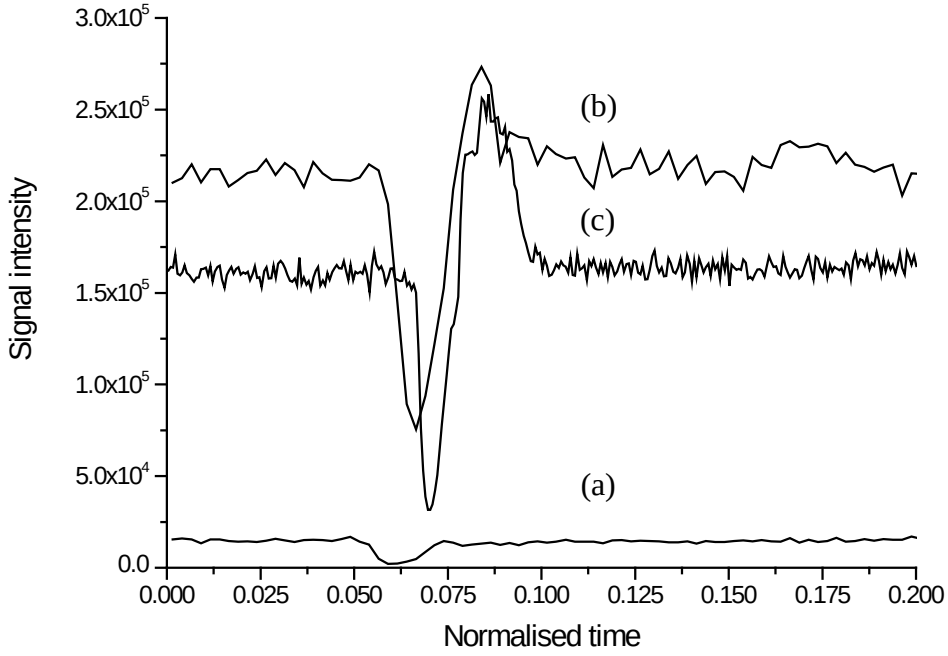

Figure 4.5 The plots showing the noise contributions for each of the three columns for extracted ion chromatograms of phenylalanine. Note the time axis is expressed as a fraction of the total run time, i.e. normalised time between 0 to 1. Each plot represents the first 20% of the total time. (a) curtain flow column, (b) 2.1 mm i.d. conventional column and (c) 4.6 mm i.d. conventional column. The response corresponding to the void time is represented by the dip in the baseline.

The measurement of the baseline noise as illustrated in Figures 4.5 - 4.7 stems from injections undertaken on all columns using exactly the same mobile phase composition for all columns tested, that is, the mobile phase was prepared in bulk and the same supply was used throughout. Further, the analyses undertaken on the curtain flow column were bracketed by the conventional columns. The order of analysis was conventional 2.1, curtain flow and then conventional 4.6. Possible changes in the nature of the mobile phase could therefore not have been responsible for these observations. In addition, all analyses were completed within 24 hours of continuous LCMS operation. At present, this remains an experimental observation and the cause of this effect is believed to come from reduced matrix effect at high velocities. This should be the focus of further studies. As a consequence of the reduced noise the limits of quantification derived from the CF column were substantially lower than on either of the standard columns. This shows another advantage of the CF mode of operation: sensitivity in analysis. Purists may argue that quantification in HPLC-MS is usually undertaken using peak area, rather than peak height, but we stress here that it is the measure of the signal height relative to the noise that determines sensitivity, hence establishes the limits of quantification.

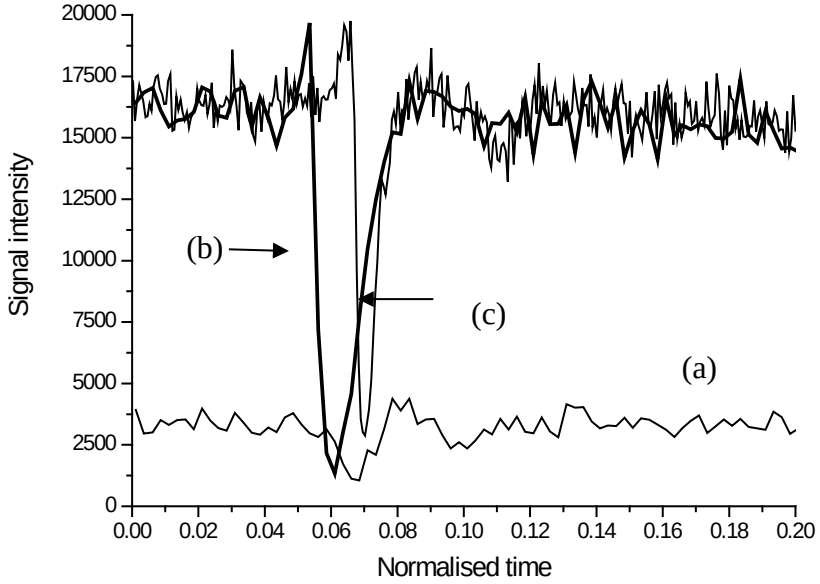

Figure 4.6 The plots showing the noise contributions for each of the three columns for extracted ion chromatograms of methionine. Note the time axis is expressed as a fraction of the total run time, i.e. normalised time between 0 to 1. Each plot represents the first 20% of the total time. (a) curtain flow column, (b) 2.1 mm i.d. conventional column (bold) and (c) 4.6 mm i.d. conventional column.

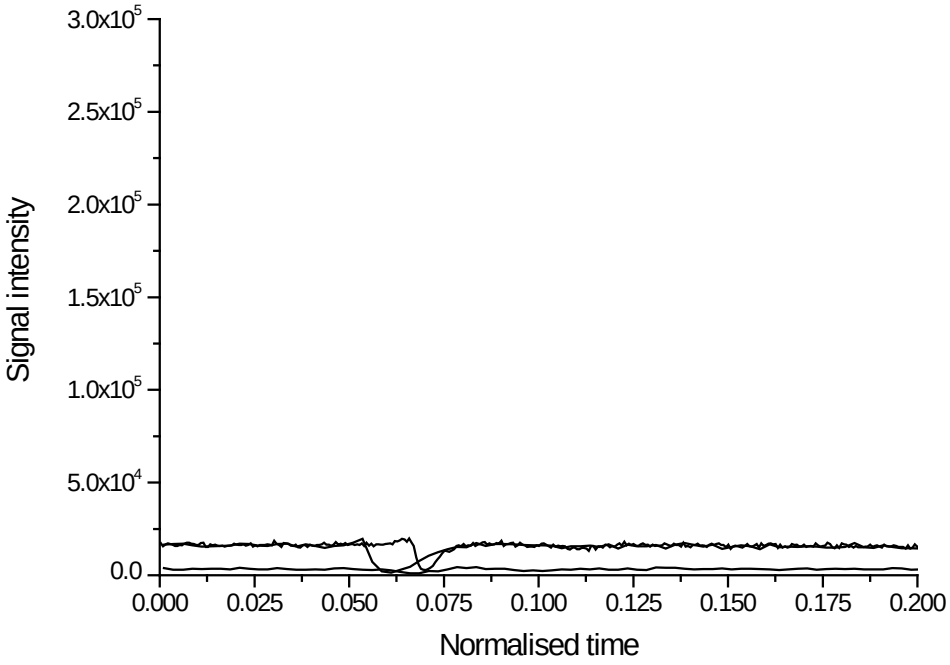

Figure 4.7 Plot of the baseline noise response for the EIC for m/z 150 (methionine) on the same scale as that for phenylalanine in Figure 4.5. Data illustrated is the same as in Figure 4.6.

A measure of system reproducibility was obtained by 15 replicate injections of the 100 ng/mL standard for each amino acid. The level of precision in the measurement of the peak height is detailed in Table 4.2.

Amino Acid	2.1mm Conventional (R.S.D)	4.6 mm Conventional (R.S.D)	Curtain flow (R.S.D)
Histidine	ND	4.4	2.1
Lysine	4.0	3.8	4.8
Arginine	5.3	3.5	8.7
Valine	5.9	3.9	4.5
Methionine	7.2	3.9	2.7
Tyrosine	9.8	5.3	3.0
Isoleucine/Leucine	5.5	2.7	1.1
Phenylalanine	4.3	3.6	2.8
Threonine	7.5	2.6	3.4
Tryptophan	4.1	3.3	2.4
Mean	**6.0**	**3.7**	**3.5**

Table 4.2 Measurement of the reproducibility in the determination of the peak height for each amino acid based on the analysis of the 100 ng/mL standard for each amino acid. Total injections = 12 on each column.

For all amino acids, the R.S.D measured for injection to injection reproducibility was the smallest on the CF column (average = 3.5%), followed by the 4.6 mm conventional column (average = 3.7%) then the conventional 2.1 mm i.d. column (average = 6.0%). Essentially there was no significant difference between the reproducibility of the CF and conventional 4.6 mm i.d. columns. However, both columns outperformed the conventional 2.1 mm i.d. column. Note, histidine was not detected at this concentration on the 2.1 mm i.d. conventional column.

Finally, a preliminary study (Table 4.3) was undertaken on the measurement of amino acids in a sample of apple juice. In total, only four of the amino acids were detected in this sample, even when the analysis was undertaken on an undiluted juice. Nevertheless, for the amino acids that were detected, the amount of each amino acid detected was always within 3.5 to 5.3% of the mean of the concentrations measured across all three columns within the set. This shows excellent agreement between analyses undertaken on the curtain flow column and conventional columns.

Amino Acid	2.1 mm Conventional (ppm)	4.6 mm Conventional (ppm)	Curtain Flow (ppm)
Histidine	ND	ND	ND
Lysine	ND	ND	ND
Arginine	ND	ND	ND
Valine	ND	ND	ND
Methionine	ND	ND	ND
Tyrosine	2300	2140	2080
Isoleucine/Leucine	1600	1720	1590
Phenylalanine	2310	2130	2310
Threonine	2360	2200	2240
Tryptophan	ND	ND	ND

Table 4.3 Calculated concentrations of each amino acid in apple juice derived from analyses undertaken on all three columns. The analysis was undertaken on a 1:10 diluted sample of apple juice.

4.4 Conclusion

AFT columns functioning in the CF mode of operation show promise as a powerful addition to an analyst's toolbox. Using these columns the sample through-put was increased 5-fold compared against standard columns of the same internal diameter, while analytical sensitivity increased also by as much as 10-fold. Analytical through-put on the CF columns was the same as the through-put on conventional columns with the same internal diameter as the virtual column. However, the analytical sensitivity (S/N) on the CF column was as much as 66-fold higher. These gains were obtained because the solvent volume load to the MS was reduced since AFT columns selectively extract mobile phase (and solute) from the radial central region of the column, subsequently also reducing the baseline noise response in the detector. It is hard to argue against the benefits of these columns for users of LCMS. Gains were observed in through-put and sensitivity, and in addition, the injection to injection precision in the measurement of peak height was better on the CF column compared to either conventional column.

Chapter 5.

Improving Quantification Using Curtain Flow Chromatography Columns in the Analysis of Labile Compounds: A Study on Amino Acids

5.1 Introduction

The performance of CF chromatography column technology with MS detection was evaluated for the analysis of unstable compounds i.e. thermally and/or solvent labile compounds. The CF column design allows for separations that are faster and/or more sensitive than conventional columns, depending on how exactly the CF column is configured – this was detailed in Chapter 4. For example, when mass spectroscopy is used as a detector, the CF column can yield separations that are 5-times faster than conventional columns of the same internal diameter. Or when the internal diameter of the conventional column is reduced in order to yield the same analytical through-put as the CF column, the sensitivity on the CF column can be as much as 66-fold higher than the conventional column [109].

This chapter examines the assay reliability using curtain flow AFT columns when applied to the analysis of labile compounds. The analysis of amino acids was used as a test, comparing the outcome for conventional HPLC columns to the AFT columns.

5.2 Experimental

5.2.1 Chromatography Columns.

The columns used in this chapter were detailed in Chapter 2, and more specifically, they are the same set of columns used in Chapter 4.

5.2.2 Chemicals and Reagents

Refer to Chapters 2 and 4.

5.2.3 Instrumentation UPLC-MS/MS

Refer to Chapters 2 and 4.

5.2.4 Mass Spectrometry Parameters

Refer to Chapters 2 and 4.

5.2.5 Quantification Protocol

Reliable quantitative analysis necessitates optimal performance of the mass spectrometer, as well as a suitable sample analysis protocol so as to maintain sample and quality control standard integrity through-out the assay. Often calibration standard curves are established, and standards re-analysed

periodically throughout the assay. The frequency of repetition is dependent on the accepted level of analytical variability; a factor determined by the sample stability and the instrumental drift. The more labile the samples/standards, the greater the frequency of repetition of re-analysis of the calibration standards. In addition, or perhaps as a rapid check, system suitability tests (SST) are often incorporated into the assay sequence in order to provide a check on the change in sensitivity that may occur during the assay. A change in the sensitivity of the SST is an indication of either or both, instrumental drift or standard stability.

In the work undertaken here, an injection sequence of analysis was undertaken according to the following protocol: three SST injections of a single standard at 100 ng/mL, five levels of calibration standards, each injected in triplicate, sample injections (each in triplicate – totalling 12 injections), a second calibration curve (five levels injected in triplicate) and finally three replicates of the same SST sample as per the first injection within this sequence. In total, there were fifty nine injections with 50 injections between each set of SST standards and 20 injections between the first standards in each of the replicate calibration curves. The purpose of this injection protocol was to effectively evaluate the benefits of analytical speed in the analysis of compounds that degrade at the bench, hence highlighting a beneficial feature of Active Flow Technology (AFT). The same sequence protocol was undertaken on each of the three column formats.

5.2.6 Column Testing.

Column performance tests were undertaken to demonstrate the loss in column efficiency as a function of the injection volume. These tests were undertaken on the 2.1 mm i.d. conventional column only. The test mixture comprised three alkylbenzenes - toluene, propylbenzene and butylbenzene. The concentrations of these three alkylbenzenes were adjusted such that for each injection volume the mass load remained constant. The mobile phase composition was 40/60 water/methanol, and the flow rate was 0.44 mL/min, injection volumes were 1, 5, 10 and 20 µL. Detection was set at 254 nm.

5.3 Results and Discussion

The total analysis time required for undertaking the testing protocol described in Section 5.2.4 was 4.5 h for the conventional 2.1 mm i.d. column and the 4.6 mm i.d. CF column, and 13 h for the conventional 4.6 mm i.d. column. Amino acids were chosen for this study because of their instability in an unregulated atmospheric environment. As such, no effort was made to prolong their

storage lifetime, since the purpose of this study was to highlight the importance of a high speed separation protocol to improve assay reliability. System suitability test standards were monitored to gauge the extent of the change in sensitivity over a period of time.

Since the mobile phase velocity was five times greater on both the CF and 2.1 mm i.d. columns compared to the conventional 4.6 mm i.d. column, each separation was completed five times faster than on the conventional 4.6 mm i.d. column. This is shown in Figure 5.1, illustrating for example, the extracted ion chromatogram of phenylalanine. The retention time of phenylalanine was 2.26 min on the 4.6 mm i.d. column, which was 5 times that on the 2.1 mm i.d. column, consistent with the difference in the flow velocities between these columns. Likewise the retention time on the CF column was 5 times less than on the 4.6 mm i.d. conventional column, while approximately the same as on the 2.1 mm i.d. column.

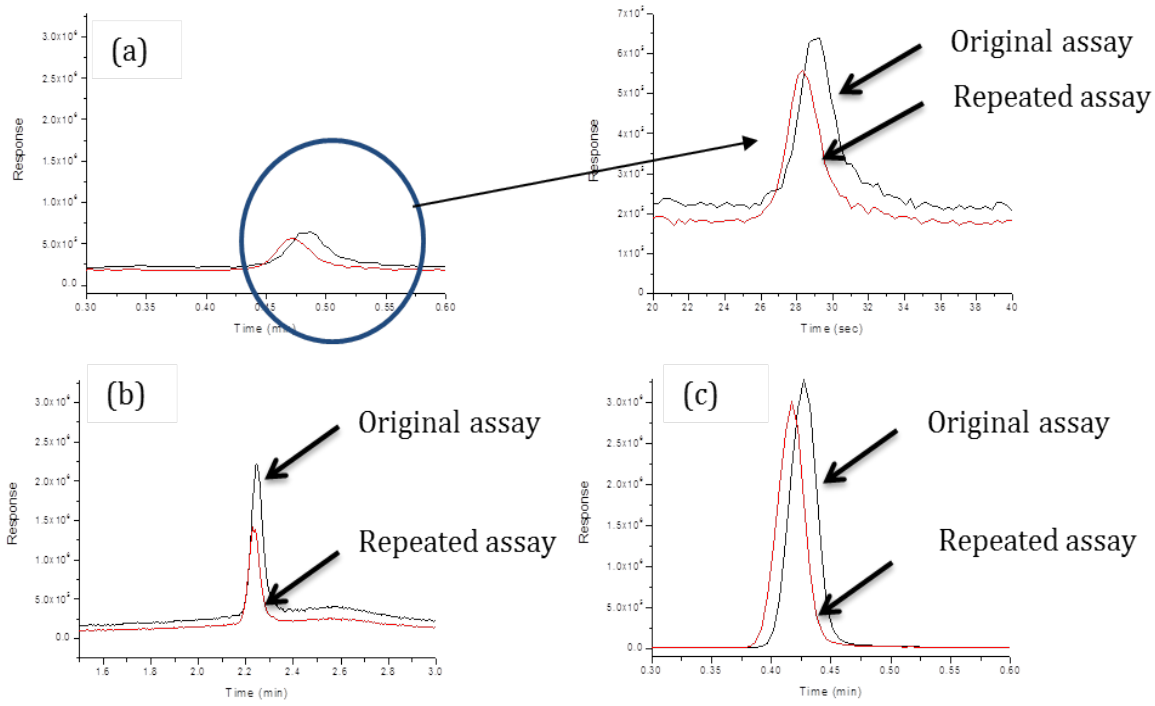

Figure 5.1 Extracted ion chromatograms of phenylalanine derived from each of the three columns. Trace (a) is the chromatogram obtained on the 2.1 mm i.d. conventional column, trace (b) for the 4.6 mm i.d. conventional column and trace (c) is the CF column.

The chromatograms in Figure 5.1 also show that there is a greater signal response for the analysis employing the CF column, compared to both the conventional columns, especially in comparison against the 2.1 mm i.d. conventional column. The gain in signal response observed on the CF column was 7.7 times that of the 2.1 mm i.d. column, which exceeds that of the 5-fold load difference between these columns. Moreover, the actual gain in analytical sensitivity, as measured

according to the signal to noise response was as much 66-fold, with an average gain of 37-fold depending on the amino acid [109]. Interestingly, the gain in signal response for the conventional 4.6 mm i.d. conventional column, compared to that on the 2.1 mm i.d. column, exactly matches the ratio of the injection volumes, i.e., 1.04:5 (Figure 5.1). Hence effectively, irrespective of the format for conventional columns the same level of signal response was observed. It must be remembered that electrospray ionisation was employed, which is concentration sensitive. This was detailed in prior work [3].

Unless specific methodology is employed that enhances sensitivity by virtue of changing the nature of the solute injection plug relative to the mobile phase environment [110,111], injection volumes across different column formats should always be scaled to match that of the column cross-sectional area since the height to a theoretical plate does not remain constant as the injection volume increases. When injection volumes are not scaled, the separation efficiency on a 4.6 mm i.d. column will be greater than on a 2.1 mm i.d. column because signal sensitivity is also related to separation efficiency, i.e., narrow distributions present taller peaks.

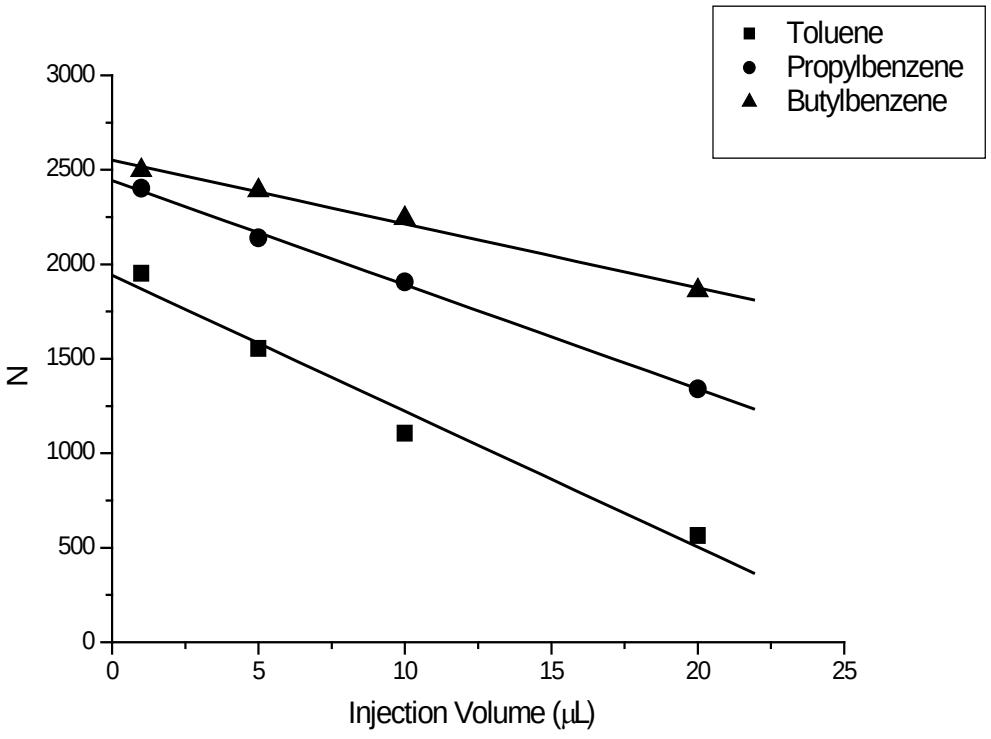

Figure 5.2 Plot of column efficiency (N) versus injection volume, for alkylbenzenes tested on a conventional 2.1 mm i.d. column.

The data shown in Figure 5.2 for example details the loss in column performance as a function of injection volume. Here a loss in column efficiency of 70% was apparent as the injection volume was increased from 1 to 20 µL on a 4.6 mm i.d. column, for the weakly retained analyte, toluene. Even as the retention increased the loss of efficiency was substantial, i.e. 45% and 25% for propylbenzene and butylbenzene respectively. As a result, there was a disproportional peak height with respect to sample load and column format as a function of injection volume for a constant mass load, i.e. sensitivity effectively decreases as the injection volume decreases due to loss of efficiency and the subsequent band broadening, as shown for the elution of the toluene band in Figure 5.3.

Hence for rigorous comparison, it is appropriate to ensure the column efficiency is maintained across the different column formats. Thus injection volumes are scaled to the column internal diameter.

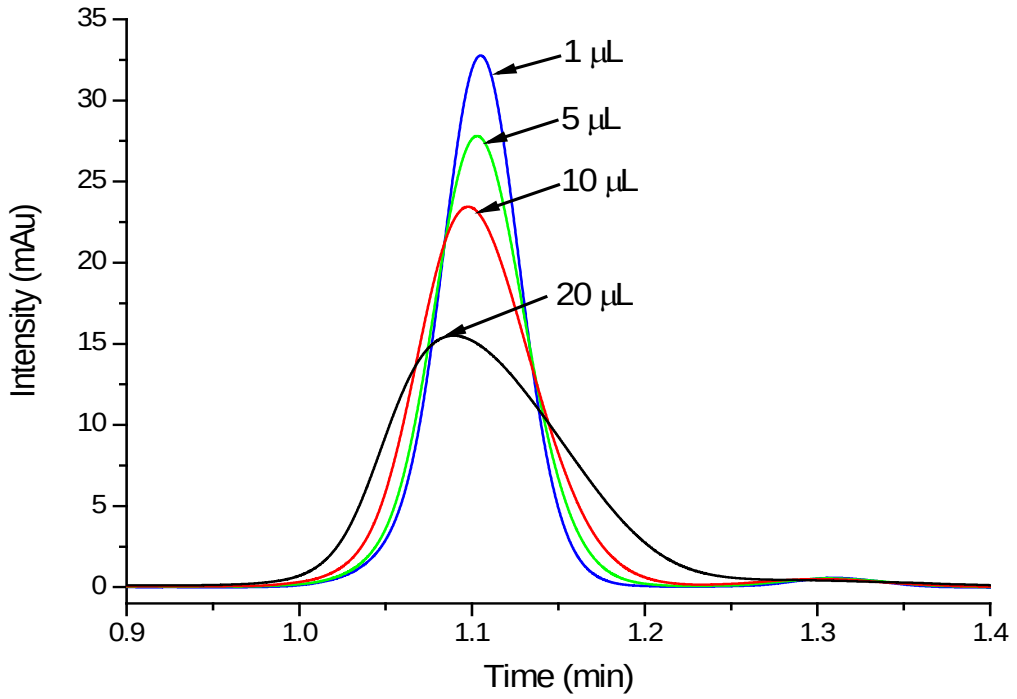

Figure 5.3 Illustration of the peak shape for the toluene band as a function of the injection volume. Flow rate 0.44 mL/min, mobile phase 40/60 water/methanol (column 2.1 mm format).

Calibration curves for the amino acid standard series were linear, irrespective of the column format. Curves for five of the amino acids tested are shown in Figure 5.4 (a - c), and the metrics of these curves are given in Table 5.1. Of note, is that r^2 were always greater than 0.98, irrespective of the amino acid, or column employed for the assay.

The chromatographic profiles of phenylalanine are shown in Figure 5.5 as an example of the change in sensitivity that was apparent between replicate analyses of the calibration data, being 2.25 hours between injections on both the CF and 2.1 mm i.d. columns, and 7.5 hours on the conventional 4.6 mm i.d. column. In the case of the CF column, the change in peak height of phenylalanine for example (a reflection of the sensitivity and sample stability) decreased by the least, 7%. In comparison a higher decrease in peak height was observed on the 2.1 mm i.d. conventional column (22%), while a very large decrease in peak height was observed on the 4.6 mm i.d. column (37%).

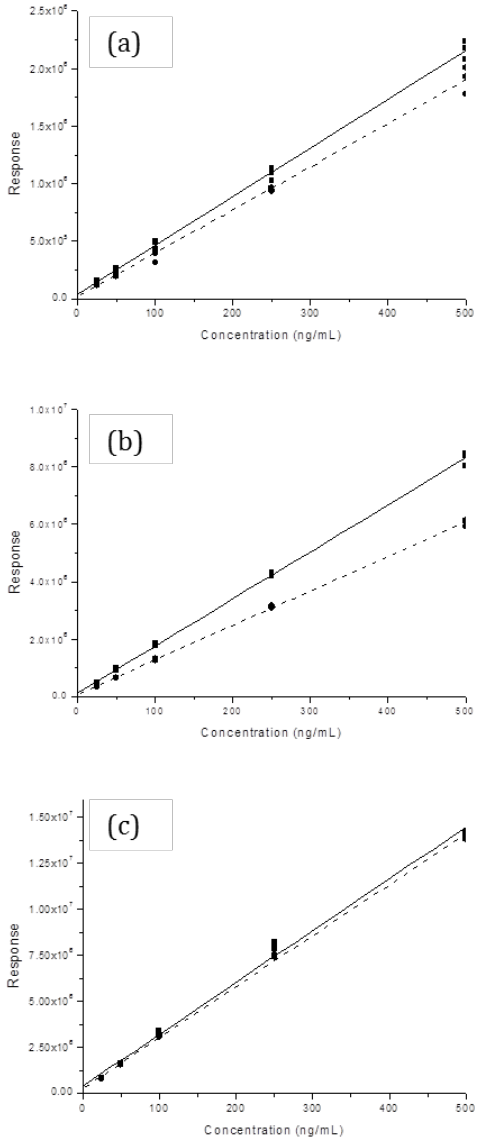

Figure 5.4 Calibration curves for phenylalanine obtained on each of the columns: Figure (a) is the calibration curve obtained on the 2.1 mm i.d. conventional column, figure (b) for the 4.6 mm i.d. conventional column and figure (c) is the CF column.

Column (calibration curve)	Methionine	Tyrosine	Threonine	Tryptophan	Phenylalanine
4.6 mm i.d. conv. column *(1^{st} curve – slope/r^2)*	2074/0.994	2904/0.994	5942/0.995	5466/0.998	17068/0.996
4.6 mm i.d. conv. column *(2^{nd} curve – slope/r^2)*	1479/0.992	2084/0.995	4424/0.997	4130/0.998	12386/0.998
2.1 mm i.d. conv. column *(1^{st} curve – slope/r^2)*	680/0.998	1100/0.987	1682/0.998	1133/0.994	4450/0.989
2.1 mm i.d. conv.column *(2^{nd} curve – slope/r^2)*	592/0.996	1032/0.983	1422/0.985	947/0.995	3855/0.986
4.6 mm i.d. CF *(1^{st} curve – slope/r^2)*	4600/0.984	7401/0.993	10046/0.998	10045/0.999	30261/0.992
4.6 mm i.d. CF *(2^{nd} curve – slope/r^2)*	4182/0.981	6884/0.993	9239/0.997	9283/0.999	29034/0.996

Table 5.1 Slope and correlation coefficient for each set of calibration data for each amino acid on the conventional 2.1 and 4.6 mm i.d. columns and the 4.6 mm i.d. CF column.

This greater decrease in peak height, apparent when comparing the CF column to the 4.6 mm i.d. conventional column is easily explained by virtue of the fact the total analysis was 3.5 times faster in the CF mode. Obviously, the sample degradation across the period of time required on the 4.6 mm conventional column is greater.

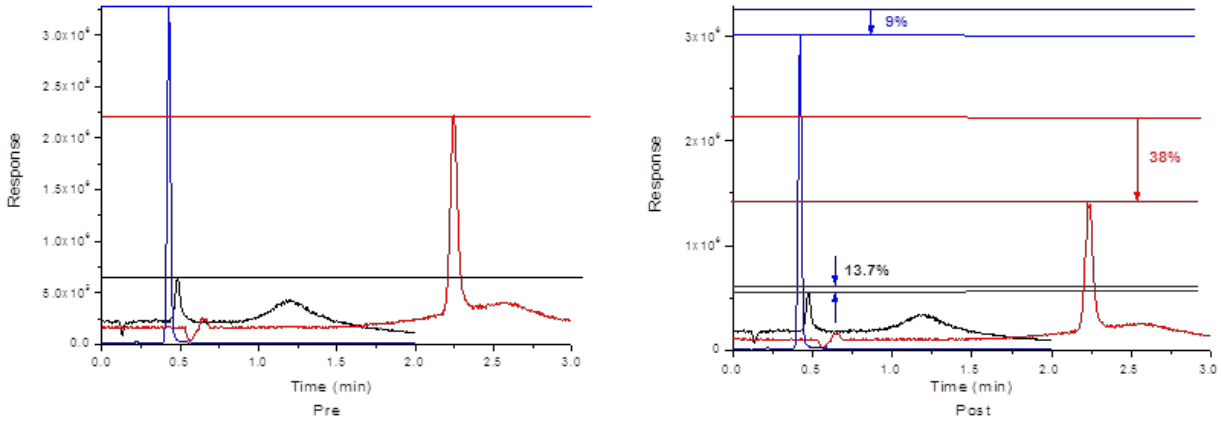

Figure 5.5 (a) Extracted ion chromatograms of phenylalanine derived from each of the three columns at the beginning of the sequence. Black trace is the chromatogram obtained on the 2.1 mm i.d. conventional column, red trace is for the 4.6 mm i.d. conventional column and blue trace is CF column. Pre-beginning of the sequence; Post-end of the sequence.

However, it is less obvious as to why the difference in change in signal response on the CF column and the 2.1 mm i.d. column was as large as that observed, since these analyses were completed in the same period of time. We suspect, that this difference reflects the fact that on the 2.1 mm i.d. column the analysis was closer to the limits in quantification and subsequently, the uncertainty in quantification was greater. This is supported by the larger R.S.D values recorded on replicate analyses on the 2.1 mm i.d. format column compared to the CF column [109], and the higher noise response of baseline data [109]. Irrespective, these trends were consistent across all amino acids tested, and the range in degradation varied between 7 to 12% on the CF column, 11 to 30% on the 2.1 mm conventional column, and 35 to 41% on the 4.6 mm i.d. conventional column. These relative changes were far greater than the R.S.Ds. of the replicate injections for each amino acid tested on each of the three columns. The data in Table 5.2, for example, presents the relative standard deviations for the system suitability tests undertaken on the 100 ng/mL standard solution for the five amino acids reported here. On the 4.6 mm i.d. conventional column, the R.S.D were between 0.7 to 3% for all amino acids. On the 2.1 mm i.d. conventional column the R.S.Ds were between 3 to 8%, while on the CF 4.6 mm i.d. column the R.S.Ds were between 0.9 to 4%.

As a result of the standard degradation, the calibration curves were also affected. The changes observed on the CF column were relatively minor, greater on the convention 2.1 mm i.d. column, but substantial greater on the 4.6 mm i.d. conventional column. These differences in calibration had a significant effect on the quantified data obtained from the calibration over the extended period of the analysis. For example, the accuracy in the determination of the concentration

of the back-calculated concentration of the system suitability tests varied by 7% when quantification was based on the first calibration set, compared to the second calibration set for phenylalanine, when analysed on the CF column. When the same analysis was undertaken using the 2.1 mm i.d. conventional column, the variation over the same period of time was 22%, and for the 4.6 mm i.d. column, where the analysis exceeded 13 hours, the variation in the back-calculated concentrations of the system suitability was more than 38%. This degree of variation for all system suitability test standards was consistent across each of the amino acids tested as detailed in Table 5.2.

Column	**Time between SST injections (h)**	**R.S.D for System Suitability Test (100 ng/mL) (%) (Amino Acid Degradation (%))***				
		Methionine	**Tyrosine**	**Threonine**	**Tryptophan**	**Phenylalanine**
4.6 mm i.d. conventional	13	3.0 (41)	1.3 (40)	3.0 (35)	0.77 (35)	1.8 (38)
2.1 mm i.d. conventional	4.5	6.0 (19)	7.8 (11)	4.1 (26)	3.6 (29)	4.2 (22)
4.6 mm i.d. CF	4.5	1.8 (7.8)	3.4 (9.6)	4.0 (8.8)	2.5 (12)	0.92 (6.6)

*Degree of standard degradation (expressed as %, based on change in peak height)

Table 5.2 Injection reproducibility and degree of standard degradation for each amino acid on each of the three columns.

The above data demonstrates the importance of frequent calibration in the analysis of labile compounds. It also shows that greater accuracy in the analysis is obtained when the through-put is increased, since there is less degradation occurring in the shorter period. Hence, higher through-put enables less frequent calibration, which improves the sample to standard ratio, favouring a greater rate of sample analysis.

5.4 Conclusion

The separation speed afforded by CF column technology when coupled to MS detection can significantly increase analytical productivity. Sample through-put can be maximized, yielding a decrease in the required number of standards in order to maintain the appropriate levels of quantitative reliability. High speed analyses are especially important in the analysis of labile compounds, such as amino acids. The next most important step in gaining further advances in sample through-put is to design high speed injection processes that will enable HPLC-MS analyses in time frames consistent with direct injection MS.

Chapter 6.

Using Active Flow Technology Columns to Achieve Near ‘Direct’ Injection Through-put in HPLC-MS

6.1 Introduction

The separation powers of high performance liquid chromatography (HPLC) and mass spectrometry are complimentary as they are effectively orthogonal. HPLC provides a means to physically resolve components as they migrate through a stationary phase media, by means of chemical or physical selectivity. The MS separates these species further according to their mass to charge ratio, or effectively, the period of time required by specific molecular fragments to traverse a magnetic field. Hence the combination of these two separation processes has resulted in an extremely powerful technique that dominates many analytical assays. There is no doubt, however, that if it were possible, users of mass spectrometry would prefer to do away with the HPLC component since HPLC is a serious source of limitation with respect to assay through-put, since significant residence time is required to separate components within the HPLC column, usually between 5 to 30 minutes. That being said, the more complex the sample, the greater the benefit from the front end separation provided by the HPLC. Nevertheless, the ideal technique to satisfy high through-put is by direct injection of solute into the MS. Realistically this can only be achieved for simple sample matrices or samples that have a well-defined component identity.

While the HPLC process limits the through-put of HPLC-MS analyses due to the time required to undertake the separation, the MS is also a source of limitation in assay throughput. There is a limit to the volume of solvent that can be processed by the MS. In effect, it is the interface between HPLC and MS that is the primary limitation to the power of the technique.

In this chapter, Active Flow technology (AFT) functioning in a parallel segmented flow (PSF) mode was utilised for the analysis of amino acids at very high through-puts. Since the volumetric flow that elutes from the active flow technology column is reduced in proportion to the segmentation ratio, the volume of mobile phase that enters the mass spectrometer is reduced. This enables separations to be undertaken at higher volumetric flow rates without compromising the flow limitations of the MS. It is the purpose of this study to demonstrate the application of these columns in narrow bore formats for ultra-high speed separations with MS detection that rival direct injection speed of analysis, but with the added advantage of significant separation of components prior to analysis using the MS.

6.2 Experimental

6.2.1 Chromatography Columns

The columns used in this chapter were packed with 5 µm particles, in either 50 or 30 mm in length and either 4.6 or 2.1 mm i.d. See Section 2.1.2 for further details.

6.2.2 Chemicals and Reagents

Section 2.1.1.

6.2.3 Instrumentation

Section 2.4.

6.2.4 Mass Spectrometry Parameters

Section 2.1.3.

6.2.5 Chromatographic Separation

Column Efficiency

The analysis of alkylbenzenes was undertaken using isocratic elution conditions (water/methanol mobile phase (40/60)). The column performance was tested at either 5 mL/min (in the case of the 4.6 mm i.d. columns), or at 2.5 mL/min (in the case of the 2.1 mm i.d. columns). Injection volumes were either 1 µL (2.1 mm i.d. format columns) or 5 µL (4.6 mm i.d. format columns). Detection was by UV at 254 nm with an acquisition frequency of 200 Hz. The number of theoretical plates was measured using the second moment method.

Amino Acid Analysis

Amino acid separations were performed in both isocratic elution mode using a water/methanol (95/5), (+0.1% formic acid) mobile phase, and in gradient mode, where the initial mobile phase was 5/95 water/methanol (+0.1% formic acid) running to 35/65 water/methanol (+0.1% formic acid). For the conventional 4.6 mm i.d. column the gradient period was 6 minutes and on the PSF column the gradient period was 1.2 minutes (since the volumetric flow rate was 5x higher). Detection was achieved using electrospray ionisation in positive ion mode using single reaction monitoring (SRM) with the following parameters: vaporiser temp at 500^{o}C, capillary temp at 350^{o}C, sheath gas at a rate of 60 units, auxiliary gas flow at 40 units and sweep gas flow at 5 units. Spray voltage was maintained at +3.5 kV. Collision energy and tube lens offset was individually optimised for each compound.

The mobile phase flow rate was adjusted such that for all experiments the volume presented to the MS was always 1 mL/min. That is for the conventional 2.1 mm i.d. column the flow rate through the column was 1 mL/min, while the 2.1 mm i.d. PSF column had a total flow rate of 6 mL/min but only 1 mL/min entered the MS since slightly less than 20% of the flow exited the central port of the PSF column into the MS.

6.3 Results and Discussion

In this study a range of columns were employed. These columns had various internal diameters and were either in conventional mode or PSF mode. Prior to analyses undertaken using MS detection, HPLC-UV was used to measure the performance of conventional and PSF columns (4.6 or 2.1 mm i.d.) at pressures between 300 – 350 bar. For the 4.6 mm i.d. conventional and PSF columns, plate counts were measured at the flow rate of 5 mL/min, using toluene, propylbenzene and butylbenzene as test solutes. For the 2.1 mm i.d. conventional and PSF columns, plate counts were undertaken at 2.5 mL/min. In both the 4.6 and 2.1 mm i.d. PSF formats the outlet segmentation ratio was 20%, that is, 20% of the flow was allowed to exit the column via the central outlet exit port. Under these conditions the 4.6 mm i.d. PSF column emulated a virtual 2.1 mm i.d. column, and the 2.1 mm i.d. PSF column emulated a virtual 1 mm i.d. column.

Table 6.1 details the plate counts, measured using the second moment method. The gains in separation performance for the PSF columns compared to traditional columns were more substantial for the 2.1 mm i.d. formats, achieving as much as a 65% increase in N for the butylbenzene band. This performance gain is pictorially visualised in Figure 6.1, which shows the overlay of the butylbenzene peaks for the conventional (black) and PSF (red - dashed) columns. The degree of peak fronting is greatly reduced when the PSF columns are utilised. From this plate count data it is evident that the separation efficiency of the PSF column is far superior to that of the conventional column when operated near the pressure limits of the column. Together with the ability to separate the wall or peripheral flow from the central flow stream when using PSF columns means that only the most efficiently transported solute is sent to the detector, in the following experiment, the MS detector. Hence a lower volumetric proportion of the mobile phase is transported to the MS, enabling greater through-put at higher efficiency.

Compound	N (= tr^2/σ^2) (4.6 mm Conv.)	N (= tr^2/σ^2) (4.6 mm PSF)	N (= tr^2/σ^2) (2.1 mm Conv.)	N (= tr^2/σ^2) (2.1 mm PSF)
Toluene	1667	1918	708	909
Propylbenzene	1905	2557	1037	1532
Butylbenzene	2252	2751	1039	1711

Table 6.1 Plate counts measured using the second moment method. Mobile phase 60/40 water/methanol, flow rates 5 mL/min on the 4.6 mm i.d. columns, and 2.5 mL/min on the 2.1 mm i.d. columns, UV detection.

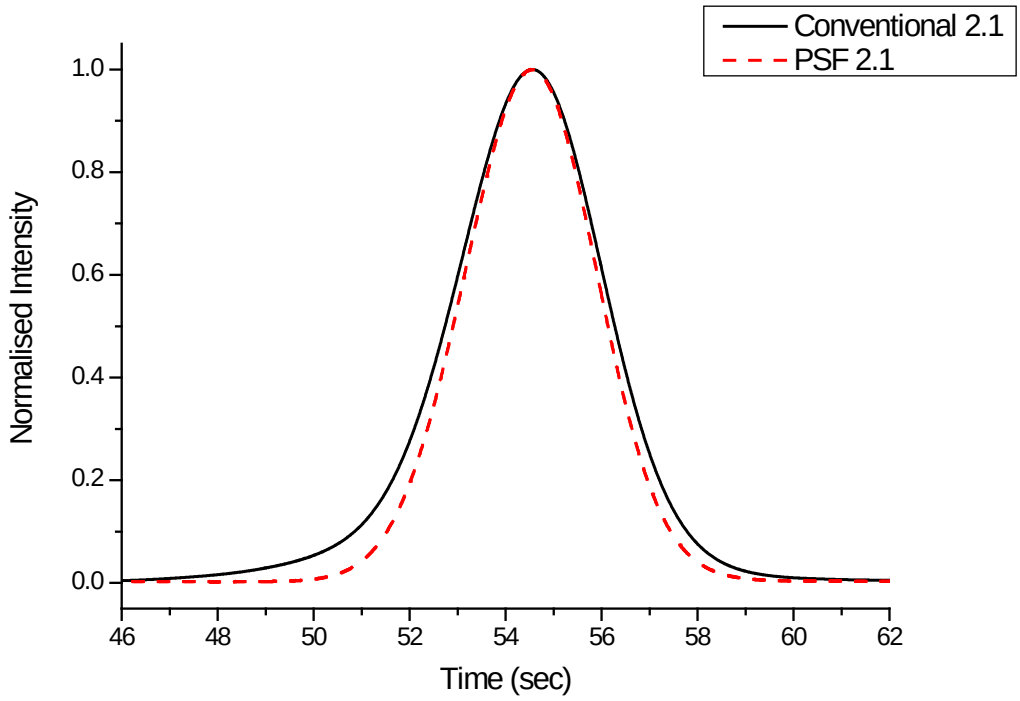

Figure 6.1 Illustration of the peak profiles for butylbenzene eluting from the 2.1 mm i.d. format columns. The flow rate on both the conventional and the PSF columns was 2.5 mL/min.

In this study, comparison was made between separations obtained on conventional columns and PSF columns. In order to do so, flow to the MS was kept constant, irrespective of the column. The flow rate to the MS was always 1 mL/min, which means that the PSF column could be operated at higher flow rates, thus improving analytical through-put. The flow rate of 1 mL/min entering the MS was chosen because this provided for stable and reliable MS operation, although at this flow rate the MS is close to its limits of operation given the high aqueous content of the mobile phase.

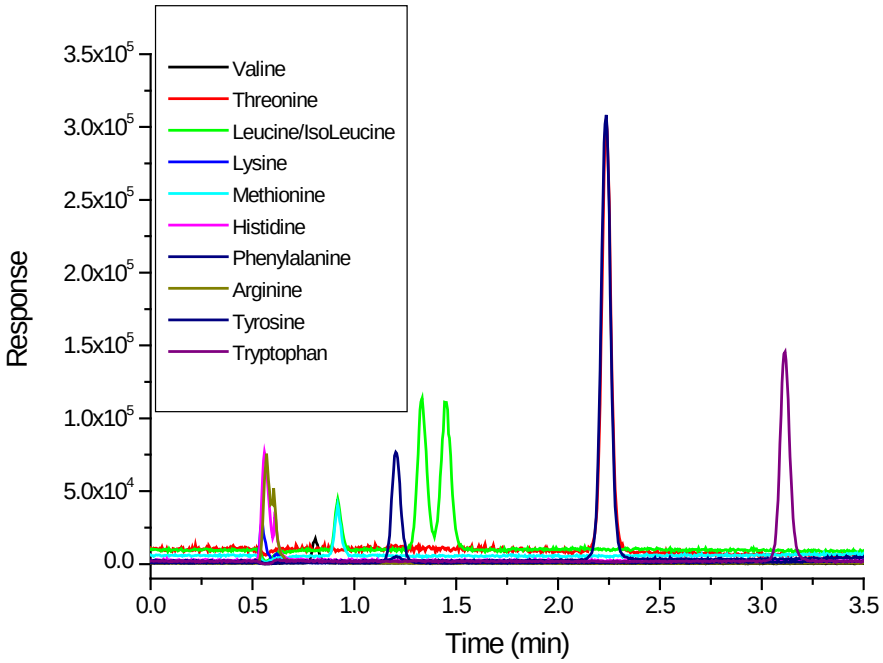

Figure 6.2 Extracted ion chromatograms of the amino acid separations undertaken on a 50 × 4.6 mm i.d. conventional column at flow of 1 mL/min; MP composition was 5% methanol in isocratic mode. Flow to the MS detector was 1 mL/min.

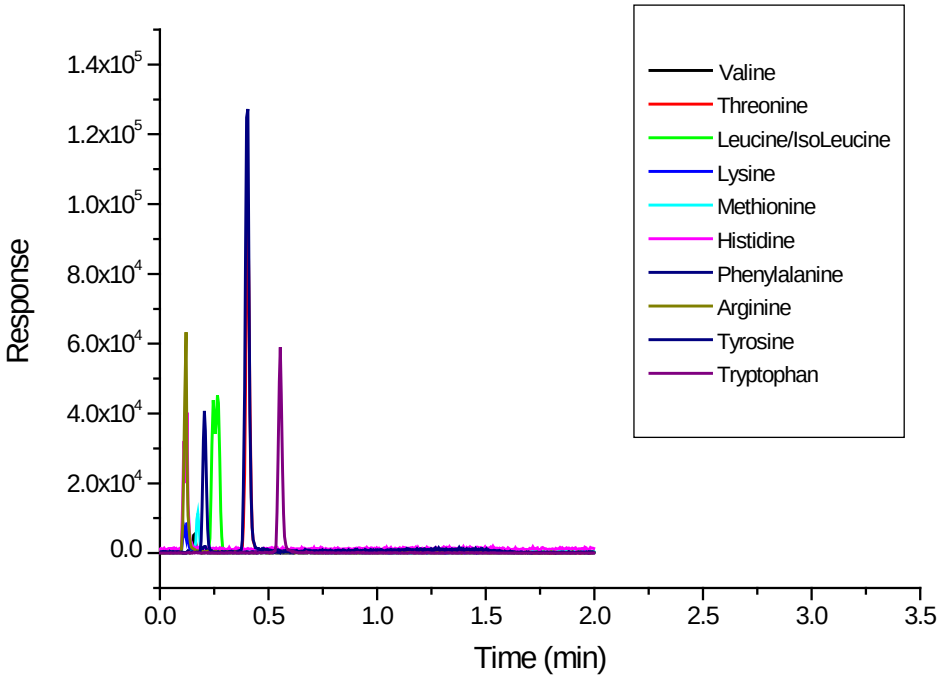

Figure 6.3 Extracted ion chromatograms of the amino acid separations undertaken on a 50 × 4.6 mm i.d. PSF column at flow of 5 mL/min; MP composition was 5% methanol in isocratic mode. Flow to the MS detector was 1 mL/min.

The amino acid test mixture was analysed on all columns using this limiting condition of operation for the MS detector. Under these conditions the extracted ion chromatograms for each of the amino acids in the standard test mixture were recorded. When the 4.6 mm i.d. column was employed, separations were undertaken using gradient elution, and the resulting separations are shown in Figure 6.2 and Figure 6.3 for the conventional and PSF columns respectively. The separation undertaken on the conventional column was at the flow rate of 1 mL/min, satisfying the limiting MS condition, while the separation undertaken on the PSF column, with a 20% outlet segmentation ratio, was at the flow rate of 5 mL/min, also satisfying the limiting MS condition (gradient steepness was scaled in accordance to the different flow rates between each column). Under these separation conditions, the analysis on the PSF column was completed in 20% of the time required for the same separation using a conventional column, but there was a slight loss in sensitivity. For visual comparison, the time axis in Figure 6.3 is scaled the same as in Figure 6.2, highlighting the gain in analytical through-put achievable when using PSF columns in conjunction with MS detection. At the higher flow rate on the PSF column, however, there was a slight loss in resolution for some components, most notably, leucine and iso-leucine.

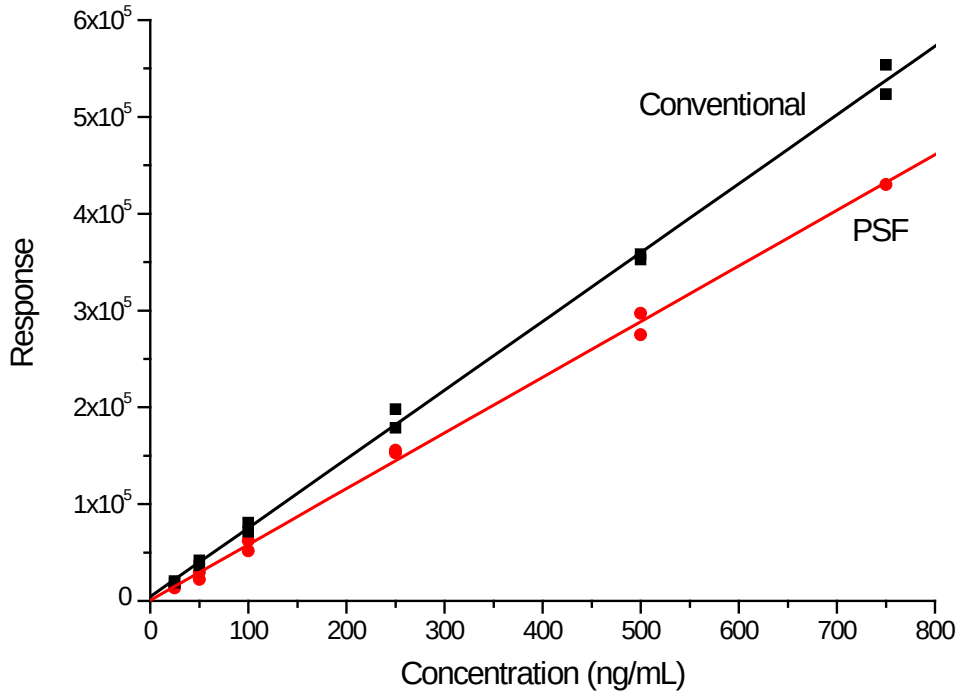

Figure 6.4 Calibrations obtained for tyrosine on conventional and PSF columns. Chromatography conditions are same as in Figures 6.2 and 6.3.

In order to improve analytical through-put using conventional columns the analyst has two options: either (1) to use a higher volumetric flow rate through the column, and employ a post-column flow stream splitter, or (2) decrease the column internal diameter, and at the same time maintain the same flow rate to the MS, without the need for post-column flow stream splitting. The second choice is usually employed in modern HPLC-MS analyses, largely for convenience. Hence, in this work the use of narrow bore columns was also adopted as a means of maximising sample through-put with the MS detection. To further minimise cycle time for analyses, isocratic elution was employed rather than gradient elution, which requires significant column re-equilibration time before subsequent analyses. The separation that was achieved on the conventional 2.1 mm i.d. column is illustrated in Figure 6.5, at the flow rate of 1 mL/min all amino acids eluted within 40 seconds, albeit, with numerous overlapping bands. However, given the orthogonal separating power of the MS, these co-eluting species were easily identifiable by the MS and hence there was no problem in their detection. Although 40 seconds run time could be deemed as a high-speed separation, PSF columns allow for even faster separations. For example, the 2.1 mm i.d. PSF column was operated at the flow rate of 6 mL/min, and the outlet segmentation ratio was adjusted to deliver 1 mL/min to the MS. Under these conditions the separation was completed in less than 6 seconds, and this separation is illustrated in Figure 6.6. This chromatographic separation is almost identical to that obtained on the conventional column, but it was 6-times faster. In fact, this 6 second separation approaches the time scale achieved for direct injection, but with the benefit of a physical separation step prior to the MS analysis. Note, on the 2.1 mm format columns sensitivity between the conventional mode of operation and the PSF mode was almost constant, unlike the situation for the 4.6 mm i.d. columns, as stated above. A limitation, however, of the separation obtained on the PSF column is related to the speed of data acquisition of the MS. Using a volumetric flow rate of 6 mL/min and a segmentation ratio around 18% results in very narrow bands, some peaks were detected with just 2 data points using the MS, hardly enough for quantitative purposes, so quantification is not reported here. This was the case even when the acquisition rate of the MS was set at 500 Hz, but since 10 components were being scanned for a primary and a daughter ion, the effective scan rate was far too slow for these ultra-high speed separations. Clearly, even for this very simple sample mixture, containing just 10 components, the limitations of the acquisition rate of the MS would likely severely limit the accuracy of the quantitative analysis and in order to fully accommodate the separation power of the PSF column, greater improvements in MS technology is required.

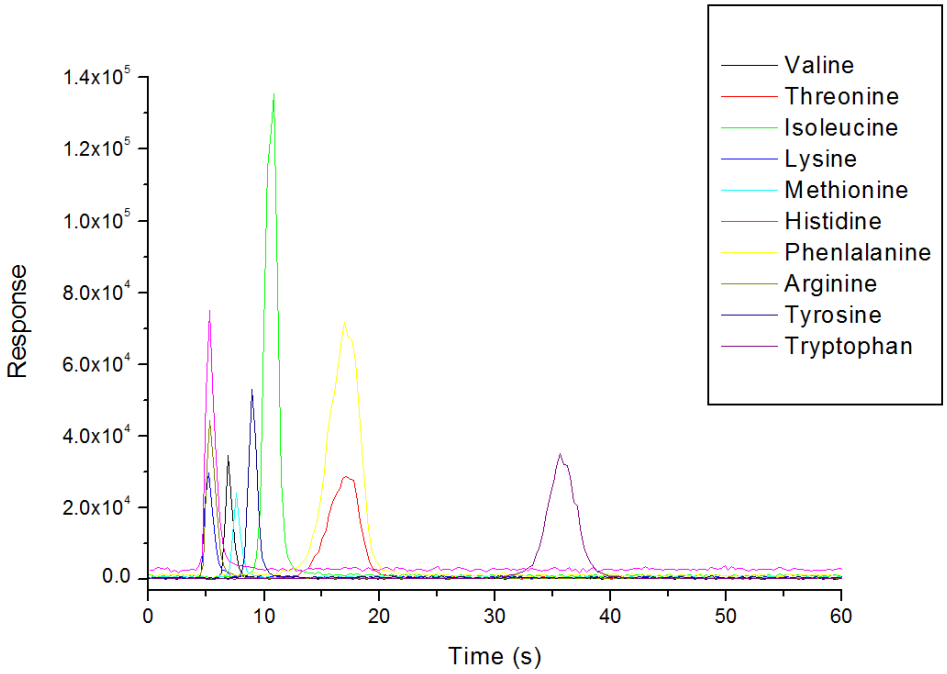

Figure 6.5 Extracted ion chromatograms of the amino acid separations undertaken on a 30 mm × 2.1 mm i.d. conventional column at flow of 1 mL/min.; MP composition was 5% methanol in isocratic mode. Flow to the MS detector was 1 mL/min.

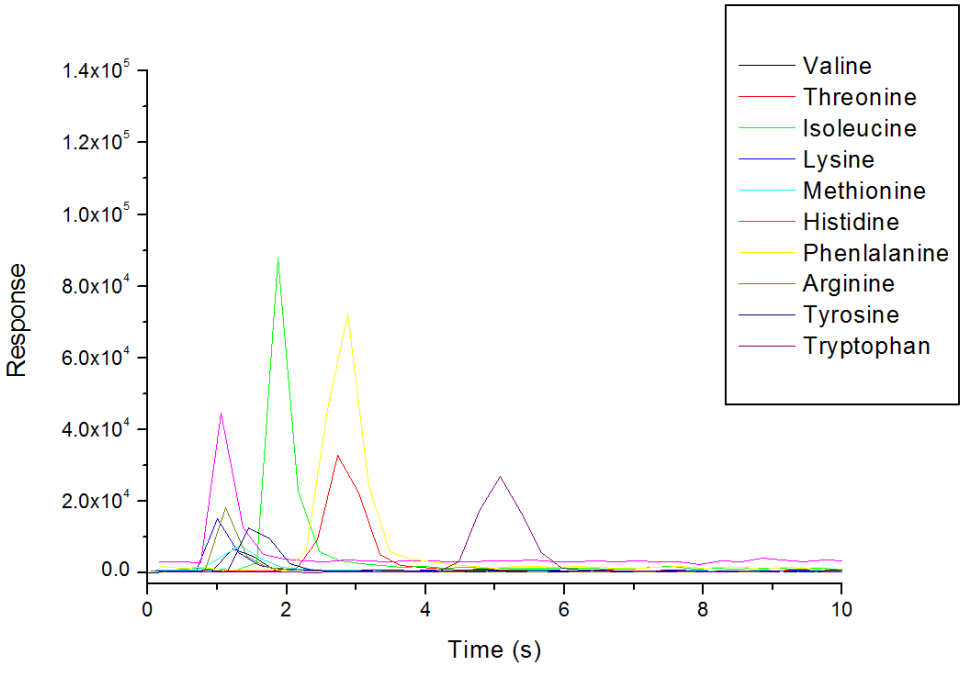

Figure 6.6 Extracted ion chromatograms of the amino acid separations undertaken on a 30 mm × 2.1 mm i.d. conventional column at flow of 1 mL/min.; MP composition was 5% methanol in isocratic mode. Flow to the MS detector was 1 mL/min.

In this study it is important to emphasise that maximised through-put was the primary separation objective, and neither the conventional nor the PSF column were operated at their optimal flow velocity with respect to separation efficiency. However, the PSF column being driven significantly harder than the equivalent i.d. conventional column. The PSF column operating at 6 times the flow rate as the same i.d. conventional column still yielded a separation performance quite similar to the conventional column, showing clearly that ultra-high speed separations are very feasible with active flow technology columns enabling what could be described as ‘pulsed direct injection’ HPLC-MS, where a pulse is established by the residence time on a chromatographic column.

6.4 Conclusion

Using PSF column technology separations for the first time approached the through-put limits of direct injection MS techniques. The true benefit, however, is that the PSF column provides a physical separation step not available in direct injection protocols, and this provides for the separation of components of a mixture, which improves the quality of the data from subsequent MS analyses. A limitation of the MS when coupled to PSF column technologies for separations taking less than 6 seconds is that the MS scan rate may be too slow to enable appropriate quantification of components, but it is still very useful for qualitative identification of these components. Improvement of quantitative analyses undertaken using MS detection requires advances in MS technology, and must be addressed as PSF technology expands the limits of performance in HPLC-MS assays.

Chapter 7.

Pulsed Direct Injection for Ultra-Fast HPLC MS Analyses

7.1 Introduction

In this chapter a new development in HPLC-MS is presented, whereby, the speed of the analysis is essentially equivalent to direct injection protocols applied in analyses using MS alone. This technique is referred to as pulsed direct injection HPLC-MS. The key to this technique is use of Active Flow Technology (AFT) columns as they can enable the radial central portion of the flow to be sampled from the column and directed to a detector, discarding the peripheral flow to waste, and hence reducing the volumetric load to the MS detector. Furthermore, the radial central region of the flow through the column is the most efficient region of the solute migration, free from wall effects. In this study the internal diameter of the AFT column was 2.1 mm, the flow rate was 4.5 mL/min and 21% of this flow was sampled from the radial central region of the column; thus the flow to the MS detector was just 0.9 mL/min. The study presents details of the injection to injection reproducibility in this analysis, highlighting the substantial benefit of being able to undertake ultra-high through-put HPLC-MS .

Recently, Agilent technologies introduced a new analytical technique referred to as '*RapidFire'*, which is effectively a high throughput MS screening process for the analysis of relatively simple samples [112,113]. In *RapidFire*, samples are displaced onto a cartridge that contains an adsorption media, typically for the removal of salts, and then eluted to the MS. The capacity of the adsorption cartridge is limited, but it nevertheless serves to provide a very basic sample clean-up step prior to the MS, since in many analyses the removal of salts with just a few theoretical plates is sufficient to provide adequate quantitative information. Analyses are then undertaken at the speed effectively equivalent to direct injection, albeit, the cartridge approach to providing sample clean-up, offers very limited separation capacity.

In Chapter 6 it was demonstrated that AFT columns show great promise in providing a means to yield very fast, and very efficient HPLC-MS analyses, in the same time frame as *Rapidfire*, but with a chromatographic separation step that comprises sufficient theoretical plates to yield chromatographic separation. In this chapter the focus is on how AFT columns can be utilised to achieve ultra-high speed separations when coupled to MS detection, effectively emulating direct injection protocols. In order to demonstrate this objective an analysis of amino acids in fruit and vegetable juices has been undertaken and the protocol and results are discussed.

7.2 Experimental

7.2.1 Chemicals and Reagents

Section 2.1.1.

The stock solution of amino acids were prepared by weighing individual standard amino acids and combined to prepare a mixed stock standard in methanol, which contained the ten amino acids tested in this study. The concentration of each of the ten amino acids in this stock standard was 100 μg/mL. A working range of calibration standards from 40 to 500 ng/mL was prepared by the appropriate dilution of the mixed stock solution using 5% methanol solution. Apple juice and beetroot juice samples were prepared by diluting the '*as supplied*' product, 1:25 and filtered through 0.22 μm nylon filter.

Column performance was assessed using butylbenzene as an efficiency marker; prepared in 20/80 water/methanol at a concentration of 13 mg/mL.

7.2.2 Chromatography Columns.

In this chapter a set of Hypersil GOLD columns (50 × 2.1 mm, 5 μm P_d) were utilised. This column set comprised one conventional format column and one AFT column kitted out in parallel segmented flow (PSF) mode, operated such that it emulated a 1.0 mm i.d. column, i.e., the outlet segmentation ratio was set at 21% through the column radial central exit port.

7.2.3 Instrumentation HPLC-MS/MS

Section 2.1.4. The auto injector was not used in this set of experiments.

7.2.4 HPLC-MS/MS analysis

Separations were performed using isocratic elution and the mobile phase composition was 95/5 water/methanol (+ 0.1% formic acid). Experiments involving MS detection were undertaken using only the AFT column operated in PSF mode. The mobile phase flow rate was operated such that LC flow was 4.5 mL/min, the PSF outlet segmentation ratio was 21% and therefore the volume delivered to the MS detector was 0.9 mL/min, which was close to the maximum operating range of this mass spectrometer for the given mobile phase composition.

For all samples and standard solutions, ten replicate injections were made of 5 μL. In order to process these injections in the time frame necessary to reach essentially direct injection analytical speed, a home built injector was incorporated into the instrument. The injector cycle time was reduced to 6 seconds for a 5 μL injection volume, made *via* a 5 μL fixed volume loop. The overall

injection to injection cycle time was 24 seconds; 6 second injection and 18 second chromatographic run time.

Analyses were undertaken in positive ion mode using electrospray ionisation with mass spectrometry detection utilising the Thermo TSQ Vantage mass spectrometer in single reaction monitoring (SRM) mode. The generically optimised MS parameters for the detection of the ten amino acids were: Vaporiser temperature at 500°C, capillary temperature at 350°C, sheath gas was set at the rate of 60 units, auxiliary gas flow at 40 and sweep gas flow at 5 units. Optimum spray voltage was maintained at +3.5 kV. Collision energy was set at 20 to optimise for all analytes and tube lens offsets were individually optimized for each compound. Data processing was performed using Thermo Xcalibur Qual Browser (Thermo Fisher Scientific, San Jose, USA).

Column Efficiency Testing using HPLC with UV Detection

Analysis of column efficiency was performed under isocratic elution conditions according to the methodology described in Section 3.2.3. The column performance was tested at flow rates ranging from 0.04 to 2.5 mL/min, at 25 separate flow rates. The test analyte was butylbenzene, with UV detection at 254 nm. HETP curves were subsequently constructed; data was not corrected for extra column contributions.

7.3 Results and Discussion.

An important aspect of AFT columns is that the relative efficiency in the separation process (compared to conventional columns) increases as the flow rate increases. This enables high speed separations to be undertaken with less loss in theoretical plates, as compared to a conventional column. To show the performance gain of AFT columns at high volumetric flow rates, plots of HETP versus flow velocity for columns packed with 5 μm Hypersil GOLD stationary phases in both conventional and AFT modes, in 2.1 mm i.d. formats are shown in Figure 7.1. Relative to the conventional column, the performance of the AFT column improved as the flow rate increased, such that at 2.5 mL/min, the gain in efficiency was in the order of 65%. That is, 1711 theoretical plates were attainable on the AFT column compared to 1039 plates on the conventional column. Indeed, in order to obtain the same number of theoretical plates on the conventional column as that on the AFT column, the conventional column would need to be operated at just under 2/3^{rds} of the flow velocity as for the AFT column.

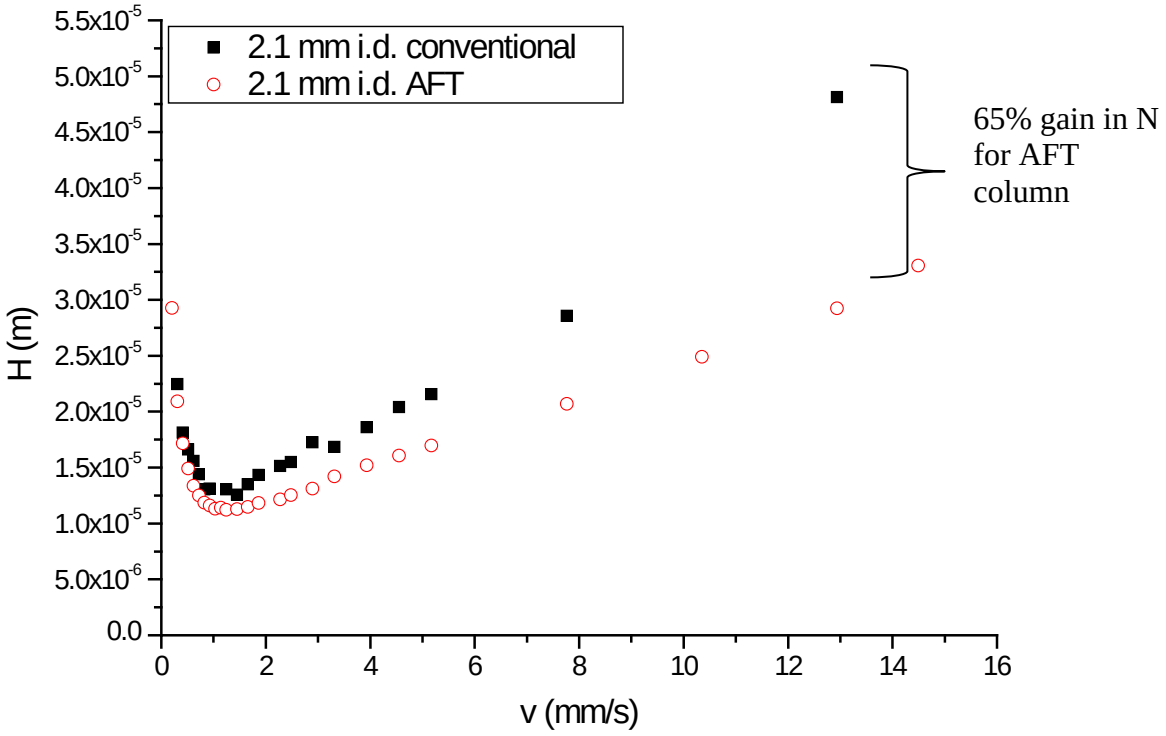

Figure 7.1 HETP curves acquired for the solute butylbenzene on a conventional 50 × 2.1 mm column (squares) and an AFT 50 × 2.1 mm column (hollow circles); both packed with 5 µm Hypersil GOLD particles. The AFT column was operated in parallel segmented flow mode, with 21% of the solvent from eluting from the radial central exit port. Only the radial central flow was processed by the UV detector.

Since less separation power is lost at high flow velocities when AFT columns are employed compared to conventional columns, 2.1 mm i.d. AFT columns were then utilised in ultra-high speed separations incorporating MS detection. A study was conducted, which demonstrated the through-put and analytical precision of AFT columns for the analysis of real samples, such as amino acids. In Chapters 4, 5 and 6, amino acids were also tested. Hence this set of compounds serves as a useful reference to demonstrate the power of AFT in pulsed direct injection mode.

The chromatograms shown in Figures 7.2 and 7.3 are ten replicate injections of a 10 component amino acid mixture obtained on an AFT 2.1 mm i.d. column (50 × 2.1 mm) operating in PSF mode, such that 21% of the solvent flow eluted via the radial central exit port. Note that in Figure 7.2 continuous data acquisition was necessary because the stop-start process of the data acquisition process adversely delayed the analysis through-put. Data acquisition was subsequently stopped and restarted only for each new sample of standard. The chromatographic analysis undertaken in Figure 7.2 utilised a volumetric flow rate of 4.5 mL/min, with 0.9 mL/min being directed to the MS detector. The chromatograms in Figure 7.3 are the ten extracted ion

chromatograms of phenylalanine; extracted from the chromatographic data displayed in Figure 7.2. In these analyses, the ten replicate injections were undertaken in less than 4 minutes.

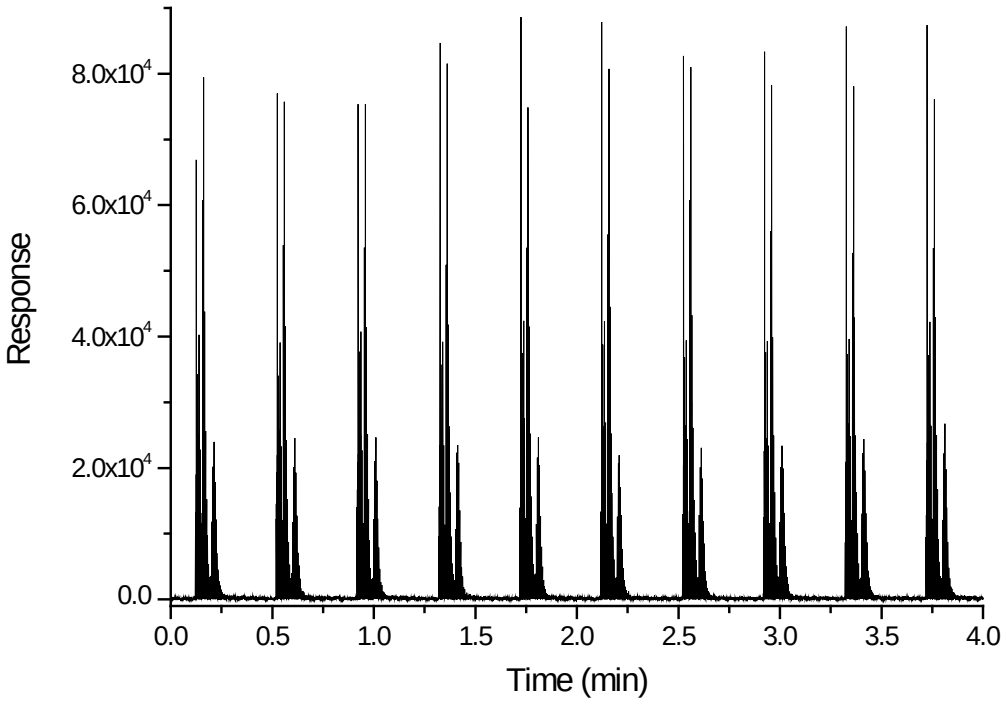

Figure 7.2 Total ion chromatograms (10 replicate injections) of 10 amino acids (200 ng/mL).

The exact injection protocol allowed for a 6 second injection period and an 18 second separation. The analysis time for the separation could have been reduced further, as no components were observed to elute beyond 15 seconds, but to avoid any cross contamination between samples especially in the analysis of the juices, 3 seconds of additional runtime was included between each injection. A set of calibration standards for the 10 amino acids were then tested under the exact same protocol as described for the analyses undertaken in Figures 7.2 and 7.3. Since the analytical through-put was very high, such that the data acquisition of the MS was approaching its limit of operation, a generic set of MS operating conditions was employed for all amino acids. This resulted in good sensitivity for some amino acids, but relatively poor sensitivity for others, in particular valine, methionine, lysine and tyrosine. In total, five calibration standards were tested for each amino acid, and each standard was analysed in replications of ten.

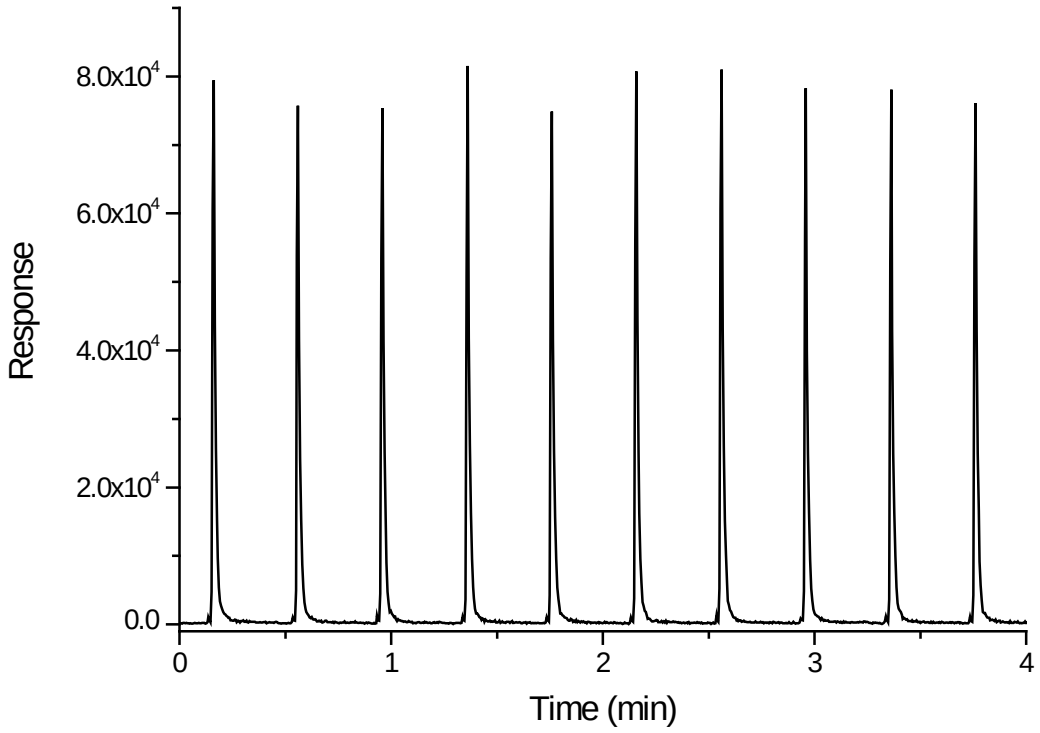

Figure 7.3 Extracted Ion chromatograms (10 replicate injections) of phenylalanine (200 ng/mL).

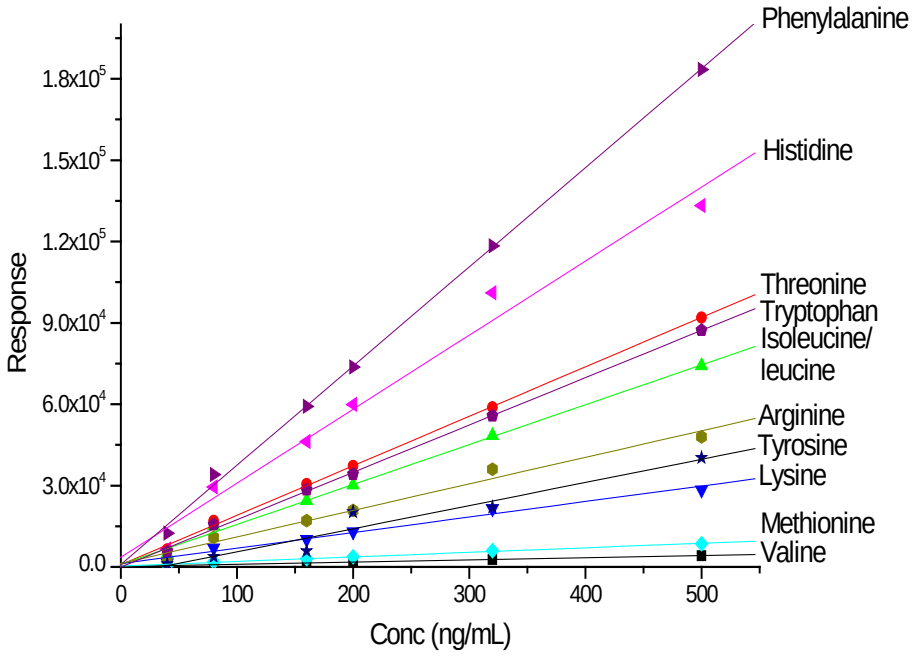

Figure 7.4 Calibration curves based on peak area for each amino acid.

The calibration data (derived from peak area integration) for all amino acids yielded linear curves with average r^2 values of 0.986. The calibration curves (based on peak area measurements) are shown in Figure 7-4, and the r^2 values, together with the precision of each set of standards for each amino acid are given in Table 7.1. For each of the amino acids that exhibited strong signal intensity the R.S.D in injection to injection replication was typically less than 5% based on peak area and 8% based on peak height, Table 7.2. For the amino acids that showed relatively poor sensitivity under this generic set of MS conditions, the R.S.D values were poorer, but improved at higher concentrations (see Table 7.1 for details).

Quantification based on peak height displayed greater variability, reflective of the limited number of data points across each peak: a factor that results from very narrow bands being extracted from the very high speed chromatographic separations. Nevertheless, typical R.S.D for the amino acids that displayed the more substantial levels of detection response was in the order of 7% or less (Table 7-2), with r^2 values for calibration curves derived from this data always being greater than 0.98 (Table 7-2).

Conc. (ng/mL)	**Val RSD%**	**Thr RSD%**	**Ile/Leu RSD%**	**Lys RSD%**	**Met RSD%**	**His RSD%**	**Phe RSD%**	**Arg RSD%**	**Tyr RSD%**	**Trp RSD%**
40	15	3.5	3.2	11	21	4.6	2.5	5.5	13	3.8
80	13	3.0	2.9	2.7	6.6	2.6	2.7	2.9	6.9	3.5
160	8.7	3.1	3.7	4.8	3.2	2.3	1.6	2.8	6.6	3.7
200	8.7	1.8	3.6	5.1	6.6	3.8	2.7	2.9	2.1	3.3
320	8.8	1.6	3.8	3.6	5.8	1.3	1.9	2.3	3.8	2.8
500	7.6	1.2	4.1	4.7	2.0	2.9	2.9	4.3	4.9	3.4
r^2 calibration curve	***0.998***	***0.999***	***0.997***	***0.976***	***0.993***	***0.979***	***0.999***	***0.980***	***0.939***	***0.999***

Table 7.1 Injection to injection precision (RSD) of each amino acid at each level of standard concentration based on peak area measurements. Number of replicates for each concentration = 10. Calibration curve linear correlation (r^2) values are included.

Conc. (ng/mL)	Val RSD%	Thr RSD%	Ile/Leu RSD%	Lys RSD%	Met RSD%	His RSD%	Phe RSD%	Arg RSD%	Tyr RSD%	Trp RSD%
40	19	7.2	5.3	17	14	5.7	3.2	6.4	11	7.6
80	15	4.3	4.3	3.6	10	6.4	2.4	5.8	7.3	4.1
160	12	4.6	4.6	6.0	10	4.7	2.2	3.9	5.7	3.6
200	14	3.5	3.4	5.9	8.4	8.5	3.2	6.4	4.2	5.3
320	7.2	2.6	3.9	4.5	7.0	2.9	2.2	5.4	3.0	2.8
500	7.8	2.3	4.4	6.1	3.5	4.7	4.3	6.2	5.7	4.6
r^2 calibration curve	***0.993***	***0.998***	***0.995***	***0.971***	***0.982***	***0.969***	***0.998***	***0.960***	***0.939***	***0.998***

Table 7.2 Injection to injection precision (RSD) of each amino acid at each level of standard concentration using peak height measurements. Number of replicates for each concentration = 10. Calibration curve linear correlation (r2) values are included.

A simple analysis of the amino acid content of juices was then undertaken: apple and beetroot juices were tested. Data is presented in Table 7.3. All of the amino acids were detected in the beetroot sample, and all but methionine and tryptophan were detected in apple juice. The concentration of some amino acids in both samples was outside of calibration range. However, this analysis was done simply to show the qualitative capabilities of the technique rather than optimising it as a quantitative method.

Juice	Val	Thr	Ile/Leu	Lys	Met	His	Phe	Arg	Tyr	Trp
Apple (RSD)	72.6 (12)	68.6 (3.4)	135 (2.9)	85.4 (3.3)	ND	37.6 (2.8)	67.5 (3.9)	61.5 (2.6)	75.0 (6.3)	ND
Beetroot (RSD)	1150 (6.4)	290 (2.7)	2550 (2.7)	147 (7.1)	170 (6.1)	210 (3.1)	289 (2.7)	242 (6.1)	2277 (6.3)	541 (3.5)

Table 7.3 Concentration (ng/mL) and (RSD) values of each amino acid for apple and beetroot samples using area responses.

7.4 Conclusion.

Ultra-high speed analyses of amino acids were undertaken using AFT chromatography columns with MS detection. The AFT columns employed here had internal diameters of 2.1 mm, and these columns were operated at 4.5 mL/min. Subsequently, separations of the amino acids were feasible in less than 15 seconds, with injection to injection precision generally less than 5%, dependent on the standard concentration. Because these AFT columns enabled very high flow rates to be employed with MS detection, high sample through-put was achievable that effectively emulated direct injection protocols.

The analyses in this study were subsequently based on ten replicates per standard (or sample) across five concentration standards, with two samples; the entire analysis being completed in less than 25 minutes (total number of injections being 60). This exceptional gain in analytical through-put, with the excellent level of precision that was obtained suggests that AFT columns coupled with MS detection should find widespread application in analytical laboratories that require high sample through-put.

Effectively, the study presented here shows that HPLC-MS, with AFT columns can operate with direct injection through-put, but with the benefits of a significant separation step.

Chapter 8.

Validation of the Pulsed Direct Injection Process

8.1 Introduction

Faster analysis is ever demanding need in every chromatography and mass spectroscopy field. In the previous Chapter the technique 'pulsed direct injection HPLC' was introduced. The basis of this technique was the employment of Active Flow Technology (AFT) columns in concert with high speed injection processes and mass spectrometry detection. In this chapter this technique was assessed for its robustness and compatibility with LC-MS/MS. This technique requires the use of AFT columns. The pulsed direct injection technique offers near direct injection speeds with a significant separation step prior to detection. An advantage of this technique is smaller back pressure due to large particle size employed in active flow technology columns which eliminates necessity of UHPLC instruments.

Cycle times of amino acid assays that utilised this technique were around 20 seconds, enabling high level replication of injections and high sample to standard ratios in standardisation protocols. These outcomes were achieved using columns packed with 5 – micron particles, overcoming the need for high pressure systems. Assays were typically operated at 4 to 5 mL/min on 2.1 mm i.d. columns. On ordinary 2.1 mm format columns such flow rates would be very detrimental to the separation performance, as demonstrated in Chapter 3. However, on AFT columns the separation efficiency remains high at very high velocities since the outlet fitting on the AFT column selectively transports only the most efficient migration zone from within the column to the MS. Subsequently 5 – micron particle packed AFT columns actually outperform conventional 1.9 micron particle packed columns, but at much lower back pressures.

In concert with MS detection AFT columns provide for a very powerful combination as both the HPLC and the MS provide orthogonal separation power. It is the fact that band overlap can be tolerated in the HPLC separation since overlapping species can be further isolated in the MS. Yet this raises another problem, how reliable is quantification of overlapping species when the transport of these components occurs at very high velocities?

It is therefore the aim of the current chapter to evaluate the reliability of data derived from pulsed injection AFT-HPLC. Specifically quantitative information will be assessed based on peak areas and peak heights, in situations where bands elute pure from the HPLC, or as co-eluting binary or tertiary mixtures. The effects of selected ion monitoring, and to what extent can this be employed to detect specific analytes in a peak containing co-eluting compounds was also evaluated.

8.2 Experimental.

8.2.1 Chemicals and reagents

For details refer to Section 2.1.2.

Preparation of all stock solutions was done by weighing each compound from solid and dissolving in methanol at the concentration of 100 μg/mL for each compound.

Working standard solutions were prepared follows: A mixed pharmaceutical solution was prepared combining 1.0 mL of each pharmaceutical stock standard (100 μg/mL) (acetaminophen, caffeine and piroxicam) and made up to 100 mL in 40% methanol, which gave a concentration of 1000 ng/mL. A second mixed standard solution was created by combining 1 mL of each stock standard solution of amino acids (threonine, histidine, phenylalanine, arginine, tyrosine and tryptophan) (100 μg/mL) and made up to 100 mL in 5% methanol, yielding a final concentration of 1000 ng/mL.

8.2.2 Instrumentation

Chromatographic separations and MS detection were carried out using the Thermo Ulitmate 3000 UHPLC as described in Section 2.1.4 and Section 7.2.3.

Instrumental method for amino acid analysis

The mobile phase flow rate was operated such that the volume presented to the column was 4.5 mL/min with 15% of the flow exiting the column from the radial central outlet port. Consequently 0.7 mL/min was presented to the MS detector. The separation was carried out in an isocratic mode with mobile phase composition of 5% methanol, 95% water and 0.1% formic acid using an AFT Hypersil GOLD HPLC column (50 × 2.1 mm i.d., 5 micron particle size). The maximum operating pressure of 450 bar was reached at this mobile phase composition using the flow rate of 4.5 mL/min.

Instrument methods for pharmaceutical compound analysis

For the analysis of the 3-component pharmaceutical sample the mobile phase flow rate was 3 mL/min with 15% of the flow exiting the column from the radial central exit port. Therefore 0.45 mL/min was presented to the MS detector. The chromatographic separation was undertaken in an isocratic mode with a mobile phase composition of 40% methanol, 60% water and 0.1% formic acid. The separation was performed on an AFT Hypersil GOLD HPLC columns (50 mm × 2.1 mm

i.d., 5 micron particle size). The maximum operating pressure was reached for this mobile phase composition at 3 mL/min.

8.2.3 Instrument set up

Pulsed direct injection mode was achieved using quaternary pump (Ultimate 3000) and a home-made injector. The reason for by-passing the conventional injector was to avoid long cycle times (2-3 min) associated with the operation of the conventional injector. To accommodate high throughput, data acquisition was set in continuum. Sample was injected from the reservoir connected to a 6-port, 2-position injection valve (Rheodyne) and loaded into a 5 μL injection loop following each analytical run, typically every 12 seconds, using an in-house built syringe pump that over-filled the loop (3×) in a 6 second period.

To minimise the band broadening, great care was taken to minimise the post column volume. In order to achieve that, the connection between the central port of the PSF column outlet and MS ion source was the shortest pre-cut tubing at hand, 5 cm viper tubing (0.13 mm diameter).

8.3 Results and Discussion.

In this Chapter four sets of experiments were designed to assess the new PDI technique for reproducibility, peak shape and robustness of the analysis, capability of MS instrumentation and data acquisition. Each of the experiments had 30 injections. Firstly, PDI was employed to test the data acquired of a single component, piroxicam. This test gave a bench mark of accuracy and precision when applying the maximum acquisition rate on a single component at a specific (3 mL/min) flow rate. Secondly, the data acquisition process was tested on a three component mixture using the same acquisition rate as for the single component, but this time, acquisition rate was shared between three compounds (piroxicam, caffeine and acetaminophen). The separation conditions were designed so that the acetaminophen and caffeine co-eluted but piroxicam was baseline resolved. Precision data is detailed for these two sets of experiments in Table 8.1. From this data it is apparent that multiple ion monitoring reduces the level of precision especially when peaks are processed using peak height. For example, the reproducibility in the peak area and peak height of the single component piroxicam was 1.15% and 2.94% respectively, while for the same compound, in the 3-component mixture the RSD increased to 1.38% and 4.25% respectively.

Piroxicam (n=30)	RSD (%)	
	Area	Height
Single component	1.15	2.94
In 3 component mix	1.38	4.25

Table 8.1 Piroxicam data as a single component and in a 3 component mixture.

The probable reason for this is that the bands eluting from the AFT column are very narrow and consequently have few points that define peak despite the acquisition rate being 1000 Hz. As a consequence the actual apex of the peak may not be precisely defined and as such variation in peak height was more substantial than the variation in peak area. Thus increasing the number of compounds being monitored, adversely affects the accuracy and precision.

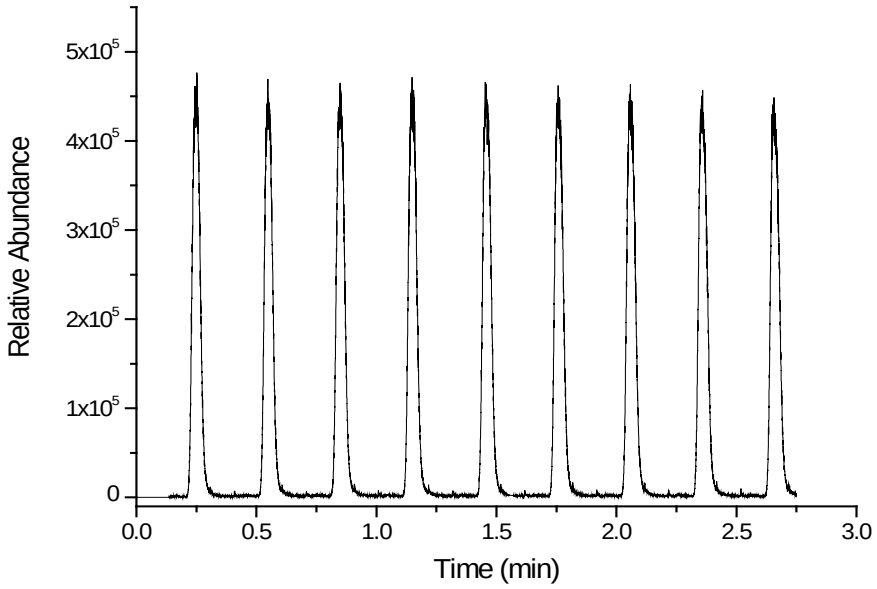

Figure 8.1 Extracted Ion Chromatogram of Piroxicam in a single component sample (10 injections).

The maximum number of points across the peak was found when only the piroxicam was monitored as a single component sample (Figure 8.1 and 8.2) compared to the when piroxicam was monitored as one component in a mixture of three and thus acquisition was split equally across the three components. This shows that the reduction of points across the peak leads to higher R.S.Ds, especially when data was processed based on peak height 4.25% RSD compared to 2.9% based on peak area for piroxicam as a single component in a 3 mix component (Table 8.1). Two further experiments were undertaken, which were designed to test the capability and robustness of the mass

spectrometer when PDI was employed for more complex samples; a six component amino acid sample (threonine, histidine, phenylalanine, arginine, thyrosine and thryptohan), whereby the first three amino acids co-eluted (histidine, tyrosine and arginine), then phenylalanine and threonine co-eluted and finally tryptophan eluted as a single peak in the same manner as for piroxicam (described above).

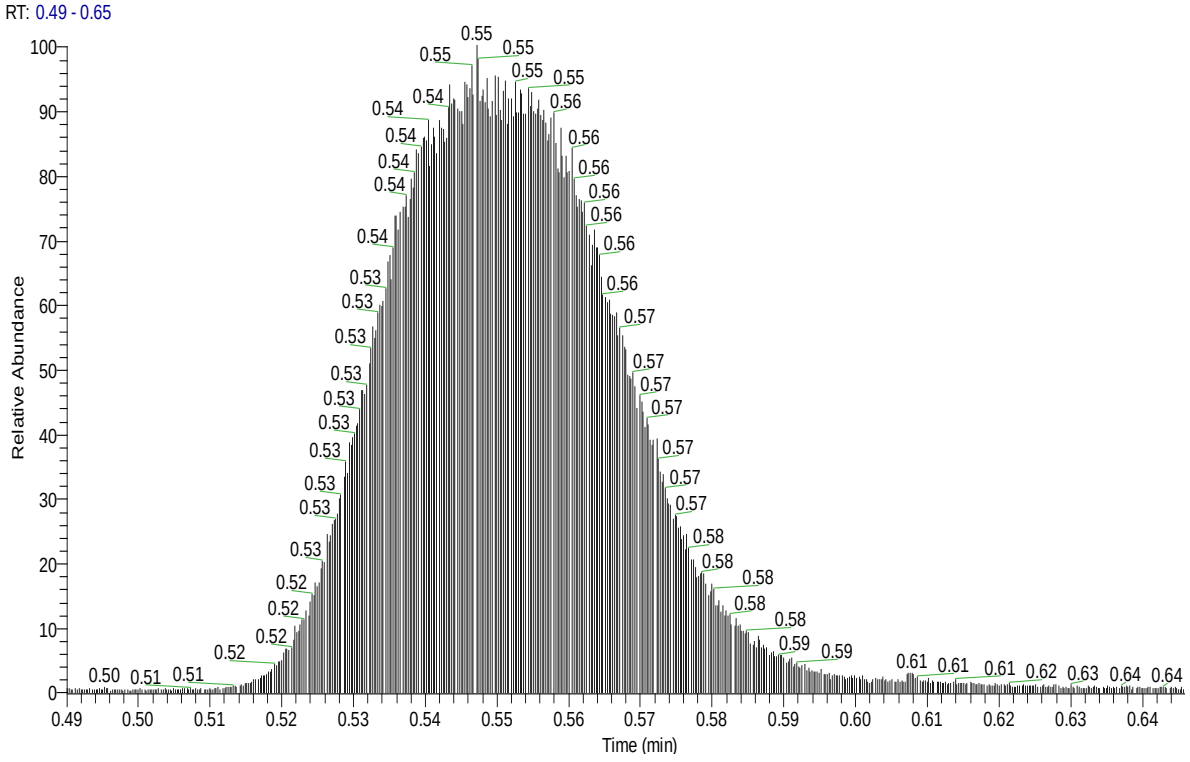

Figure 8.2 Extracted ion chromatogram of piroxicam in single component sample.

Additionally, these same six amino acids were quantified in a set of experiments whereby total of 20 components were monitored so as to mimic the analysis of a more complex sample. Thus data acquisition was shared between the '20' components. These additional MRMs were added to further challenge and strain the MS data acquisition. This experiment was conducted to assess and compare the accuracy and precision for the analysis of six amino acids when monitored as a '6' component sample and as a '20' component sample. Analysis of the data in Table 8.2 revealed that the relative standard deviations in the area responses for the six amino acids in both tests was around 4%, irrespective of whether or not 6-components were monitored or 20. However, in both cases, the RSDs were higher than for the 3- or 1-component pharmaceutical samples. As expected, however, the RSDs were larger in both experiments when data was based on peak height, approximately 12%. Similarly, as in the two experiments that tested the pharmaceuticals, the trend

of increasing RSD with fewer data points across the peak width was apparent, as is the case when more MRMs were monitored.

Interestingly, the first three overlapping bands (histidine, arginine and tyrosine) were found to have lower RSDs compared to the second band of 2-coeluting components.

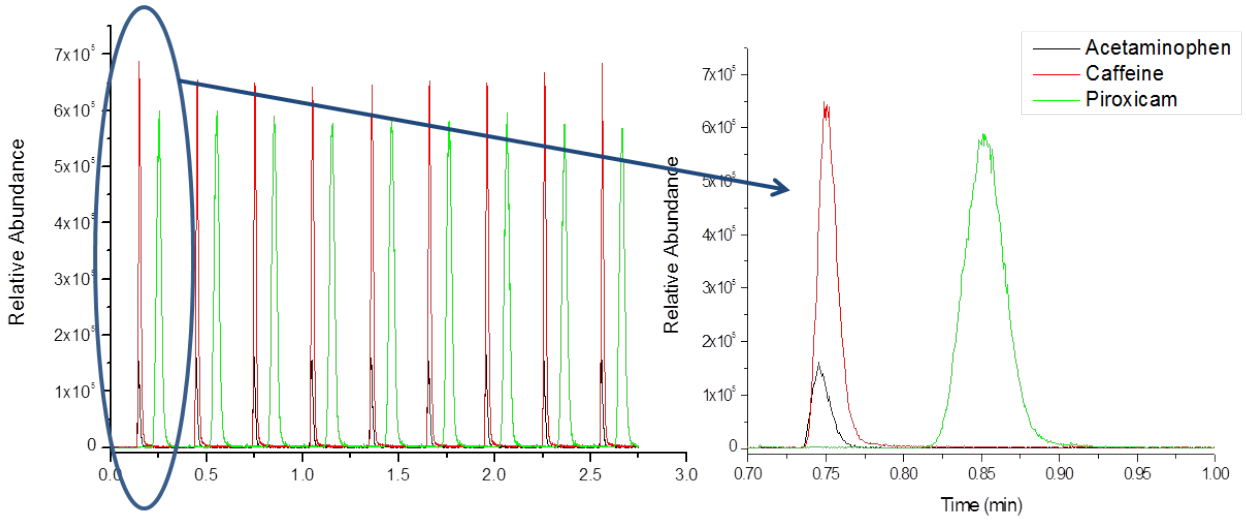

Figure 8.3 Extracted Ion Chromatogram of 3 Pharmaceuticals: acetaminophen, caffeine and piroxicam (10 injections).

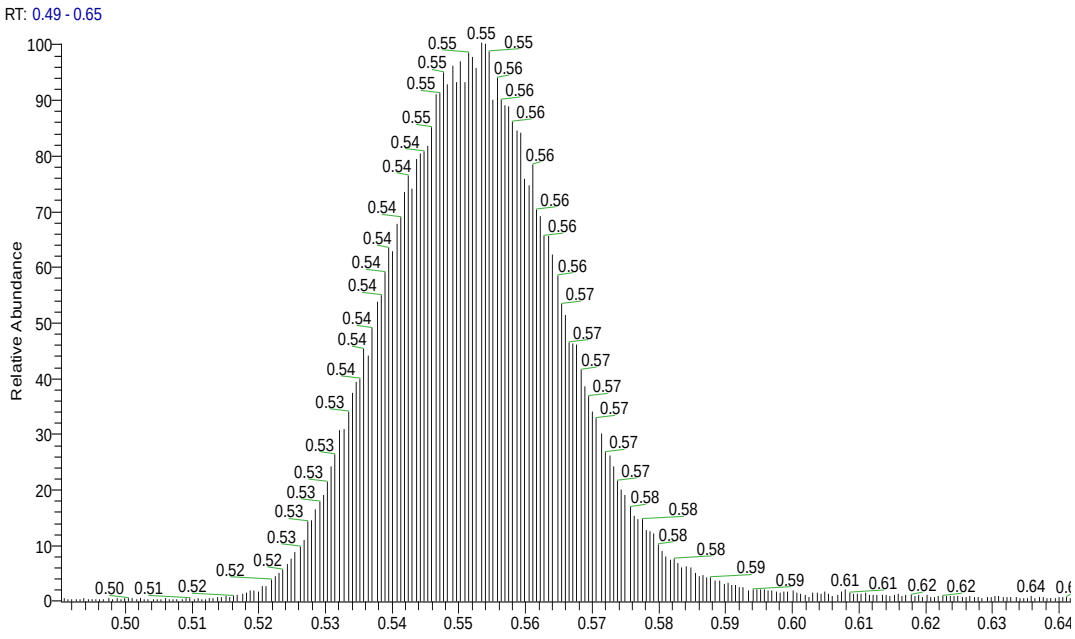

Figure 8.4 Extracted ion chromatogram of Piroxicam in a three component sample mix.

6 Amino Acids (n=30)	Threonine		Histidine		Phenylalanine		Arginine		Tyrosine		Tryptophan	
	Area	Height	Area	Height	Area	Height	Area	Height	Area	Height	Area	Height
RSD in 6 mix component	3.0	11.1	6.3	17.6	3.6	17.6	10	10.7	4.1	9.7	3.3	11.5
RSD in 20 mix component	1.7	9.0	5.2	13.3	4.2	20.8	2.4	6.1	4.4	10.7	1.7	10.7

Table 8.2 RSD values for 6 amino acids in 6 and 20 component mixes.

		Histidine		Arginine		Tyrosine	
First Band		Area	Height	Area	Height	Area	Height
	6 mix	6.26	17.6	10	10.7	4.07	9.67
	20 mix	5.19	13.3	2.37	6.1	4.45	10.7
Second Band		Threonine		Phenylalanine			
		Area	Height	Area	Height		
	6 mix	3.02	11.1	3.57	17.6		
	20 mix	1.7	8.96	4.16	20.8		
Third Band		Tryptophan					
		Area	Height				
	6 mix	3.27	11.5				
	20 mix	1.66	10.7				

Table 8.3 RSD of respective amino acids in different eluting bands. See Figure 8.5 for chromatogram.

This indicates that overlapping bands should ideally be chromatographically resolved for best quantification, given the current limitations to the rate of data acquisition of the TSQ Vantage MS. That being said, monitoring twenty compounds appeared to be within the limits of MS

capability provided peak area was used for quantification, where the peak area RSD was 4.1%, and for the peak height, 12.4 % (Table 8.2). This shows promise as a technique for very high through-put assays.

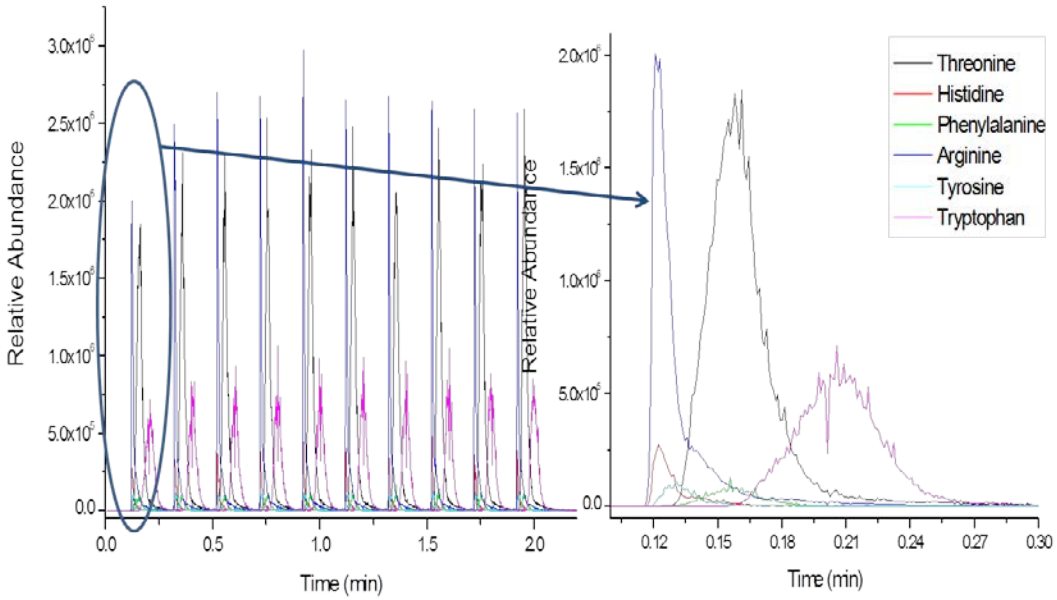

Figure 8.5 Six Amino acids zoomed in (one injection).

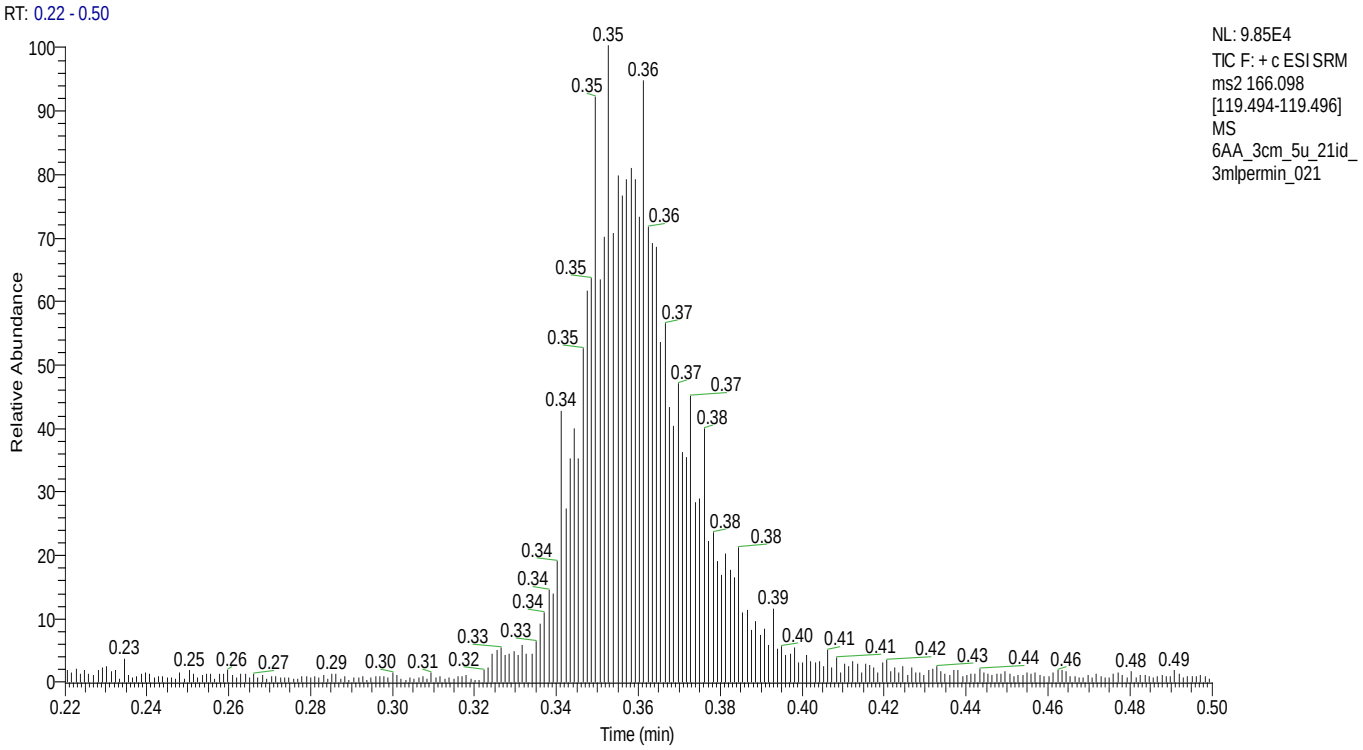

Figure 8.6 Extracted Ion Chromatogram of phenylalanine in 6 compounds sample mix -95 points across the peak derived from Figure 8.5.

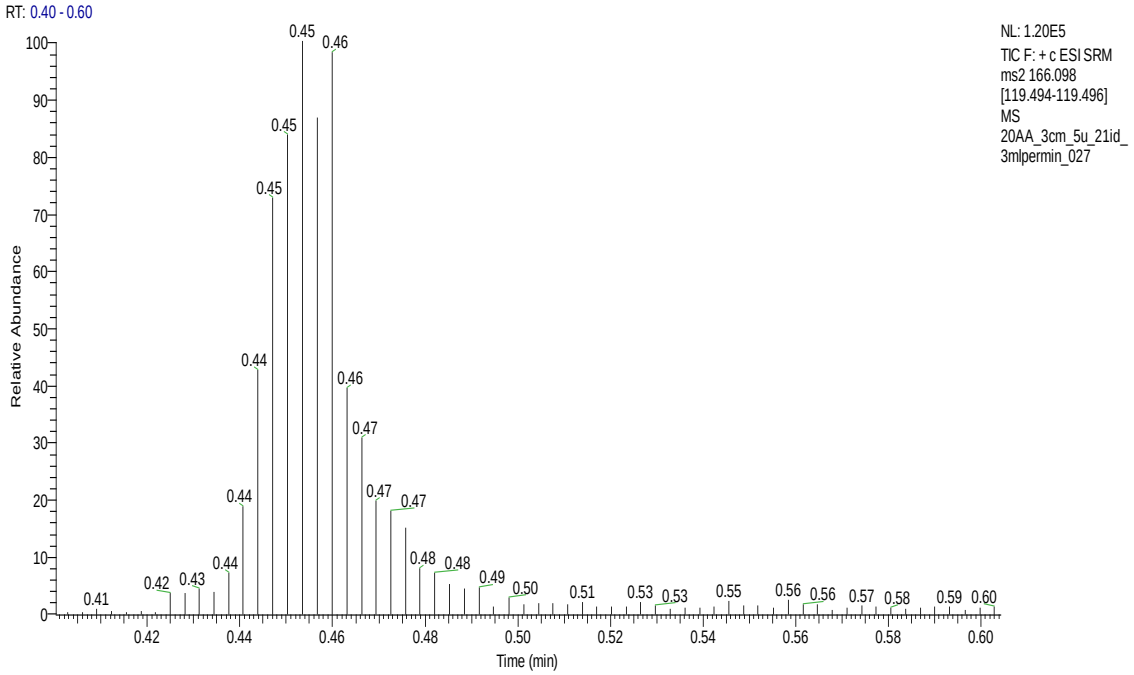

Figure 8.7 Phenylalanine in 20 compounds mix – 25 points across the peak derived from Figure 8.5.

Chapter 9.

Future Directions: Application of Pulsed Direct Injection and Active Flow Technology in Reaction Monitoring

9.1 Introduction

Understanding reaction mechanisms and reaction kinetics are important parameters in the optimisation of drug development, especially for large scale pharmaceutical companies. For that reason, industry strives to develop processes that enable reaction monitoring in order to gain a greater understanding of their drug development strategies [114]. Understanding the reaction mechanism(s) gives the synthetic chemist the opportunity to control and optimise the reaction efficiency and possibly reduce the cost of the drug production/and or maximise the yield or potentially minimise the level of contamination from undesirable side reactions. Often spectrophotometric methods are employed to monitor reaction processes. However, the formation of by-products, or the presence of multiple reaction components may make it difficult to understand data derived from spectrophotometric or calorimetry analyses. In order to improve the clarity of the information obtained from reaction monitoring a separation step that serves to isolated reaction components is desirable. Quite often, this separation step, prior to the detection of reaction components or reaction products is a lengthy procedure, and this may limit the quality of information obtained, especially if reaction intermediates are short lived, or the reaction kinetics fast. As such, the use of mass spectrometry in reaction motoring is gaining popularity [114] because MS offers the advantage of being able to selectively monitor targeted species from within more complex mixtures. A limitation, however, is that ion-suppression, or simply just the number of components entering the MS simultaneously may make it difficult to determine exactly the reaction process. Therefore a chromatographic separation step, if undertaken rapidly, would be beneficial.

In Chapters 7 and 8 the technique referred to as Pulsed Direct Injection (PDI) was introduced, which utilises Active Flow Technology (AFT) columns to gain speed in high-throughput analysis, especially those involving MS detection. This chapter details how PDI may be potentially applied to Live Reaction Monitoring (LRM). To illustrate this, a simple example of the concept is presented, whereby, the decomposition of three amino acids in the presence of dilute nitric acid is monitored.

9.2 Experimental.

9.2.1 Chemicals and reagents

Details of chemicals and reagents used are outlined in Chapter 2. Specific details are outlined below.

9.2.2 Standard preparation

Three separate stock solutions of phenylalanine, tyrosine and tryptophan were prepared by individually weighing each amino acid from solid and dissolving each in methanol at the concentration of 100 μg/mL for each compound. A working standard solution was prepared by combining 1.0 mL of each amino acid stock standard (100 μg/mL) and diluting to 25 mL in 5% methanol/1 M HNO_3, yielding a final concentration of 4 mg/mL.

9.2.3 Instrumentation

Chromatographic separations and MS detection were carried out using the Thermo Ulitmate 3000 UHPLC as described in Chapters 2 and 7.

9.2.3.1 Instrumental method for amino acid analysis

The amino acid mixture, undergoing decomposition, was analysed using a similar protocol as described for the amino acid analysis in Chapter 8, with minor modification. Specifically, the mobile phase flow rate was operated such that the volume presented to the column was 4 mL/min with 20% of the flow exiting the column from the radial central outlet port. Consequently 0.8 mL/min was presented to the MS detector. The separation was carried out in an isocratic mode with mobile phase composition of 5% methanol, 95% water and 0.1% formic acid using an AFT Hypersil GOLD HPLC column (30 mm × 2.1 mm i.d., 5 micron particle size).

9.2.4 Instrument set up

Instrument set up was as same as for Pulsed direct injection and is outlined in Chapter 7.

9.3 Results and Discussion.

This chapter demonstrates the potential for PDI employing AFT columns for Live Reaction Monitoring, using the degradation of amino acids in the presence of nitric acid as an example case. While not specifically monitoring a synthetic reaction mixture, the degradation of the amino acid

mixture could be monitored in real time; a proof in principle of the concept and capabilities of Live Reaction Monitoring.

The chromatogram shown in the Figure 9.1 presents the total ion count for the three amino acids. Data was collected in continuum with a total of 60 injections undertaken in a 15 minute period. Periodically the data acquisition process was stopped – a limitation of the propriety software used to drive the LCMS. Such obstacles for the continuous live reaction monitoring will be overcome in future applications. Nevertheless the data is sufficient to demonstrate proof of principle.

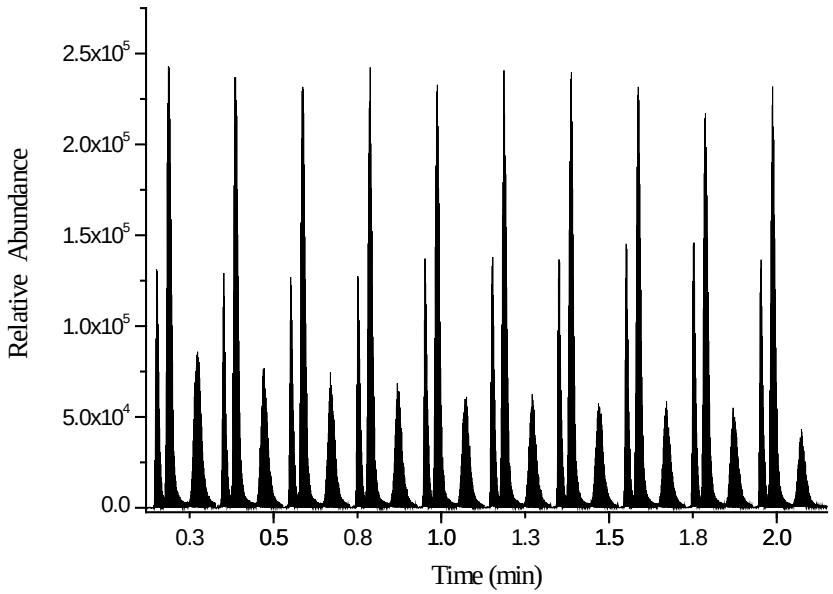

Figure 9.1 Total Ion Count for 10 injections of phenylalanine, tryptophan and tyrosine, prepared in 5M Nitric acid.

At the flow rate of 4 mL/min through the 2.1 × 30 mm column the time frame of each individual separation was 6 seconds with an injection to injection cycle time of 12 seconds (6 seconds being required for sample injection). Greater throughput could readily be achieved since in this particular protocol the operating pressure was well below the limitations of the column (~ 6000 p.s.i.).

Extracted ion chromatograms of phenylalanine, tyrosine and tryptophan are presented in Figures 9.2, 9.3 and 9.4 respectively. From these chromatograms it is apparent that the rate of degradation was fastest for tryptophan (a 90% loss in 15 minutes), whereas the phenylalanine and tyrosine were fairly stable in the acidic solvent environment, losing 15% and 11% in the 15 minute period respectively. The rate of degradation is illustrated in Figure 9.5.

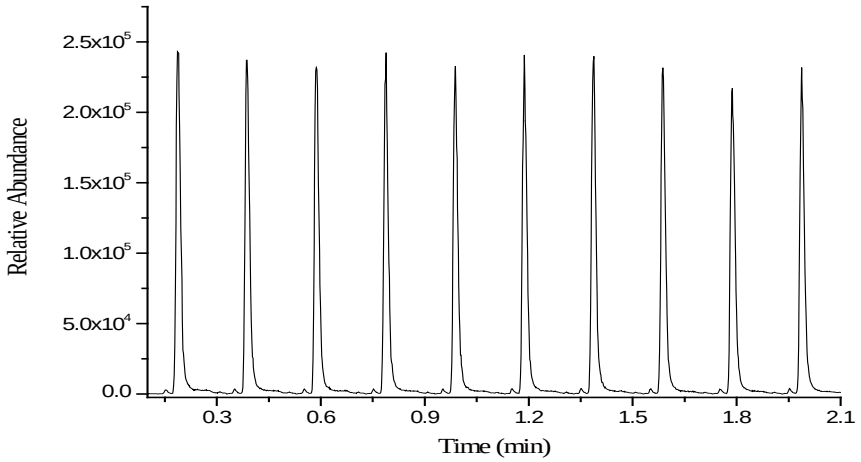

Figure 9.2 Extracted Ion Chromatogram of phenylalanine derived from Figure 9.1.

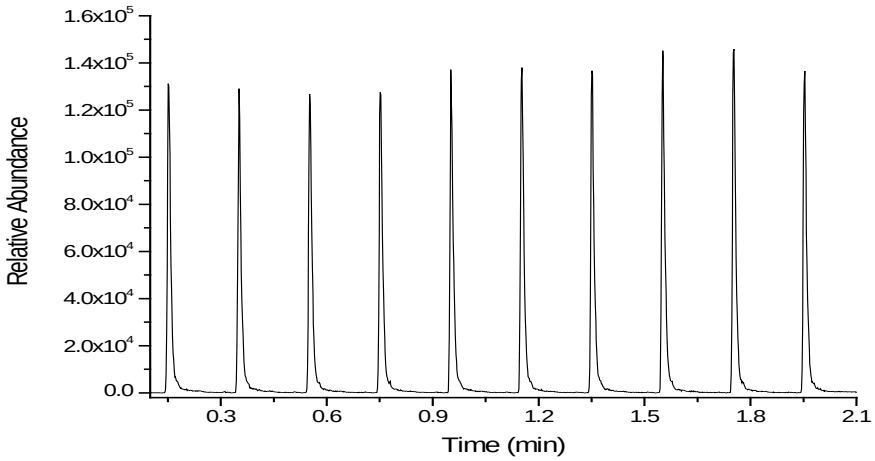

Figure 9.3 Extracted Ion Chromatogram of tyrosine derived from Figure 9.1.

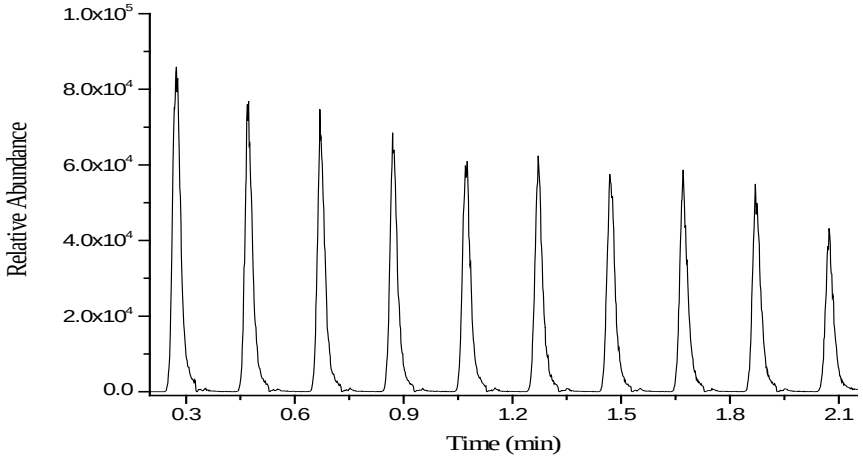

Figure 9.4 Extracted Ion Chromatogram of tryptophan derived from Figure 9.1.

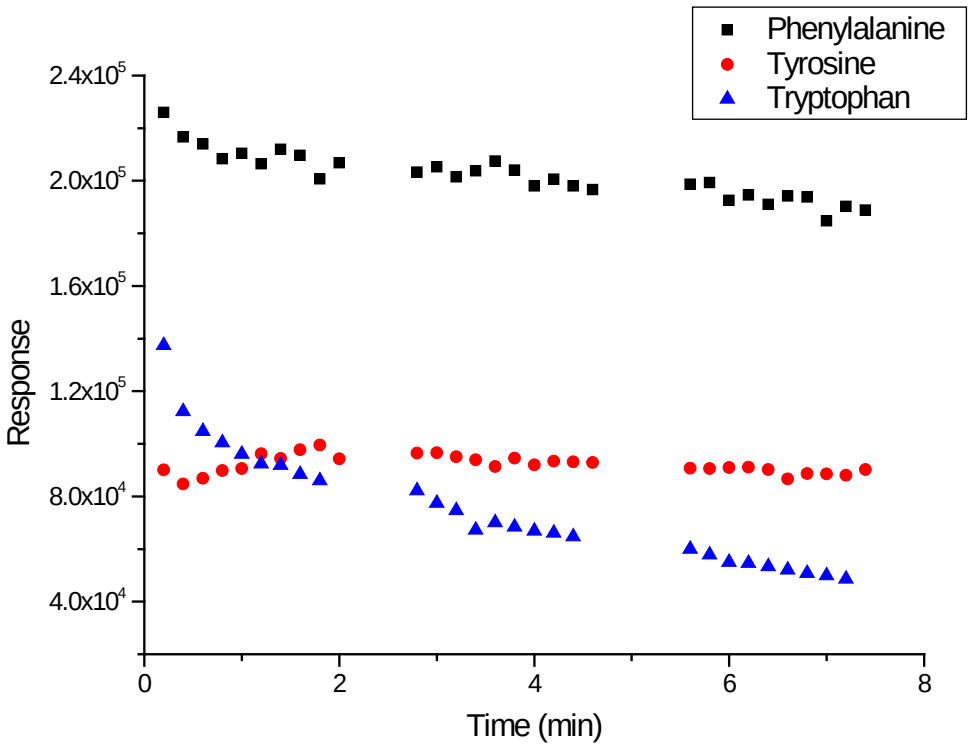

Figure 9.5 Degradation of three amino acids over 7 minutes. (Note, tyrosine was relatively stable in 5M Nitric acid)

9.4 Conclusion.

As a proof of principle, Live Reaction Monitoring was successfully achieved using the new technique of Pulsed Direct Injection and AFT columns. LRM can be applied and utilised in monitoring reactions that require fast and frequent sampling points. The use of AFT columns offers separation step that is comparative to direct injection analysis, but with a substantial separation step prior to the MS. This separation step can be significant in MS analysis as it could potentially minimise matrix effects and allow better characterisation of the products produced during drug synthesis.

Chapter 10.

Conclusions

10.1 Concluding Remarks

The benefits of analyses undertaken using HPLC with MS detection are clear. Furthermore, high speed and high resolution separations are an essential component of our modern analytical requirements. This hyphenated method of analysis provides separation power expressed across two effectively orthogonal dimensions, while at the same time, the MS detector provides quantitative information on the amount of sample, as well as potentially the identity of the sample components. However, the hyphenation of these two techniques is not without problems. HPLC without MS detection could be faster; likewise MS without HPLC could also be faster. The benefit of the separation power by the HPLC and selectivity in detection of the MS make it worth the burden of persisting with the limitation of the coupling. At the crux of the problem lies the simple fact that the capacity of the MS to desolvate large volumes of mobile phase prior to the detection source is limited. To overcome this limitation, two strategies are currently available: (a) post column flow stream splitting, which samples a portion of the mobile phase eluting from the column and hence reduces the amount of solvent entering the MS without sacrificing chromatographic speed; or more commonly nowadays, (b) employing narrow bore columns, which function at the same linear velocities as standard analytical scale columns, but with lower solvent usage. It is important to note that when flow stream splitting processes are employed, the sampling occurs such that it corresponds to the axial flow direction within the column, hence the amount of sample reaching the column reduces in proportion to the split ratio, although the concentration of the sample remains constant.

This thesis explored how a new column technology referred to as active flow technology (AFT) improves the interface between the HPLC and the MS, enabling wider bore columns to behave as if they were narrow bore, thus the MS could better manage the solvent flow. As such, the conclusions to this thesis are that AFT columns are an ideal front end separation device for applications that employ MS, further reasoning is provided below.

Chapter 3 addressed the first objective of this thesis by demonstrating that AFT columns packed with 5 micron particles provided efficiency that exceeded UHPLC technology (1.9 micron particles) when both types of columns were operated near the maximum pressure – hence throughput. The added advantage of the AFT columns over that of the UHPLC columns was that the AFT columns operated at around half the back pressure, yielding around 30 - 70% more theoretical plates per separation depending on retention factor. The performance gain of the AFT column is especially advantageous for high-throughput analysis with mass spectrometry detection,

which is enabling since only around 20% of the flow from the column is directed to the detector. Hence, an AFT column operating at 5 mL/min presents just 1 mL/min to the detector. While it is tempting to equate the AFT flow splitting process to post-column flow stream splitting, this should be avoided since AFT flow stream splitting samples the elution band in the radial direction, not so the axial direction. Hence the concentration of the band is increased relative to a sample eluting from a conventional column; hence sensitivity increases.

Another objective of the preliminary investigations into the implementation of AFT into MS analyses was to demonstrate that AFT columns with MS detection yielded increased sensitivity compared to columns in conventional format. This was extensively explored and successfully demonstrated in Chapter 4 when AFT CF columns were employed. As a result of the radial, rather than axial, flow stream splitting process, AFT columns directed the more efficient migration zone, at higher concentration to the detector. Hence detection sensitivity was enhanced. This was demonstrated in Chapter 4 for the analysis of amino acids; sensitivity was found to increase by as much as 10-fold in signal response and 66-fold when assessed according to S/N when AFT columns were compared to conventional columns having the same internal diameter as the virtual AFT column of the same 'virtual' diameter. At the same time through-put was increased up to 5-fold compared to conventional columns of the same physical internal diameters. The data metrics – i.e., peak height etc., showed gains in the injection to injection precision for peak height (AFT vs. conventional) with R.S.D of 3.5% compared to 6.0% when the virtual 2.1 AFT column was compared to the conventional 2.1 mm i.d. column.

Following the advantages of speed, sensitivity and data analysis that were apparent with AFT column, Chapter 5 showed how quantification of labile compounds benefited from higher through-put. Over the course of the assays for both the AFT and conventional columns, the amount of samples were shown to degrade by around 38% for the conventional columns, but only 9% when AFT - CF columns was used. The outcome was a direct result of being able to undertake the separations at high through-put when using AFT columns. Chapter 5 also demonstrated how higher throughput contributed towards improved assay robustness.

The use of AFT columns in parallel segmented flow mode for high throughput analyses was further explored in Chapter 6, leading AFT columns to be employed in a manner that resembled direct injection MS analysis – i.e, MS without chromatography. In Chapter 6 only narrow bore column formats were explored. Operational flow rates were as high as 6 mL/min through a 2.1 mm i.d. PSF column and approximately 20% of the flow exited from the radial central outlet port. In that manner the AFT – PSF column was effectively functioning as a virtual 1.0 mm i.d. column. At this flow rate, the separation of the amino acids was completed within 6 seconds. Interestingly,

sensitivity was not adversely affected, even though the PSF column was operated well above the flow optimum, compared to the conventional 2.1. mm i.d column, which was operated near the flow optimum. The analysis time of the conventional column was completed in 40 seconds – seven times longer than the AFT column.

Robustness for these near direct injection separations was not assessed at this stage since the MS detector was unable to operate with a sufficiently high data acquisition frequency. Hence there were too few data points defining peaks. Experiments in Chapter 7 and 8 addressed these issues, but the residence time of the small inside the column was increased in order for better peak definition to be established.

In order for near direct injections to become a viable process, the injector itself must be changed. Injectors using robotics to transfer solutions and syringe pumps to wash needles operate on a time scale which is far too long. So for the work in Chapters 7 and 8, home-made injector was employed, thus all work in Chapters 7, 8 and 9 by-passed the conventional injector supplied with the instrument. The application of AFT in these high through-put separations was termed Pulsed Direct Injection as injection and separation through the column was direct in pulses to the MS, at speeds equivalent to direct injection protocols. To accommodate for the detector data acquisition frequency limitations, the flow through the column was slowed and subsequently, the separation of the amino acids was feasible in around 15 seconds, with injection to injection precision of 5% across five different standard concentrations. This technique demonstrated high-throughput analysis, with 60 injections completed in around 25 minutes (10 replications for each standard).

Lastly, Chapter 9 addressed the final thesis objective, specifically developing new technology that enabled live reaction monitoring (LRM) suitable for the optimization of organic synthesis. Operating AFT columns in PDI mode enabled live reaction monitoring of the degradation of amino acids in acidic solution; 60 injections were completed in less than 15 minutes. The injection to injection cycle time was 12 seconds. Although an organic synthesis was not tested, the amino acids served as an example to show proof of principle.

References

[1] H.D. Dewald, Journal of Chemical Education 76 (1999) 33.
[2] J. J. Thomson, L.G. Rays of Positive Electricity and Their Applications to Chemical Analysis, London, UK, 1913., Longmans Green, London, UK (1913).
[3] N.M. AB, The Nobel Prize in Physics Nobelprize.org, 2014.
[4] M. Grayson, Journal of The American Society for Mass Spectrometry 22 (2011) 1301.
[5] J.B. Fenn, M. Mann, C.K. Meng, S.F. Wong, C.M. Whitehouse, Science 246 (1989) 64.
[6] B. Gologan, Z. Takáts, J. Alvarez, J. Wiseman, N. Talaty, Z. Ouyang, R.G. Cooks, Journal of the American Society for Mass Spectrometry 15 (2004) 1874.
[7] Z. Ouyang, Z. Takáts, T.A. Blake, B. Gologan, A.J. Guymon, J.M. Wiseman, J.C. Oliver, V.J. Davisson, R.G. Cooks, Science 301 (2003) 1351.
[8] J.B. Fenn, Angewandte Chemie International Edition 42 (2003) 3871.
[9] C.M. Whitehouse, R.N. Dreyer, M. Yamashita, J.B. Fenn, Analytical Chemistry 57 (1985) 675.
[10] M. Yamashita, J.B. Fenn, Journal of Physical Chemistry 88 (1984) 4451.
[11] M. Yamashita, J.B. Fenn, Journal of Physical Chemistry 88 (1984) 4671.
[12] P. Kebarle, L. Tang, Analytical Chemistry 65 (1993) 972A.
[13] A.P. Bruins, Mass Spectrometry Reviews 10 (1991) 53.
[14] M. Karas, U. Bahr, T. Dülcks, Fresenius' Journal of Analytical Chemistry 366 (2000) 669.
[15] C.E.C.A. Hop, Journal of Mass Spectrometry 31 (1996) 1314.
[16] J.F. Anacleto, S. Pleasance, R.K. Boyd, Organic Mass Spectrometry 27 (1992) 660.
[17] T.F.S. Inc., Quantiva Ion source with capillary needle spraying towards the orifice of the sample cone 2013.
[18] M.S. Wilm, M. Mann, International Journal of Mass Spectrometry and Ion Processes 136 (1994) 167.
[19] M. Wilm, M. Mann, Analytical Chemistry 68 (1996) 1.
[20] R. Körner, M. Wilm, K. Morand, M. Schubert, M. Mann, Journal of the American Society for Mass Spectrometry 7 (1996) 150.
[21] S.A. Trauger, W. Webb, G. Siuzdak, Spectroscopy 16 (2002).
[22] E.D. Hoffmann, V. Stroobant, Mass Spectrometry Principles and Applications, John Wiley & Sons, Chichester, UK, 2001.
[23] K.L. Brown, G.W. Tautfest, Review of Scientific Instruments 9 (1956) 696.
[24] J.S. Allen, Review of Scientific Instruments 18 (1947) 739.
[25] H.E. Stanton, W.A. Chupka, M.G. Inghram, Review of Scientific Instruments 27 (1956) 109.
[26] W.J. Fies Jr, International Journal of Mass Spectrometry and Ion Processes 82 (1988) 111.
[27] R.D. Collins, Vacuum 19 (1969) 105.
[28] M.S.B. Munson, F.H. Field, Journal of the American Chemical Society 88 (1966) 2621.
[29] D.F. Torgerson, R.P. Skowronski, R.D. Macfarlane, Biochemical and Biophysical Research Communications 60 (1974) 616.
[30] S. Banerjee, S. Mazumdar, International Journal of Analytical Chemistry 2012 (2012) 40.
[31] K. Tanaka, H. Waki, Y. Ido, S. Akita, Y. Yoshida, T. Yoshida, T. Matsuo, Rapid Communications in Mass Spectrometry 2 (1988) 151.
[32] R. Kaufmann, Journal of Biotechnology 41 (1995) 155.
[33] M. Mann, G. Talbo, Current Opinion in Biotechnology 7 (1996) 11.
[34] M. Dole, L.L. Mack, R.L. Hines, R.C. Mobley, L.D. Ferguson, M.B. Alice, The Journal of Chemical Physics 49 2240.
[35] M. Wilm, Mol Cell Proteomics 10 (2011) M111.009407.

[36] N.B. Cech, C.G. Enke, Mass Spectrometry Reviews 20 (2001) 362.
[37] A.T. Blades, M.G. Ikonomou, P. Kebarle, Analytical Chemistry 63 (1991) 2109.
[38] B.P. Pozniak, R.B. Cole, Journal of the American Society for Mass Spectrometry 26 (2015) 369.
[39] G. Diehl, U. Karst, Analytical and Bioanalytical Chemistry 373 (2002) 390.
[40] R.B. Cole, Electrospray and MALDI Mass Spectrometry, John Wiley & Sons, New Jersey, NJ, USA, 2010.
[41] K. Tang, J.S. Page, R.T. Kelly, I. Marginean, in: J.C. Lindon (Ed.), Encyclopedia of Spectroscopy and Spectrometry (Second Edition), Academic Press, Oxford, 2010, p. 467.
[42] G. Taylor, Disintegration of Water Drops in an Electric Field, 1964.
[43] A.P. Bruins, Journal of Chromatography A 794 (1998) 345.
[44] A. Gomez, K. Tang, Physics of Fluids 6 (1994) 404.
[45] D.B. Hager, N.J. Dovichi, J. Klassen, P. Kebarle, Analytical Chemistry 66 (1994) 3944.
[46] D. Duft, T. Achtzehn, R. Müller, B.A. Huber, T. Leisner, Nature 421 (2003) 128.
[47] L. Rayleigh, The London, Edinburgh, and Dublin Philosophical Magazine and Journal of Science 14 (1882) 184.
[48] M.G. Ikonomou, A.T. Blades, P. Kebarle, Analytical Chemistry 62 (1990) 957.
[49] R.B. Cole, Journal of Mass Spectrometry 35 (2000) 763.
[50] P. Kebarle, M. Peschke, Analytica Chimica Acta 406 (2000) 11.
[51] G. Schmelzeisen-Redeker, L. Bütfering, F. Röllgen, International Journal of Mass Spectrometry and Ion Processes 90 (1989) 139.
[52] S. Nguyen, J.B. Fenn, Proceedings of the National Academy of Sciences 104 (2007) 1111.
[53] J. Iribarne, B. Thomson, The Journal of Chemical Physics 64 (1976) 2287.
[54] B. Thomson, J. Iribarne, The Journal of Chemical Physics 71 (1979) 4451.
[55] P. Kebarle, Journal of Mass Spectrometry 35 (2000) 804.
[56] Z. Olumee, J.H. Callahan, A. Vertes, The Journal of Physical Chemistry A 102 (1998) 9154.
[57] T.R. Covey, R.F. Bonner, B.I. Shushan, J. Henion, R. Boyd, Rapid Communications in Mass Spectrometry 2 (1988) 249.
[58] J.R. Chapman, R.T. Gallagher, E. Barton, J.M. Curtis, P.J. Derrick, Organic Mass Spectrometry 27 (1992) 195.
[59] M. Mann, C.K. Meng, J.B. Fenn, Analytical Chemistry 61 (1989) 1702.
[60] M. Tswett, Berichte der Deutschen botanischen Gesellschaft vol. 24 (1906) pages 316.
[61] R. Kuhn, A. Winterstein, E. Lederer, Zeitschrift für physiologische Chemie (1931) 141
[62] A.J. Martin, R.L. Synge, Biochemical Journal 35 (1941) 1358
[63] T.H. Walter, R.W. Andrews, TrAC Trends in Analytical Chemistry 63 (2014) 14.
[64] R.A. Shalliker, Hyphenated and alternative methods of detection in chromatography, CRC Press, 2011.
[65] L. Nováková, H. Vlčková, Analytica Chimica Acta 656 (2009) 8.
[66] F. Gritti, C.A. Sanchez, T. Farkas, G. Guiochon, Journal of Chromatography A 1217 (2010) 3000.
[67] M. Rodriguez-Aller, R. Gurny, J.-L. Veuthey, D. Guillarme, Journal of Chromatography A 1292 (2013) 2.
[68] D. Guillarme, J.-L. Veuthey, Journal of Chromatography A 1292 (2013) 1.
[69] H.H. Maurer, Journal of Chromatography A 1292 (2013) 19.
[70] D. Guillarme, J. Schappler, S. Rudaz, J.-L. Veuthey, TrAC Trends in Analytical Chemistry 29 (2010) 15.
[71] R.A. Shalliker, B.S. Broyles, G. Guiochon, J Chromatogr A 888 (2000) 1.
[72] F. Gritti, G. Guiochon, Journal of Chromatography A 1218 (2011) 1592.
[73] C. Ho, C. Lam, M. Chan, R. Cheung, L. Law, L. Lit, K. Ng, M. Suen, H. Tai, The Clinical Biochemist Reviews 24 (2003) 3.
[74] W.F. Smyth, P. Brooks, Electrophoresis 25 (2004) 1413.

[75] W.F. Smyth, J Chromatogr B 824 (2005) 1.
[76] M.S. Rashed, M.P. Bucknall, D. Little, A. Awad, M. Jacob, M. Alamoudi, M. Alwattar, P.T. Ozand, Clinical Chemistry 43 (1997) 1129.
[77] M. Piraud, C. Vianey-Saban, K. Petritis, C. Elfakir, J.P. Steghens, A. Morla, D. Bouchu, Rapid Communications in Mass Spectrometry 17 (2003) 1297.
[78] R.M. Shawky, H.S. Abd-Elkhalek, S.E. Elakhdar, Egyptian Journal of Medical Human Genetics 16 (2015) 165.
[79] B. Wild, B. Green, E. Cooper, M. Lalloz, S. Erten, A. Stephens, D. Layton, Blood Cells, Molecules, and Diseases 27 (2001) 691.
[80] U. Krishnamurti, M.W. Steffes, Clinical Chemistry 47 (2001) 1157.
[81] S.K. Manna, A.D. Patterson, Q. Yang, K.W. Krausz, J.R. Idle, A.J. Fornace Jr, F.J. Gonzalez, Journal of Proteome Research 10 (2011) 4120.
[82] M.-J. Motilva, A. Serra, A. Macià, Journal of Chromatography A 1292 (2013) 66.
[83] J. O'Mahony, L. Clarke, M. Whelan, R. O'Kennedy, S.J. Lehotay, M. Danaher, Journal of Chromatography A 1292 (2013) 83.
[84] P.J. Taylor, Clinical Biochemistry 38 (2005) 328.
[85] H. Trufelli, P. Palma, G. Famiglini, A. Cappiello, Mass Spectrometry Reviews 30 (2011) 491.
[86] A. Cappiello, G. Famiglini, P. Palma, H. Trufelli, Journal of Liquid Chromatography and Related Technologies 33 (2010) 1067.
[87] F. Gosetti, E. Mazzucco, D. Zampieri, M.C. Gennaro, Journal of Chromatography A 1217 (2010) 3929.
[88] L. Nováková, H. Vlčková, D. Šatínský, P. Sadílek, D. Solichová, M. Bláha, V. Bláha, P. Solich, Journal of Chromatography B 877 (2009) 2093.
[89] T. Bueters, J. Dahlström, K. Kvalvågnaes, I. Betnér, S. Briem, Journal of Pharmaceutical and Biomedical Analysis 55 (2011) 1120.
[90] M. Camenzuli, School of Science and Health, University of Western Sydney, Sydney, 2013.
[91] S. Pravadali-Cekic, School of Science and Health, University of Western Sydney, Sydney, 2014.
[92] R.A. Shalliker, M. Camenzuli, L. Pereira, H.J. Ritchie, Journal of Chromatography A 1262 (2012) 64.
[93] D. Kocic, S. Hua, G.R. Dennis, R.A. Shalliker, Microchemical Journal 118 (2015) 193.
[94] J.H. Knox, G.R. Laird, P.A. Raven, Journal of Chromatography A 122 (1976) 129.
[95] R.A. Shalliker, V. Wong, G. Guiochon, Journal of Chromatography A 1161 (2007) 121.
[96] M. Camenzuli, H.J. Ritchie, J.R. Ladine, R.A. Shalliker, Analyst 136 (2011) 5127.
[97] M. Camenzuli, H.J. Ritchie, J.R. Ladine, R.A. Shalliker, Journal of Chromatography A 1232 (2012) 47.
[98] D. Foley, L. Pereira, M. Camenzuli, T. Edge, H. Ritchie, R.A. Shalliker, Microchemical Journal 110 (2013) 127.
[99] M. Camenzuli, H.J. Ritchie, J.R. Ladine, R.A. Shalliker, Analyst 136 (2011) 5127.
[100] M. Camenzuli, H.J. Ritchie, J.R. Ladine, R.A. Shalliker, Journal of Separation Science 35 (2012) 410.
[101] M. Camenzuli, J.M. Terry, R.A. Shalliker, X.A. Conlan, N.W. Barnett, P.S. Francis, Analytica Chimica Acta 803 (2013) 154.
[102] K. Tang, J.S. Page, R.D. Smith, Journal of the American Society for Mass Spectrometry 15 (2004) 1416.
[103] L.R. Snyder, J.J. Kirkland, J.W. Dolan, Introduction to modern liquid chromatography, John Wiley & Sons, 2011.
[104] W.J. Lough, I.W. Wainer, High performance liquid chromatography: fundamental principles and practice, CRC Press, 1995.
[105] F. Gritti, G. Guiochon, Analytical Chemistry 80 (2008) 5009.

[106] K. Kaczmarski, F. Gritti, J. Kostka, G. Guiochon, Journal of Chromatography A 1216 (2009) 6575.
[107] D. Åsberg, J. Samuelsson, M. Leśko, A. Cavazzini, K. Kaczmarski, T. Fornstedt, Journal of Chromatography A 1401 (2015) 52.
[108] J. De Vos, M. De Pra, G. Desmet, R. Swart, T. Edge, F. Steiner, S. Eeltink, Journal of Chromatography A 1409 (2015) 138.
[109] D. Kocic, L. Pereira, D. Foley, T. Edge, J.A. Mosely, H. Ritchie, X.A. Conlan, R.A. Shalliker, Journal of Chromatography A 1305 (2013) 102.
[110] J. Samuelsson, P. Forssén, T. Fornstedt, Journal of Separation Science 36 (2013) 3769.
[111] R. Arnell, P. Forssén, T. Fornstedt, Analytical Chemistry 79 (2007) 5838.
[112] Y.D. Thibodeaux SJ, McGee JE. 2013 in: C.N. Sittampalam GS, Nelson H, et al. (Ed.), Assay Guidance Manual [Internet], Eli Lilly & Company and the National Center for Advancing Translational Sciences, 2013.
[113] P.J. Bingham, K. Maegley, C.T. Krivacic, Cancer Research 74 (2014) 5155.
[114] K.M. Roscioli, X. Zhang, S.X. Li, G.H. Goetz, G. Cheng, Z. Zhang, W.F. Siems, H.H. Hill Jr, International Journal of Mass Spectrometry 336 (2013) 27.